Titre: Title:	The Impacts of Surface Engineering on the Environment and the Material Flows
Auteur: Author:	Mohamad Kaddoura
Date:	2024
Type:	Mémoire ou thèse / Dissertation or Thesis
Référence: Citation:	Kaddoura, M. (2024). The Impacts of Surface Engineering on the Environment and the Material Flows [Thèse de doctorat, Polytechnique Montréal]. PolyPublie. https://publications.polymtl.ca/59643/

POLYTECHNIQUE MONTRÉAL

affiliée à l'Université de Montréal

The impacts of surface engineering on the environment and the material flows

MOHAMAD KADDOURA

Département de mathématiques et de génie industriel

Thèse présentée en vue de l'obtention du diplôme de *Philosophiæ Doctor*

Génie industriel

Octobre 2024

POLYTECHNIQUE MONTRÉAL

affiliée à l'Université de Montréal

Cette these intiulée:

The impacts of surface engineering on the environment and the material flows

présentée par **Mohamad KADDOURA**

en vue de l'obtention du diplôme de *Philosophiæ Doctor*

a été dûment acceptée par le jury d'examen constitué de :

Robert LEGROS, président
Manuele MARGNI, membre et directeur de recherche
Guillaume MAJEAU-BETTEZ, membre et codirecteur de recherche
Mourad BEN AMOR, membre et codirecteur de recherche
Clara SANTATO, membre
Shanonn LLOYD, membre externe

DEDICATION

To my late father,

To my mother,

ACKNOWLEDGEMENTS

I would like to start by thanking my supervisors: Manuele, Guillaume and Ben for all the experience they brought in and the fruitful discussions.

Thanks to everyone at CIRAIG who made my stay so welcoming and joyful, especially the McCarold squad. Thank you Maxime for the coding help and the fun nights out. Thank you Anne-France for the enjoyable discussions and the continuous encouragement during our "coffee breaks." Thank you Titouan for being my first friend in Montréal and all the fourth-floor discussions. Thank you Han for being a lovely roommate. Thank you Carla for being part of the adventure since day one. Thank you Anne for the nice hiking trips. Thank you Elliot for your positivity. Thank you Ivan for your kindness. Thank you Geoffrey for always offering your couch. Thank you Jasmine and Olli for the good times and the frequent tabbouleh. Thank you Marit for the nice gatherings in general and the endless laughter in Leiden. Thank you Laura for the pleasant runs during COVID.

Thanks to my family who supported me through this journey and helped me persevere.

Thanks for the financial support I received from GreenSEAM & CREATE-SEED (NSERC), CIBC Bank, CIRODD, and FRQNT through scholarships.

RÉSUMÉ

Les technologies d'ingénierie de surface (ES) sont largement utilisées dans les secteurs de l'énergie et des transports, protégeant les pièces de l'usure et améliorant leur efficacité énergétique. Cela conduit à une réduction des émissions de gaz à effet de serre (GES) pendant la phase d'utilisation, avec une augmentation des émissions associées à la production de matériaux de revêtement et au processus de revêtement qui doit être prise en compte. Un autre problème important réside dans les pertes dissipatives se produisant tout au long du cycle de vie du composant, qui sont rarement évaluées. Avec l'augmentation prévue de l'utilisation de l'ES et son importance dans diverses applications, il est important d'évaluer les impacts environnementaux (et les avantages) et l'impact sur les pertes de matériaux pour garantir que ceux-ci sont minimisés dans l'industrie. L'analyse du cycle de vie (ACV) et l'analyse des flux de matériaux (AFM) sont les principaux outils d'écologie industrielle utilisés pour ces évaluations. Ces outils peuvent prendre du temps, en particulier dans la phase de collecte de données, et peuvent entraver de telles études dans le développement futur de technologies innovantes. Il est donc nécessaire de disposer d'une approche efficace pour effectuer l'ACV, et éventuellement l'AFM, sans compromettre la confiance dans les résultats.

Une revue de la littérature a montré que ces outils sont rarement utilisés pour l'ES et ne sont pas conçus pour des évaluations prospectives à grande échelle. Les compléter par des modèles d'évaluation intégrés qui suivent des scénarios cohérents permettrait cela. De plus, pour simplifier la méthodologie de l'ACV, les approches actuelles (par exemple, l'ACV simplifiée et de sélection) compromettent généralement la simplicité avec la confiance dans les résultats. L'utilisation de l'analyse d'incertitude pour guider la collecte de données permettrait de réduire les efforts tout en se concentrant sur les données conduisant à la plus grande amélioration des résultats.

L'objectif général de la thèse est d'anticiper et d'évaluer les impacts de l'ingénierie de surface sur l'environnement et l'utilisation des matériaux à différentes échelles d'adoption. Trois objectifs spécifiques ont été définis en conséquence. Le premier est d'évaluer les impacts environnementaux de l'adoption prospective à grande échelle de nouvelles technologies d'ingénierie de surface. Le deuxième est de quantifier les pertes dissipatives associées aux technologies d'ingénierie de surface et de suggérer des stratégies d'économie circulaire pour les réduire. L'objectif final est de

développer une méthodologie pour orienter les efforts de collecte de données dans l'ACV à l'aide de l'analyse d'incertitude.

Tout d'abord, l'ACV a été liée au modèle d'évaluation intégré MESSAGE pour évaluer les avantages et les impacts environnementaux prospectifs de la nouvelle application de l'ES. L'application de technologies SE innovantes au secteur de l'énergie a le potentiel de réduire les émissions annuelles de CO2-eq de 1,8 Gt en 2050 et de 3,4 Gt en 2100 dans un scénario de trajectoire socio-économique optimiste. Cela correspond à une réduction annuelle de 7 % et 8,5 % dans le secteur de l'énergie en 2050 et 2100, respectivement. En outre, les émissions de GES liées aux processus de revêtement sont largement compensées par les économies de GES des technologies de conversion d'énergie où les technologies SE innovantes sont appliquées.

Par la suite, une AFM paramétrée a été réalisée pour quantifier les pertes dissipatives des SE dans les secteurs de l'énergie et des transports en 2014 en utilisant le modèle ETP de l'AIE. Les résultats montrent que le processus de revêtement contribue le plus aux pertes dissipatives (jusqu'à 39 %). Le combustible à oxygène à haute vitesse (HVOF) a eu la plus grande part de pertes, avec 15,5 ktonnes de NiCrSi perdues pendant l'étape de revêtement. L'amélioration de l'efficacité du dépôt, la récupération de la poudre non adhérente et le décapage du revêtement des composants en fin de vie sont des stratégies clés d'efficacité des matériaux pour réduire les pertes de matériaux (jusqu'à 50 %).

Enfin, un cadre a été proposé pour réduire le temps nécessaire à la collecte de données dans l'ACV à l'aide d'une analyse d'incertitude. Le cadre nécessite de modéliser l'incertitude des paramètres d'entrée et de les propager via des simulations de Monte Carlo. Une analyse de sensibilité globale est ensuite utilisée pour classer les paramètres en fonction de leur contribution à la variabilité de sortie, et la collecte de données est priorisée en conséquence. Une étude de cas comparant les technologies de fabrication additive a été réalisée pour opérationnaliser le cadre, confirmant l'hypothèse de réduction du temps de collecte des données, tout en soulignant certaines limites du cadre.

Les principales limites de ce projet de recherche sont que les applications d'ingénierie de surface n'étaient pas souvent documentées, et donc les études étaient limitées aux secteurs de l'énergie et des transports. De plus, en raison du manque de données, de nombreuses hypothèses ont dû être

formulées pour modéliser les inventaires de revêtements nécessaires aux composants. Au fur et à mesure que davantage de données deviennent disponibles, des modèles plus représentatifs pourraient être générés. Pour le cadre d'ACV efficace en termes de temps proposé, il s'est avéré difficile de définir la distribution d'incertitude pour la collecte des données de dépistage, et de meilleures directives sont nécessaires pour garantir la validité des résultats.

Bien que l'ingénierie de surface puisse conduire à une réduction des émissions de GES, en particulier dans le secteur de l'énergie, des efforts supplémentaires doivent être faits pour réduire les pertes dissipatives de matériaux. Les évaluations futures pourraient bénéficier du cadre d'ACV proposé pour réaliser des études plus rapides et stimuler l'innovation dans le domaine.

ABSTRACT

Surface engineering (SE) technologies are widely used in the energy and transportation sectors, protecting parts from wear and tear, and improving their energy efficiency. This leads to reduced greenhouse gas (GHG) emissions during the use phase, with increased emissions associated with the production of coating materials and the coating process that needs accounting for. Another significant issue lies in dissipative losses occurring throughout the component's life cycle, which are rarely assessed. With the expected increase in the use of SE and its importance in various applications, assessing the environmental impacts (and benefits) and the impact on the material losses (especially in terms of GHG emissions) is important to ensure those are minimized in the industry. Life cycle assessment (LCA) and material flow analysis (MFA) are the main industrial ecology tools used for such assessments. Those tools could be time consuming, especially in the data collection phase, and might hinder such studies in future development of innovative technologies. Thus, there is a need for an efficient approach to perform LCA, and possibly MFA, without compromising the confidence in the results.

A literature review showed that those tools are seldom used for SE and are not designed for prospective large-scale assessments. Complementing them with integrated assessment models that follow consistent scenarios would allow for that. Furthermore, to simplify the LCA methodology, current approaches (e.g., streamlined and screening LCA) usually compromise simplicity with confidence in the results. Using uncertainty analysis to guide data collection would ensure reducing the efforts while focusing on the data leading to the most improvement in the results.

The general objective of the thesis is to anticipate and assess the impacts of surface engineering on the environment and the material use at various scales of adoption. Three specific objectives were defined accordingly. The first is to evaluate the climatic environmental impacts of prospective large-scale adoption of novel surface engineering technologies. The second is to quantify the dissipative losses associated with surface engineering technologies and suggest circular economy strategies to reduce them. The final objective is to develop a methodology to steer the efforts of data collection in LCA using uncertainty analysis.

First, LCA was linked with the MESSAGE integrated assessment model to assess the prospective environmental benefits (in terms of GHG emissions) and impacts of novel SE application.

Applying innovative SE technologies to the energy sector has the potential of reducing annual CO2-eq emissions by 1.8 Gt in 2050 and 3.4 Gt in 2100 in an optimistic socio-economic pathway scenario. This corresponds to 7% and 8.5% annual reduction in the energy sector (compared to the baseline energy generation in MESSAGE SSP1) in 2050 and 2100, respectively. Besides, GHG emissions related to the coating processes are largely offset by the GHG savings of the energy conversion technologies where the innovative SE technologies are applied.

Following that, a parametrized MFA was performed to quantify the dissipative losses from SE in the energy and transportation sectors in 2014 using the IEA ETP model. Results show that the coating process contributing most to the dissipative losses (up to 39%). High velocity oxy-fuel (HVOF) had the highest share of losses, with 15.5 ktonne of NiCrSi lost during the coating stage. Improving the deposition efficiency, recovering the unadhered powder and stripping the coating from the components at their end-of-life are key material efficiency strategies to reduce the material losses (up to 50%).

Finally, a framework was proposed to reduce the time needed for data collection in LCA using uncertainty analysis. The framework requires modelling the uncertainty of the input parameters and propagating them through Monte Carlo simulations. Global sensitivity analysis is then used to rank the parameters based on their contribution to the output variability, and data collection is prioritized accordingly. A case study comparing additive manufacturing technologies was done to operationalize the framework, confirming the hypothesis of reducing the time to collect data, while highlighting some limitations of the framework.

The main limitations of this research project are that surface engineering applications were not often documents, and thus the studies were limited to the energy and transportation sectors. Besides, due to the lack of data, many assumptions had to be done to model the inventories of coating needed for components. As more data becomes available, more representative models could be generated. For the suggested time efficient LCA framework, defining the uncertainty distribution for the screening data collection proved to be difficult, and better guidelines are needed there to ensure the validity of the results.

While surface engineering can lead to reduced GHG emissions, especially in the energy sector, more work needs to be done to reduce the material dissipative losses. Future assessments could

benefit from the proposed LCA framework to perform faster studies and drive innovation in the field.

TABLE OF CONTENTS

LIST OF TABLES

LIST OF FIGURES

LIST OF SYMBOLS AND ABBREVIATIONS

APS	Atmospheric plasma spray
CC	Climate change
CCS	Carbon capture and storage
CS	Cold spray
CVD	Chemical vapor deposition
EOL	End of life
FS	Flame spray
GHG	Greenhouse gas
GSA	Global sensitivity analysis
HVOF	High-velocity oxy-fuel
IAM	Integrated assessment model
IE	Industrial ecology
ISO	International organization for standardization
LCA	Life cycle assessment
MESSAGE	The Model for Energy Supply Systems And their General Environmental impact
MFA	Material flow analysis
PVD	Physical vapor deposition
SE	Surface engineering
SI	Sobol' index
SSP	Shared socio-economic pathway
TBC	Thermal barrier coating
TS	Thermal spray
YSZ	Yttria stabilized zirconia

LIST OF APPENDICES

CHAPTER 1 INTRODUCTION

1.1 Climate change and the need for mitigation

The impacts of climate change are being experienced around the globe at an increasing pace. Extreme weather events such as heatwaves (Tripathy et al., 2023), floods (Hunt & Menon, 2020), wildfires (Mansoor et al., 2022), and intense hurricanes (Balaguru et al., 2023) are becoming more common. Changing weather patterns affect agricultural yields, and ecosystems are struggling to adapt (Schmitt et al., 2022). In addition to their effect on the environment, global food security, water resources, and public health are also impacted (Amoak et al., 2022). Climate change is the result of a rise and accumulation in greenhouse gases driven by human activities (e.g., burning fossil fuels). Carbon dioxide is the most common emitted greenhouse gas (GHG) by human activities, where studies showed an almost linear relationship between global mean temperature change and accumulated CO_2 emissions (Friedlingstein et al., 2014). With an expected increase in GHG emissions in the coming years, urgent mitigation and adaptation actions are needed.

In 2015, more than 190 countries have recognized the urgent need for a response to climate change and agreed to limit the average global temperature increase to 1.5^{o}C above pre-industrial levels by signing the Paris agreement (Hulme, 2016). Raftery et al. (2017) found that there is only 1% chance to limit the global temperature increase to 1.5^{o}C, and the likely range is in fact 2.0-4.9^{o}C. Many countries have already foreseen the need for responding to these effects, placing climate adaptation policies and plans high on their agendas (Preston et al., 2011). For example, the European union set a target of 40% reduction of GHG emissions by 2030 compared to 1990 level, and 32.5% energy improvement (EC, 2014). This is complemented with an increased share of renewables in the energy mix, set to be 32%. Such policies to radically increase the shares of renewables might be too ambitious and costly to implement, while other incremental improvements could be more realistic and achievable.

Climate change mitigation strategies should consist of a number of measures and not a single "magic bullet" (Van Vuuren et al., 2007). In fact, stabilizing GHG concentrations at 400 ppm CO_2-eq is feasible under current technologies (ibid). Carbon capture and storage (CCS), for example, is a way to remove CO2 from the atmosphere and store it underground. The large scale deployment of those technologies, however, is still slow due to public perception (Roy et al., 2023). Other

technologies, such as electric vehicles had more adoption rates, and they can reduce GHG emissions by up to a quarter compared to gasoline cars over their lifetime (Hawkins et al., 2013). Further deployment, however, might be constraint by the limited availability of critical metals in the future (Habib et al., 2020). In this thesis, the focus will be on surface engineering, which has the potential of providing incremental GHG emission reductions in products already in use, but might also be hindered by the use of critical materials.

1.2 The role of surface engineering

Surface engineering is used in various sectors e.g., the energy sector, where it is used as a thermal-barrier coating to increase the efficiency of gas turbines (Clarke et al., 2012) and the automotive sector to reduce friction in passenger cars (Kenneth Holmberg et al., 2012). Almost one-third of energy used in transportation goes to overcome friction, and with recent advances in the field of lubrication and surface engineering, especially in terms of utilizing new materials, friction losses could be reduced by 18-40% (Kenneth Holmberg & Erdemir, 2019). The benefits of surface engineering are not restricted to the use phase of coated products, but to improved material efficiency as well. The environmental impacts of material production and processing are becoming vital (Allwood et al., 2011), emphasizing the role of material efficiency in reducing those emissions. To understand the need for producing new materials, it is important to know the causes of the end-of-life of products triggering users to replace them. Van Nes & Cramer (2006) categorized motives to replace products in four categories: wear and tear, improved utility, improved expressions, and new desires. They concluded that it is important to design for longevity during product development. Ashby (2009) also attributes the end of the physical life of a product to one of the following: fatigue, wear, corrosion, and creep. Most of the mentioned causes (e.g., corrosion and wear) are tackled with surface engineering and coating of the components to improve their characteristics extends the lifetime of products. Not only that those replacement-causing mechanisms lead to high environmental impacts (due to reduced lifetime and efficiency) but could also have massive costs. In fact, the global cost due to corrosion in 2013 was about 3.4% of the world GDP (around 2.5 trillion dollars), which could be reduced by 15% to 35% by using appropriate surface engineering technologies (Koch et al., 2016). Future development of new coating technologies and materials or the use of existing ones in new applications has the potential

for increased material and energy efficiency gains, contributing to decarbonization of the economy. The perceived environmental benefits need to be assessed against the impacts of coating to avoid shifting the burden from one life cycle stage to another.

1.3 Tools to assess the environmental impacts

Industrial ecology (IE) is a research field that empirically studies the major linkages of industrial processes within the biophysical basis of society, and is distinguished with detailed material flow analysis (MFA) and vintages of fixed assets while following up with system-wide mass balances (Pauliuk et al., 2017). Life cycle assessment (LCA) is a well-established IE method to quantify the environmental impacts of products and services in a holistic way (ISO, 2006), and is widely used by researchers and practitioners in the area of sustainability assessment (Göran Finnveden et al., 2009). Industrial ecology tools are increasingly being used in regulations across the world, especially in Europe. For example, in 2023, Denmark has made it mandatory to conduct LCA studies for new buildings (Construction, 2023). In the context of climate change mitigation, integrated assessment models (IAM) are used to provides future industrial system scenarios (Pauliuk et al., 2017). Combining IE tools with IAMs thus allows for a more robust mitigation assessment (ibid.).

1.4 Context of the research

This research is part of a strategic network focusing on green surface engineering for advanced manufacturing. The focus of this thesis is the *"green"* part of the project, more specifically the effects of a large-scale adoption of surface engineering on the environment and the material flows. Coating materials to increase their efficiency was identified as a potential application, especially in the energy sector which is responsible for significant emissions of GHGs and involves the flows of numerous materials. Surface engineering has a significant contribution potential in this application, increasing the thermal gradient of thermal-based technologies, and protecting renewables from cold conditions. Coating, however, brings into question the impacts of material dissipative losses of coating materials. Accordingly, it is important to investigate these aspects to better understand the potential and limitations of surface engineering. The work utilizes different IE tools (LCA, MFA, and IAM) and how to use them in the context of surface engineering.

CHAPTER 2 LITERATURE REVIEW

In this chapter, the existing literature around the tools and data used in the research are reviewed. It starts with an overview of the surface engineering technologies and their applications in different sectors. This is followed by a literature on Life cycle assessment (LCA) and material flow analysis (MFA), the tools used to assess the impacts on the environment and material, are reviewed.

2.1 Surface engineering

Surface engineering (SE) is "a specialized activity that is applied at or very near the final stage of material manufacture" (Dearnley, 2017). SE is mainly used to allow for the adjustment of four surface properties: mechanical (wear and friction), chemical (corrosion, permeation, temperature insulation, bio-compatibility, wettability), electrical (conductivity) and optical (transmission, reflection, absorption and color) (Bewilogua et al., 2009). Improving the surface properties reduces emissions during the use phase of the coated products. A common way to classify different coating technologies is based on the state of matter during the deposition and the film size as seen in Figure 2.1 (K. Holmberg & Matthews, 2009), and will be adopted in this thesis.

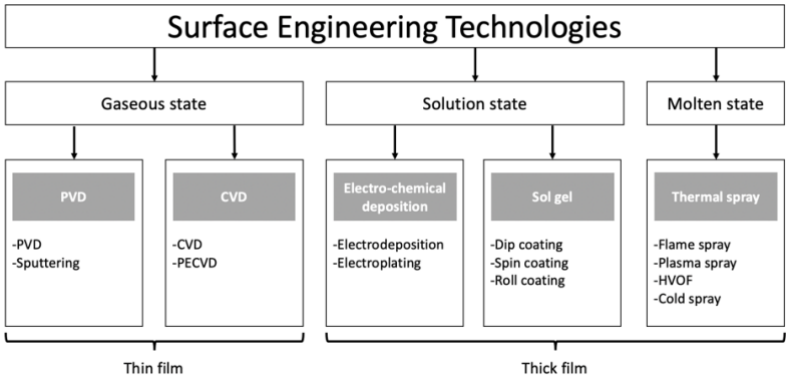

Figure 2.1 Classification of surface engineering techniques, adapted from Holmberg and Matthews (2009)

Physical vapor deposition (PVD) coatings are mainly used in the automotive and tooling industries. In the automotive industry, they can improve the durability of the engine components and enhance fuel efficiency (Bewilogua et al., 2009). For tools, coating enhances hardness and wear resistance, extending the lifetime of tools (Deng et al., 2020). Current research is focused on developing new coating materials, mainly alloy composites, to achieve superior performance (Ichou et al., 2024).

The impact of those materials and their scarcity needs to be assessed before scaling their adoption. The other trend in PVD application is extending to new areas such as renewable energy, electric vehicles and additive manufacturing (Ichou et al., 2024).

The main application for thermal spray is thermal barrier coatings (TBCs) for gas turbines and jet engines. These coatings are essential for protecting engine components from extreme temperatures, allowing for higher operating temperatures and, consequently, greater engine efficiency. The higher efficiency reduces fuel consumption, which leads to lower emissions. New materials for TBCs are pushing the boundaries of temperature tolerance, further improving fuel efficiency, and reducing the environmental footprint of aviation and energy generation (Clarke et al., 2012). Traditionally, yttria stabilized zirconia (YSZ) is the most commonly used TBC material, but with the search for increased efficiencies, pyrochlores (e.g., $La_2Zr_2O_7$ and $Gd_2Zr_2O_7$) emerged as promising candidates (Mahade et al., 2015; Vaßen et al., 2010). High Velocity Oxy-Fuel (HVOF) and cold spray technologies are also gaining traction, particularly for repairing high-value components, especially those subject to corrosion and wear, like those used in gas turbines. An advantage that cold spray repairing has, thanks to its low processing temperature, is the ability to use it on most metals and alloys, with almost no limits on the thickness growth (W. Li et al., 2018). Cold spray, as its name indicates, is done at low temperatures (but high velocities), thus has a low compressive residual stress, low thermal input, and causes no microstructural changes in the base alloy (Rech et al., 2014). The low processing temperature also means minimizing (and eventually eliminating) the damaging effects of oxidation, possible phase transformation, decomposition, grain growth and other issues with thermal additive manufacturing (W. Li et al., 2018; X. Wang et al., 2015). Kumar et al. (2005) recommended the uses of HVOF in repairing cavitation damages in turbines, exhibiting better erosion resistance compared to weld repair. Besides, cold spray could be used to repair damaged aluminium alloy components in the aviation industry (Rech et al., 2014).

Surface engineering relies on a diverse range of materials designed to modify and enhance the surface properties of the coated substrates. These materials are selected based on the specific requirements of various applications, such as wear resistance, corrosion protection, thermal stability, and friction reduction. Materials used in surface engineering are ceramics, metals, and polymers, each of which offers distinct advantages depending on the of the application. Table 2.1 summarizes the substrate and feedstock materials commonly used for each surface engineering

technology (Fotovvati et al., 2019). Iron-based (steel) substrate is the most common coated, together with aluminum, nickel and titanium alloys. For the feedstock, it is common to have some critical and rare earth metals, due to their special characteristics. This includes zirconium, niobium, tungsten, tantalum, copper, nickel, cobalt, magnesium, yttria, molybdenum, chromium and boron.

Table 2.1 Summary of the common substrates and feedstocks used in different surface engineering technologies, adapted from Fotovvati et al. (2019)

SE echnology	**Substrate**	**Feedstock**
PVD	Steel, glass, Si, KBrCAuAl, AgAuCuAl	TiCxOy, ZrC_xO_y, TiN, PE, PVDF, PTh
CVD	Glass, Si, tissue, NiCoFe	Nb_2O_5, WTiNW$Si_2Ta_2O_5CuSiO_2$, $SiSi_3N_4SiO_2$, PTFE, Ni_3Ti
CSD	Steel, Cu	$NiCoAl_2O_3$, NiCoSiC, $ZnNiAl_2O_3$, PPy
ECD	Steel, Ti6Al4V	GlassCuBG, SiO2, chitosan, grapheme, SiC
Sol gel	Si, NiTi, Steel	$TiCl_4$TEOSMTEOS, HA, PDMS, PC
Plasma Spray	Steel	$Al_2O_3ZrO_2$YSZ, Ni5Mo5.5Al, TiCNiCrBSi
HVOF	Steel, Ti6Al4V	HA, CoNiCrAlY, WC
Arc Wire	Steel	MoS_2TiCFe, Ti/Al
Cold Spray	Ti6Al4V, Al6061-T6, Al6061	HA, AlZnMgCu, Ni, MoO_3, NiAl

Future development of new SE technologies and materials has the potential for increased energy and material efficiency gains and reduced costs, helping mitigating climate change. This, however, can come on the expensive of the use of high energy demanding processes or scarce metals, and complete environmental (Section 2.2) and material (Section 2.3) assessments are needed.

2.2 Life cycle assessment

Life Cycle Assessment (LCA) is a technique used to understand and address the environmental impacts of a product or service during its entire life cycle. This includes raw material extraction and production, manufacturing, transportation, use and end-of-life treatment. The LCA could be used to identify opportunities of environmental improvement and help in decision making for stakeholders. LCA has been standardized according to the ISO 14040:2006 standard. To conduct an LCA it should include the following four phases: goal and Scope definition, inventory analysis, impact assessment and interpretation (ISO, 2006).

Most LCA studies are performed on full-market existing systems, where process data are widely available (Stefano Cucurachi et al., 2018). In the case of emerging technologies, this becomes challenging, especially in the inventory analysis stage, where data collection is already the most time intensive stage in traditional LCA studies (Laca et al., 2011; Zargar et al., 2022). In response to that, the concepts of prospective, anticipatory and ex-ante LCA have emerged (Arvidsson et al., 2023) with various guidelines to perform it (Adrianto et al., 2021; Arvidsson et al., 2018; Mendoza Beltran, Cox, et al., 2018). Other efforts to overcome the data availability issue in LCA in general, and reduce time and cost associated with it, are simplified versions of LCA (Gradin & Björklund, 2021). Screening and streamlined LCAs are the most common simplification approaches used (Arena et al., 2013; Hochschorner & Finnveden, 2003; Hung et al., 2020). Those methods do not use the full potential of LCA by eliminating some processes and impact categories and relying on lower data quality. Instead, prioritizing high quality data collection for the most “important” parameters instead is needed. Global sensitivity analysis can be used for that purpose, which ranks input parameters based on their contribution to the variance of the output (Patouillard et al., 2019).

LCA is suitable for small-scale and retrospective studies. In response to that, there has been a rise in studies complementing LCA with other tools to incorporate the prospective and large-scale elements (Section 2.2.1). To deal with the issue of the data collection in LCA under limited resources, global sensitivity analysis can help identify the significant parameters affecting the results the most (Section 2.2.2).

2.2.1 Prospective LCA

While there is not a single definition for prospective LCA, Arvidsson et al. (2018) defines it as an LCA of an emerging technology that is modeled at a future time. This is important from an eco-design perspective, where it is the easiest to alter the design to address potential environmental hotspots at early stages, but there is not enough data to have a full LCA (Chebaeva et al., 2021). Recommendations to conduct prospective LCAs highlight the importance of data selection and the differentiation between foreground and background data (Adrianto et al., 2021; Arvidsson et al., 2018; Mendoza Beltran, Cox, et al., 2018).

Various approaches are used to model the foreground inventory of early-stage technologies to account for the scaling effect. Scaling factors could be used for specific applications (e.g., for heat pumps (Caduff et al., 2014)). Piccinno et al. (2016) used an engineering-based approach to simplify calculations for the reactions relevant to different chemical processes. Computational models, like machine-learning, were also used to estimate the parameters of bio-based processes (Karka et al., 2022). Furthermore, recommendations of using learning effects (e.g., learning curves) for prospective assessments have been proposed (Thomassen et al., 2020).

To model prospective background data, integrated assessment models (IAM) have been adopted by LCA practitioners (Mendoza Beltran et al., 2020). IAMs are numerical models studying different pathways and scenarios for human and earth systems involving technology shifts and disruptions within the context of climate change mitigation and energy optimization (Huppmann et al., 2019a). Common IAMs with good coverage of energy conversion, transportation technologies, and greenhouse gases include AIM/CGE, GCAM, IMAGE, MESSAGE and MACRO/REMIND (Pauliuk et al., 2017). IAMs are usually linked to LCA to analyze the impact of future electricity supply mixes on specific technologies, e.g., comparing internal combustion engine vehicles with electric vehicles (Mendoza Beltran, Cox, et al., 2018) and alternative aluminum production routes (Pedneault et al., 2021). LCA can also be linked to IAMs to account for possible shifts of impacts between different environmental categories in the energy sector, by including additional categories to GHG emissions (Fernández Astudillo et al., 2019; Luderer et al., 2019; Pehl et al., 2017; Vandepaer et al., 2020). IAMs do not come without limitations. Most of them lack the documentation and reproducibility, making it harder for other researchers to use

them. Still, some IAMs provide open access to their model, like the MESSAGE[ix], which provides all the models used and also an easy-to-use web interface to visualize the results (Huppmann et al., 2019b). Another limitation of IAMs is while they have good coverage of energy systems, transportation technologies and greenhouse gas emissions, other aspects like material cycles and vintage tracking are still missing and should be included in the future (Pauliuk et al., 2017).

The Model for Energy Supply Systems And their General Environmental impact (MESSAGE) is a dynamic linear least-cost optimization model. It includes 43 energy conversion technologies, 11 world regions and is available in open access (Huppmann et al., 2019b). The coverage and flexibility of the model allows researchers to customise it based on their research needs. For example, it could be regionally customised to study the energy system at a country level (e.g. MESSAGE-China (Q. Liu et al., 2009) and MESSAGE-Brazil (Nogueira De Oliveira et al., 2016)). It could also be used to focus on one energy generation technology, e.g., to assess the use of nuclear power in the UAE (AlFarra & Abu-Hijleh, 2012). Furthermore, MESSAGE could be adjusted to account for different energy efficiency scenarios (Selvakkumaran & Limmeechokchai, 2013).

Recently, shared socio-economic pathways (SSPs) were introduced as new scenario framework for climate change research (O'Neill et al., 2017) and were adopted in the Intergovernmental Panel on Climate Change Sixth Assessment Report (IPCC, 2022). The scenarios are driven by narratives describing different socio-economic pathways and defined based on challenges for mitigation and for adaptation (Figure 2.2). SSPs include a marker scenario (base scenario), with possible extensions of it based on environmental policies (Fricko et al., 2017). Having consistent scenarios that are linked to IAMs makes it easier to comprehend different studies.

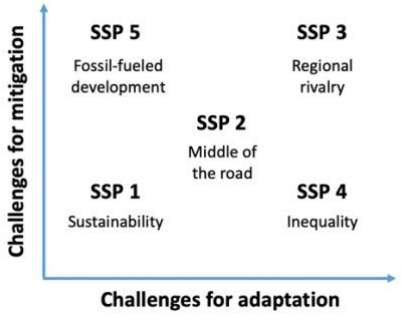

Figure 2.2 Overview of the two dimensions of the shared socio-economic pathways (SSPs), with the 5 SSPs, redrawn from (O'Neill et al., 2017)

While IAMs cover the energy sector, they do not account for the material flows in the system. Coupling the inventories of energy technologies with IAMs would enable that.

2.2.2 Global sensitivity analysis in LCA

Before exploring global sensitivity analysis, a brief introduction of uncertainty analysis in LCA is provided. Uncertainties in LCA are usually divided into epistemic and aleotory uncertainty. Epistemic uncertainty is that due to lack of knowledge or representativeness and can be reduced with more research while aleatory uncertainty is due to the inherent variability of the system (Igos et al., 2019). The first step in an uncertainty assessment is to identify and characterize the uncertainty. The most common distribution functions to characterize uncertainties in LCA are normal, triangular, uniform and lognormal distributions (Lloyd & Ries, 2007). This is followed by the uncertainty propagation**,** where stochastic methods are usually used, namely Monte Carlo (ibid.). The final step is the analysis, which could be in the form of scenario or sensitivity analysis. Sensitivity analysis aims at understanding the main source of uncertainty and address it by refining the critical elements (Igos et al., 2019) and can be done on both a local or global scale.

Different methods are available to perform a GSA, i.e., to quantify the contribution to output variance. Those include squared standardized regression coefficient, squared Spearman correlation coefficient, key issue analysis, Sobol' indices and random balance design (Groen et al., 2017a), all giving similar results. In LCA, GSA is mainly used at an inventory level, where various guidelines have been presented (Lacirignola et al., 2017; Wei et al., 2015). First order Sobol' index is the most common method, but higher order Sobol' indices might be needed in some studies to address the high degree of correlation between parameters (Wei et al., 2015). GSA could also be used for life cycle impact assessment (LCIA), where Cucurachi et al. (2016) proposes a protocol for that to ensure the development of trustable impact assessment models.

In LCA, Global sensitivity analysis is usually used to identify parameters significantly affecting the results, where decision-making is improved by treating them. This has been applied to various systems, e.g., biodiesel production (Khang et al., 2017), geothermal heating networks (Jaxa-Rozen et al., 2021), dialkylimidazolium ionic liquid production (Baaqel et al., 2023) mealworm production (Thévenot et al., 2018), and milk production (Wolf et al., 2017). GSA becomes more relevant when assessing emerging technologies, with the unpredictable pathways a technology

undergoes going from lab to industrial scale (Blanco et al., 2020). For example, Cox et al. (2018) included future energy generation scenarios from IMAGE integrated assessment model in their assessment of future battery electric vehicle. In addition to identifying the highly variable parameters, it was highlighted that future research to focus on reducing the uncertainty and improving the data quality for those parameters (Wolf et al., 2017).

Another use of GSA in LCA studies is to have simplified LCA models of specific products based on a few parameters that contribute the most to the output variability, and could be helful when dealing with emerging technologies (Lacirignola et al., 2017). For example, the GHG emissions of miscanthus cultivation was defined by a simplified model focusing on six of the 38 parameters expressing the system (Lask et al., 2021). In another study, GHG emissions from wind turbines was defined as a function of the turbine load factor and the wind turbine lifetime (Padey et al., 2013). While it is argued that such models give simple robust results for decision makers, excluding some parameters with low contribution to the variability of the results might be misleading. It is important to aim for a complete model (even with low data quality) while focusing on improving the data quality of the parameters contributing the highest to the variability of the output. Gibon and Hahn Menacho (2023) followed a similar approach to provide a parametrized LCA model for nuclear power, another energy generation technology with highly variable environmental impacts previously reported. Their models include more parameters than the others (20) and nine environmental impact categories.

Uncertainty analysis in LCA is usually used to assess the variability of the results but no to prioritize data collection. It is possible to leverage the power of identifying parameters contributing the most to the variability of the output to guide data collection and reduce the efforts in performing an LCA.

2.2.3 LCA of SE technologies

This section presents an overview of LCA studies conducted on various surface engineering technologies. The extensive list of the reviewed literature is available in Appendix E. Key aspects to consider when comparing the studies include the technologies employed, the coating materials used, and the most impactful lifecycle stages. Historically, electroplating has been the most studied surface engineering technology in LCA studies. Most studies focus on comparing chromium

electroplating, which emits hazardous hexavalent chromium, to safer alternatives. Regulatory pressure to reduce or eliminate hexavalent chromium due to its carcinogenic properties has prompted the development of substitute technologies (Pollack, 2018). While these alternatives reduce hexavalent chromium emissions, therefore reducing the impacts on human health, they may present trade-offs in other impact categories, such as global warming potential (GWP), especially when fossil-based electricity is used (Merlo & Léonard, 2021).

The reviewed studies defined different functional units, making the comparison of different technologies infeasible. The most common functional unit included both the coated area and coating thickness, followed by the coated area alone. Some studies focused on the final product which the coating is applied to or used the amount or mass of the final product as the functional unit. Surface engineering is generally performed to enhance certain properties (e.g., corrosion resistance), and using coating thickness or mass as a functional unit could discard differences in material efficiency. For example, some materials might require thinner coatings to achieve the same protective function. Furberg et al. (2021) proposed a property-based functional unit, emphasizing the desired performance outcome, which is more appropriate for comparing different coating materials. Similarly, Merlo & Léonard (2021) recommended shifting from using the amount of coating material as the functional unit to a function-based approach, such as the lifespan extension of a tool, for a more accurate comparison of environmental impacts.

Another critical factor in comparing LCA studies is the system boundaries, specifically the life cycle stages included. Most of the studies had a cradle-to-gate scope, excluding the use and end-of-life (EOL) phases. Only a limited number of studies considered pre-treatment stages, such as grit blasting, which can contribute significantly to the environmental impacts, particularly from alumina production (Guarino et al., 2017; E. Rúa Ramirez et al., 2024). Pre-treatment methods, such as sandblasting, are important for some coating applications because they improve adhesion between the substrate and coating by increasing surface roughness. Post-treatment steps, like laser remelting, can enhance coating density and adhesion while exhibiting relatively low environmental impacts (Serres et al., 2010). The use phase is often neglected in LCA studies as well, even though it can significantly influence results. This is especially important if the coating improves the energy efficiency in some applications, results in reduced emissions. Recycling at the EOL phase,

particularly when the material contributes substantially to the overall impacts, can also help reduce environmental burdens from avoided mining when included.

The majority of LCA studies relied on data from literature, patents, and laboratory experiments. Background data for these studies typically came from databases like ecoinvent, while foreground data were often derived from lab-scale experiments or company reports. To make these studies more applicable to industrial scales, researchers have adopted optimization strategies to scale-up coating technologies and account for reduced electricity consumption (Fiameni et al., 2021; Tsoy et al., 2019).

Global warming potential (GWP) was the most assessed impact category in LCA studies of surface engineering, along with human health impacts, particularly in cases where toxic materials like chromium were involved. Some studies also examined energy demand, given that electricity is often the primary contributor to the climatic environmental impact of these processes. Material demand, particularly for scarce resources such as copper or indium, was another focus of interest in several studies (Guarino et al., 2017; Haapala et al., 2009).

Sensitivity analyses in the reviewed studies often addressed the electricity mix, as electricity plays a dominant role in determining environmental impacts (namely GHG emissions). For instance, replacing fossil-based electricity with hydropower reduced the GWP of plasma spray processes by 46.65% (J. Liu et al., 2021). Deposition efficiency was another common parameter for sensitivity analysis because it has an inverse relationship with both material and energy consumption (Moign et al., 2010). Additionally, coating degradation time and coating porosity, which influence the need for recoating during a product's lifetime, were studied for their potential effects on material usage. These parameters are essential in understanding the long-term sustainability of different surface engineering technologies.

The assessed studies were retrospective in nature, describing currently used technologies. Prospective and large-scale assessments, as described earlier, are needed with an ever-growing sector. Furthermore, the impacts on the use of materials are neglected, and issues related to criticality of metal and materials losses need to be assessed.

2.3 Material availability

With various materials used in the coating process (Table 2.1), concepts related to material availability (criticality and dissipation) are explored in this section. This is followed by a literature on material flow analysis (MFA), a tool that allows us to track the flow of materials, with a focus on the surface engineering sector.

2.3.1 Criticality of metals

With complex products made up of various metals, the global demand of 55 metals has increased by almost 7 folds between 1953 and 2013. This was driven by emerging technologies, which hugely increased the demand for 32 metals that were seldomly used before the 1980s (P. Wang et al., 2018). The high demand of many metals, which are usually extracted in specific geographic areas, shows the need to quantify the 'criticality' of those metal to ensure the security of supply. Assessing the criticality would also help in the design of products and the design for recyclability. Although the idea might seem trivial to categorize elements into critical and non-critical, in practice it is a challenging task (Graedel & Allenby, 2010).

Criticality assessment was first developed by the US National Research Council (NRC, 2008), assessing the material's importance in use and the material's availability. Another methodology to quantify the criticality of different elements in the periodic table was proposed by Graedel et al. (2012). It consists of three dimensions: supply risk, environmental implications, and vulnerability to supply restrictions. This methodology could be used for risk assessment and in strategic decision makings. It is also flexible in terms of the indicators, which could be altered according to the aim of the study. It was used in a comprehensive study on the criticality of metals (Graedel et al., 2015), where 62 metals were classified according to the three criticality dimensions. The most critical metals were those mined as companions, their ores are highly concentrated in areas with geopolitical issues, are associated with high environmental impacts during their mining, and lack suitable substitutes. The results, however, could not be taken as concrete findings, but rather a directional indication.

With a strong push towards decarbonization, a transition towards renewables flourished in the past decade. This shift, although reduces GHG emissions, is associated with the use of different rare

elements. Several studies have tried to assess the role and availability of those critical metals in the future "clean" energy technologies. Elshkaki & Graedel (2013) studied the availability of materials in the future (year 2050) related to a shift to cleaner energy. Although for wind technologies there is no risks on the availability of metals (in agreement with Tokimatsu et al. (2017), but contradicting Alonso et al. (2012)), for photovoltaic solar, silver, tellurium, indium and germanium could have a constrained demand, depending on the technology used. The results are in line with another study that tried to find bottlenecks in the need of special metals for future energy systems in 2050 (Grandell et al., 2016). The most critical elements were identified as silver, tellurium, indium, dysprosium, lanthanum, cobalt, platinum and ruthenium. While Elshkaki & Shen (2019) identified almost the same elements as critical in a Chinese market perspective, they expected that technological advancements could reduce the supply risk of silver, indium, dysprosium, and terbium. One of the shortcomings of material criticality assessment methods is that they overlook the role of recycling, innovation, substitution and time horizons (Månberger & Stenqvist, 2018). Further mitigation strategies to address possible shortages include extending primary output of energy technologies, reuse and waste reduction (Moss et al., 2013). For example, 20% of the total demand of neodymium in wind turbines in 2050 could be avoided by recycling decommissioned turbines and redesigning magnets for reuse (Fishman & Graedel, 2019).

2.3.2 Material dissipative losses

Material dissipative losses are "losses of material into the environment, other material flows, or permanent waste storage that result in concentrations in the receiving medium such that recovery of these materials is technically or economically unfeasible" (Zimmermann & Gößling-Reisemann, 2013). It is especially important to reduce those losses in the case of critical materials, where the availability is already low from a supply side, and we need to ensure it stays longer in the in-use stocks. In addition to mitigating criticality and supply issues, minimizing the in-use material dissipation can reduce GHG emissions from the metal industry by 13-23% while ensuring the availability of more materials to recycle (Ciacci et al., 2016). Lifset et al. (2012) introduced the dissipation index, a measure of resource efficiency for different materials. This index can be used in the calculation of recycling rates to account for dissipative losses, which had a small but

discernible influence, emphasizing the importance of considering dissipative losses when assessing recycling.

Mineral dissipation has also been addressed in LCA studies through different life cycle impact assessment methods (LCIA) (Beylot et al., 2024). Recent methods include the environmental dissipation potential (van Oers et al., 2024), Abiotic Resource Project method (Owsianiak et al., 2022), and Average Dissipation Rate and Lost Potential Service Time (Charpentier Poncelet et al., 2022). The main challenge in developing such method is the different definitions of dissipative losses, and the inclusion of life cycle inventory (LCI) flows that correspond to the losses (Berger et al., 2020). When LCI flows are included in LCA, they can be quantified using material flow analysis (MFA).

2.3.3 Material flow analysis

2.3.3.1 Overview

Material flow analysis (MFA) is "a systematic assessment of the state and changes of flows and stocks of materials within a system defined in space and time" (Brunner & Rechberger, 2004). This includes the source of the materials, the pathways (i.e., manufacturing steps), the intermediate sink (i.e., sector where the product is used) and the final sinks. This is achieved by a mass balance between different processes and stocks in a system. In MFA, A *material* describes both substances (e.g., elements and compounds) and material goods (both having positive and negative economic values). A *process* includes transportation, transformation, or storage of materials. *Stocks* represent an amount of material stored in a process.

MFA has been the main tool used to track the flow of materials and the losses in various life cycle stages (Cullen & Cooper, 2022). Most MFA studies focused on materials with large extraction rates, e.g., aluminum, copper, and iron (ibid). However, MFAs on metals used in small quantities for specialized applications, posing greater concerns due to their criticality (Graedel et al., 2015), are still lagging. MFAs for critical materials are usually performed for specific countries (e.g., China) and mainly in the context of clean technologies (Hu et al., 2022; Zheng et al., 2022), ignoring smaller applications and higher geographical coverage.

2.3.3.2 MFA of SE technologies

Despite being labeled as one of the main drivers of dissipation (Zimmermann & Gößling-Reisemann, 2013), the use of critical materials in coatings has not been extensively assessed. To our knowledge, only one MFA study was performed for yttria-stabilized zirconia (YSZ) used as a thermal barrier coating (Figure 2.1), with a limited spatial coverage of Germany (Zimmermann, 2017). The results show that in the case of jet engines, 38% of the losses occur in the coating process and up to 28% in the material production stage. Other studies included surface engineering as an application rather than the focus of the study. Nassar (2017) assessed the stocks and flows of physical vapor deposition (PVD) as an application of tantalum. Only a portion of tantalum is deposited on the substrate during PVD sputtering, while 19-88% of it is lost, usually on the chamber walls. Leal-Ayala et al. (2015) also included wear applications when assessing the material flow of tungsten, without specifying the end products in which they are used, or whether they are used as coatings or not. From those studies, coating process appears to account for high material dissipative losses, and further coating applications must be assessed to understand the scale of it.

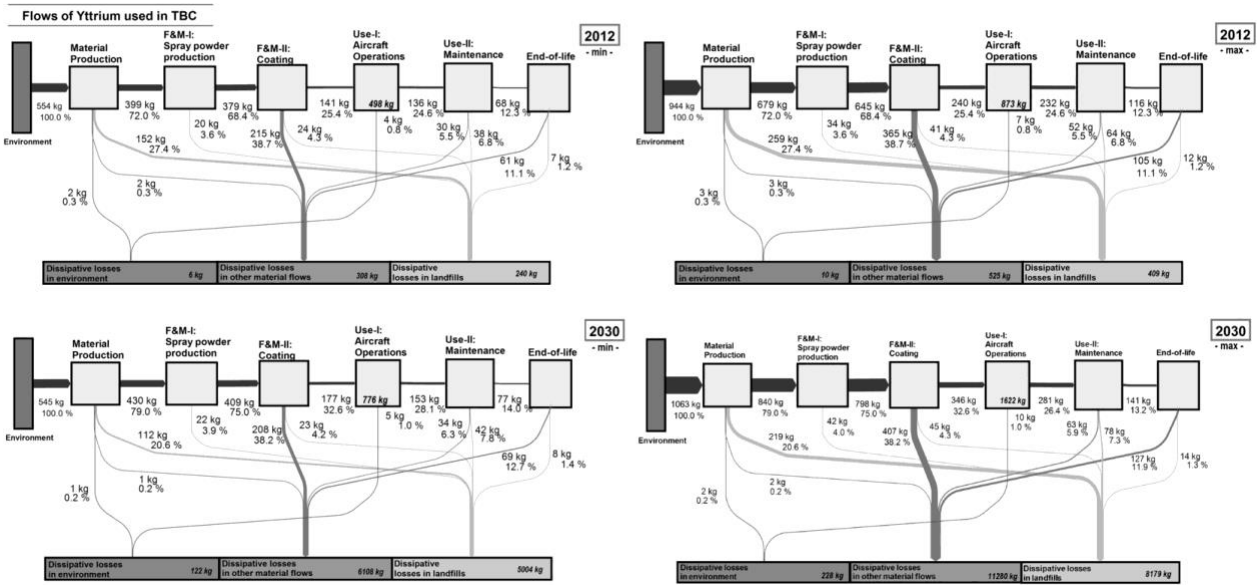

Figure 2.3 An example of a material flow analysis of Yttrium used in TBC, From Zimmermann (2017), with permissions.

Despite the wide spread of MFA studies assessing material dissipative losses, those addressing the surface engineering domain are still lagging.

CHAPTER 3 RESEARCH OBJECTIVES AND METHODOLOGY

3.1 Problem definition

With a growing pressure to decarbonize the energy and transportation sectors, a toolbox of different interferences and technologies is needed. Surface engineering (SE) technologies contribute to enhancing energy efficiency within the energy and transportation sector. Despite the extensive material-science related literature on SE, there's a notable absence of a comprehensive life cycle engineering approach tailored to assess their environmental impacts. While SE technologies offer efficiency gains that lead to reduced greenhouse gas (GHG) emissions during the use phase, there are also emissions associated with the production of coating materials and the coating process. To avoid any shift of burdens across different life cycle phases or to other environmental impact categories, it's important to adopt a holistic perspective. Besides, novel SE technologies are developed continually, and are used in increasing sectors This requires considering factors like the current and future market size of the technology, its diffusion and displacement rates, to supplement prospective LCAs, which are currently lacking in many studies.

Although thermal spray technologies extend component lifetimes and improves the energy efficiency, thereby mitigating environmental impacts, they are not without some drawbacks. A significant issue lies in dissipative losses occurring throughout the component's life cycle. Research on assessing dissipative losses in materials used in SE is scarce, often relying on limited literature and undisclosed industry communications, with a narrow geographical scope. Given the critical nature of certain coating materials, studying their fate is crucial to guide efforts in minimizing losses, factoring in the feasibility of such reduction measures. While various circularity strategies for thermal spray applications have been studied independently, a comprehensive evaluation to understand the potential pathways to transition to a more circular sector is still lacking. This would give us an idea of the potential reduction in dissipative losses in the economy and highlights circular economy strategies that should be prioritized.

Identifying the environmental and material loss hotspots requires novel eco-design of surface engineering technologies to tackle and reduce them. LCA and MFA, however, are most suitable for technologies with abundant information available, as data collection, particularly in the inventory analysis phase, is time consuming. Assessing the environmental impacts of emerging

technologies poses even greater data collection challenges. Emerging SE technologies are good examples, where modeling optimal spraying parameters and considering future electricity mix evolution are essential. Assessing the impacts on the environment and the material use requires significant resources that might hinder such studies in supporting environmentally sound design of novel technologies. To streamline LCA and reduce its time and cost intensity, simplified versions have been developed. However, significant simplifications in these methods increase the risk of displacements and misleading results. Instead, emphasis should be on a more iterative method focusing on what matters. This could be done by acknowledging data uncertainty and describing it through uncertainty information, assessing the impact of uncertain data on results, and ultimately focusing on improving the quality of uncertain input parameters that primarily influence results.

This research is therefore interested in the following general research question: how to assess the impacts of surface engineering on the environment and the material flows in a timely manner?

3.2 Objectives of the study

General objective: Anticipate and assess the impacts of surface engineering on the environment and the material use at various scales of adoption:

Specific objective 1: Evaluate the environmental impacts of prospective large-scale adoption of novel surface engineering technologies.

Specific objective 2: Quantify the dissipative losses associated with surface engineering technologies and suggest circular economy strategies to reduce them.

Specific objective 3: Develop a methodology to steer the efforts of data collection in LCA using uncertainty analysis.

3.3 General methodology

The general methodology adopted to address the main objective and specific objectives of this study is illustrated in Figure 3.1. The research combines several tools used in the industrial ecology field, particularly life cycle assessment (LCA) to assess the environmental impacts (mainly in terms of GHG emissions), material flow analysis (MFA) to quantify dissipative losses, and integrated assessment models (IAMs) for large-scale prospective scenario analysis. The sectors assessed

where the transportation, energy, and manufacturing sector, with the highest potential of improvement, and where SE is already. Varying geographic and temporal coverage was chosen depending on the scope of different case studies.

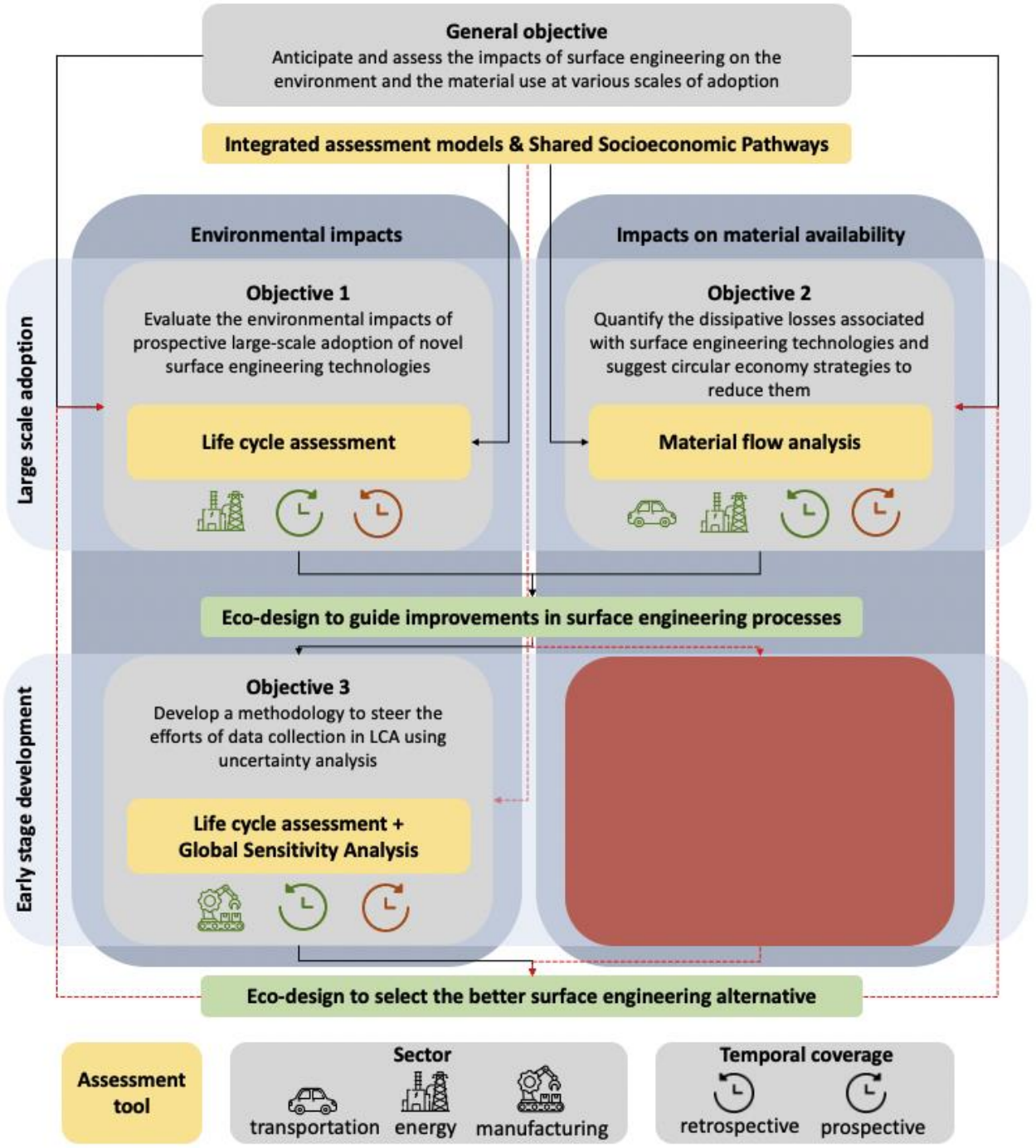

Figure 3.1 General methodology. Red represents elements not included in the thesis but could be investigated in the future.

Specific objectives and the method used to achieve them are briefly described in the following subsections.

3.3.1 Methodology addressing objective 1

The first specific objective of this study aims to quantify the **environmental** benefits and trade-offs of **large-scale** adoption of innovative surface engineering technologies to improve the energy conversion efficiency in the **energy sector** under different **prospective socio-economic** and policy scenarios. The anticipated environmental performances are assessed in terms of potential impacts on the climate, on ecosystem quality, and on human health to identify potential burden shifting to other environmental impact categories.

The first step of this sub-objective involves conducting a literature review to identify innovative surface engineering technologies in the energy sector. The energy conversion technologies studied are coal power plants, gas turbines, solar panels, and wind turbines. Due to the high uncertainty in the amount of lifetime extension achieved due to corrosion/erosion resistance in other energy conversion technologies, such applications are out of the scope of the study.

The second step involves scaling up the impacts and modeling the evolution of energy systems and the adoption of the identified surface engineering technologies in them over time and in accordance with consistent narratives of possible societal evolution pathways. The MESSAGE integrated assessment model (IAM) was used with three shared socio-economic pathways (SSPs) defining the different narratives. Three adoption scenarios (pessimistic, optimistic and optimistic + retrofit) were also defined to be consistent with the different SSPs.

Finally, to get the environmental impacts for various SE technologies, ecoinvent 3.5 database was used with IMPACTWorld+ impact assessment method. The inventory for the energy technologies was the result of the MESSAGE model, and for SE technologies, literature was used.

3.3.2 Methodology addressing objective 2

The second objective aims to quantify the **material** dissipative losses in thermal spray applications and the reduction potential of applying circular economy strategies. This was done through a parametrized **MFA** that can be enhanced when more data becomes available.

To quantify the material dissipative losses, the first step was to identify the main thermal spray applications through literature review. This was complemented with expert judgement due to the

limited information available in the literature. The main applications were found to be in the energy and transportation sectors, where the amount of coating needed for each application was calculated.

The second step was to identify key parameters affecting the losses at each life cycle stage. Those parameters were mining efficiency, material production efficiency, powder production efficiency, theoretical deposition efficiency, target deposition efficiency, post-processing efficiency, corrosion ratio, friction ratio, thermal fatigue ratio, wear ratio, powder production recycling rate, coating recycling rate, and EOL recycling rate. The parameters were defined as probability distribution functions and the resulting dissipative losses were defined as parametrized functions. A 1000 runs Monte Carlo assessment was carried out to account for uncertainties.

The final step in identifying the dissipative losses was **scaling up** the impacts based on the amount of coating used in each product (identified previously through the literature), then the number of products in the sector. The IEA ETP model was used for the **energy** and **transportation** sector scale-up.

After identifying the losses, material efficiency strategies relevant to the surface engineering sector were identified and assessed. Those included reducing the material lost in the coating stage by design, extending the lifetime of coating on the components, and recycling the powder.

To complement the assessment on dissipative losses, environmental impacts associated with the material losses were quantified using life cycle assessment. Material impacts were calculated based on ecoinvent 3.6 database characterised with impact indicators using the IMPACTWorld+ method. Climate change, ecosystem quality, and human health indicators were assessed.

3.3.3 Methodology addressing objective 3

The third objective of the research aims to reduce efforts in conducting LCA by prioritizing data collection efforts using uncertainty analysis (namely **global sensitivity analysis**). A case study on cold spray **additive manufacturing** was carried out to operationalize the proposed framework.

The first step of the framework is to define the goal and scope, particularly the desired level of confidence that an alternative is environmentally better than the other. This level of confidence is to be used later to decide when to stop the iterative process while being confidant that the results are conclusive.

The second step is the screening data collection based on a brief literature / expert judgement rather than a thorough data collection. This is followed with a completeness check, to make sure that no inputs were missed out. Here, we focus on identifying the “unknown unknowns” rather than improving the data we have for the identified inputs. This could be done using input/output tables, information from related LCAs, and applying the law of mass conservation.

The third step is modelling the uncertainty of the identified input parameters. This could be done directly using a probability distribution function or generating a lognormal one with the pedigree matrix approach.

The final step is the uncertainty analysis. This begins with a Monte Carlo simulation to know the probability that one technology has a higher impact than the other. It is followed by a global sensitivity analysis (GSA) using the first order Sobol’ indices to rank the parameters based on their contribution to the uncertainty of the results. If satisfied with the results (either the probability or the Sobol’ indices), we can finish the study and use the results. Otherwise, additional data collection for the parameter with the highest Sobol’ index should be performed, preferably from primary sources, and we iterate the final step until we are satisfied with the results.

CHAPTER 4 ARTICLE 1: INVESTIGATING THE ROLE OF SURFACE ENGINEERING IN MITIGATING GREENHOUSE GAS EMISSIONS OF ENERGY TECHNOLOGIES: AN OUTLOOK TOWARDS 2100

Authors: Mohamad Kaddoura, Guillaume Mejeau-Bettez, Ben Amor, Christian Moreau, and Manuele Margni

Submitted on March 29, 2021 and published on March 26, 2022 in Sustainable Materials and Technologies journal, Volume 32, Issue July 2022, eLocator: e00425, DOI: 10.1016/j.susmat.2022.e00425

4.1 Article presentation

The first article, which responds to specific objective 1, estimates the prospective large-scale impacts of novel surface engineering technologies in the energy sector. Different scenarios are modeled based on the shared socio-economic pathways, the evolution of the electricity mix in each and the adoption of surface engineering technologies.

The authors of this article are: Mohamad, Guillaume Majeau-Bettez, Ben Amor, Christian Moreau and Manuele Margni. It was published in the journal Sustainable Materials and Technologies in March 2022. The content of the article was also presented at the American Center for Life Cycle Assessment (ACLCA) conference in September 2021(online) the 76th LCA Forum in November 2020 (online). Supplementary material published with the article is available in Appendix A.

4.2 Manuscript

4.2.1 Introduction

Electricity and heat production was the largest contributing sector (37%) to fossil CO_2 emissions in 2018 (Crippa et al., 2019). This sector is expected to remain pivotal for climate change mitigation, where the energy demand is expected to increase by 1.3% each year until 2040 under business-as-usual scenarios (IEA, 2019). Although the use of some technologies (e.g., carbon capture and storage and renewable energy sources) to supply the increased demand provides a good potential in reducing greenhouse gas (GHG) emissions (Haszeldine, 2009; Panwar et al., 2011), a

portfolio of different mitigation options is needed to solve the climate problem (Pacala & Socolow, 2004). Improving the technical efficiency of energy technologies is a key mitigation strategy in any portfolio (Guan et al., 2018; Kwon et al., 2017; Lanzi et al., 2011) where emission mitigation and decoupling policies should focus on improving the energy efficiency (Qiang Wang et al., 2019). This justifies the European Union target of achieving a 36% energy efficiency improvement in 2030 compared to 1990, which will contribute to reaching their goal of a 55% reduction of GHG emissions (EC, 2020). Such efficiency gains will largely depend on improved surface properties. The use of surface engineering (SE) technologies thus has the potential of improving the energy efficiency in the energy sector, but surprisingly its potential role is still not widely studied in literature.

Surface engineering "encompasses all of those techniques and processes which are utilized to induce, modify, and enhance the performance – such as wear, fatigue and corrosion resistance and biocompatibility – of surfaces" (Strafford & Subramanian, 1995). Surface engineering technologies usually result in an increase in the component lifetime (e.g., by wear protection) (Nadolny et al., 2021) or a reduced energy demand in the use phase (e.g., by friction reduction) (Leiden et al., 2020). In the energy sector, surface engineering technologies could be used to further improve the efficiency of coal power plants (Hidalgo et al., 2001), gas turbines (Clarke et al., 2012), solar panels (Alamri et al., 2020) and wind turbines (Parent & Ilinca, 2011). In other energy conversion technologies, SE is mainly used to extend the lifetime of some components. Corrosion resistance coatings for critical components in biomass and waste-to-energy facilities have been recently developed to extend plant lifetimes (Kawahara, 2016). In hydroelectric power plants, novel coating materials resist abrasive erosion and extend the lifespan of hydro turbines (Sangal et al., 2018). For nuclear power applications, the coating is usually used for the fuel storage (either new or used) to protect from corrosion. A zirconium alloy is used as fuel cladding to prevent radioactive fuel from dissipating into the coolant (D. Jin et al., 2016) and copper coatings are developed as corrosion barriers for used fuel nuclear containers (Keech et al., 2014). When assessing the benefits of different coatings, it is necessary to investigate their performance under harsh conditions. For example, the reliability of thermal barrier coatings (TBCs) in gas turbine blade during erosion (Xiao et al., 2017) and the durability of icephobic coatings during deicing cycles (Janjua et al., 2017) could mean that recoating is necessary. Although the literature in the

surface engineering domain is rich from a material-science point of view, “no holistic life cycle engineering approach can be found for the specific requirements of surface engineering” to study their environmental impacts (Leiden et al., 2020).

While SE technologies provide efficiency improvements leading to lower GHG emissions in the use phase, they also incur some emissions during the production of coating materials and the coating process. To ensure that there is no shift of burden between different life cycle phases, a holistic perspective, such as life cycle assessment (LCA), should be used (ISO, 2006). Various LCA studies examined individual SE technologies, mostly focusing on the impacts of the coating process in SE (Moign et al., 2010; S. Peng et al., 2019; Serres et al., 2010, 2011), while only few included the potential benefits in terms of reduced emissions during the use phase (Bauer et al., 2008; Wigger et al., 2017). All these studies are of retrospective nature, whereas SE technologies are evolving and prospective LCAs are thus needed to anticipate and guide future technical developments. In a prospective LCA of an emerging technology, different technology alternatives should be analyzed and scenarios should be included (Arvidsson et al., 2018). Cooper and Gutowski (2020) go further and propose including the market size of the new technology now and in the future, in addition to its diffusion and displacement rates, to extend the explorative analysis of anticipatory LCAs, which is currently missing in most studies.

To bring this large-scale, prospective dimension to LCA methodology, complementary tools are needed. Integrated Assessment Models (IAMs) provide future market sizes of energy conversion technologies based on consistent socio-economic pathways, filling this gap (Adrianto et al., 2021). IAMs are numerical models that center on studying different pathways and scenarios for human and earth systems involving technology shifts and disruptions within the context of climate change and energy optimization (Huppmann et al., 2019b). The scenarios supply “descriptions of the future industrial system, such as the electricity mix, as input data to industrial ecology models for prospective assessment of specific emissions mitigation strategies not considered in IAMs” (Pauliuk et al., 2017). IAMs are usually linked to LCA to analyze the impact of evolving electricity mix supply in the future on specific technologies, e.g., comparing internal combustion engine vehicles with electric vehicles (Beltran et al., 2018) and alternative aluminum production (Pedneault et al., 2021). LCA is also linked to IAMs to account for possible shifts of impacts between different environmental categories in the energy sector, by including additional categories

to GHG emissions (Fernández Astudillo et al., 2019; Luderer et al., 2019; Pehl et al., 2017; Vandepaer et al., 2020). The scenarios are driven by narratives describing different socio-economic pathways. The shared socio-economic pathways (SSPs) are commonly used narratives, where they are defined based on challenges for mitigation and for adaptation (O'Neill et al., 2017).

The aim of this paper is to quantify the environmental benefits and trade-offs of large-scale adoption of innovative surface engineering technologies to improve the energy conversion efficiency in the energy sector under different prospective socio-economic and policy scenarios. In other words, this article explores the share of expected energy efficiencies that hinges on the successful development and deployment of innovative SE technologies. The anticipated environmental performances are assessed in terms of potential impacts on the climate, on ecosystem quality, and on human health to identify potential burden shifting. The term "innovative" refers to traditional or new technologies that are not currently used in the energy sector, or technologies that are currently used but with new coating materials. The energy conversion technologies studied are coal power plants, gas turbines, solar panels and wind turbines. Due to the high uncertainty in the amount of lifetime extension achieved due to corrosion/erosion resistance in other energy conversion technologies, such applications are out of the scope of the study.

4.2.2 Material and methods

In this study, we develop an approach to quantify the benefits and potential trade-offs of surface engineering in three main steps (Figure 4.1). The following section proceeds by explaining each step: (4.2.2.1) identifying and documenting innovative surface engineering technologies and the efficiency gains that they enable, (4.2.2.2) developing sector-specific scenarios to scale up these gains, and (4.2.2.3) assessing the potential environmental benefits and impacts of these deployment scenarios.

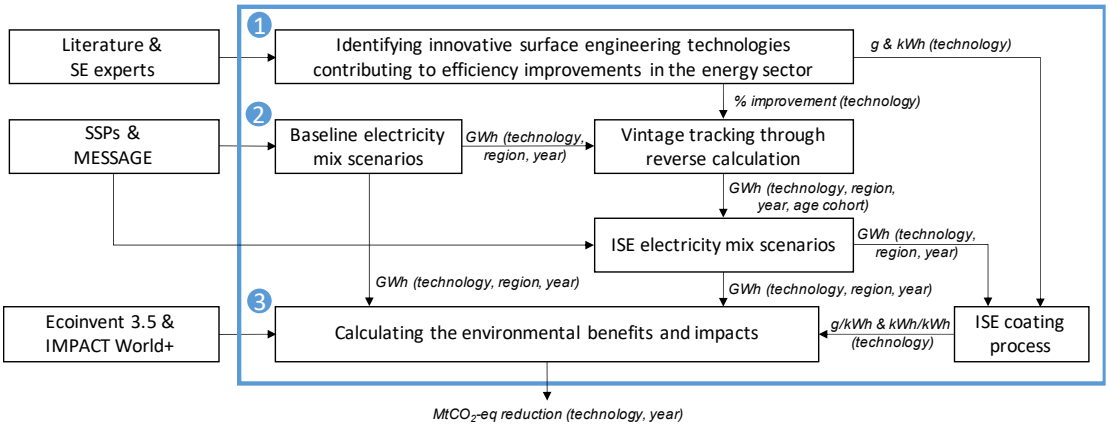

Figure 4.1 Overview of the methodology used to identify the mitigation potential of surface engineering technologies in the energy generation sector. ISE: innovative surface engineering, SSP: Shared socio-economic pathway, g: grams, kWh: kilowatt hour, GWH: gigawatt hour

4.2.2.1 Identifying innovative surface engineering technologies in the energy sector

This section gives an overview of the chosen innovative surface engineering technologies used to improve energy conversion efficiency in coal power plants, gas turbines, solar panels and wind turbines, where the current surface engineering research on energy technologies takes places.

Corrosion resistant coatings for ultra-supercritical coal power plants

Thermal power plants are described based on the conditions (pressure and temperature) where the electricity is generated. Plants operating below 538°C are termed subcritical, between 538°C and 565°C are supercritical, and above 565°C are ultra-supercritical, each with different efficiencies (Viswanathan et al., 2005). When operating at high temperatures, corrosion in the boiler is an issue and advanced materials or coatings are thus needed. In traditional coal power plants, 50/50 nickel chromium alloys are usually flame sprayed on boiler walls. Chromium oxidizes to Cr_2O_3 when alloyed with nickel, providing high temperature oxidation protection (Hidalgo et al., 2001). In ultra-supercritical conditions, higher hardness is required, thus other alloying elements should be used with nickel and chromium. Thermally sprayed NiCrBSi provides the desired properties and is currently used to protect against wear, abrasion, erosion and corrosion in various industrial applications (ibid.). Accordingly, we model NiCrBSi as the coating material to achieve efficiency improvements from ultra-supercritical power plants. We make the conservative assumption that current coal power plants are supercritical, as is typically the case in China, the country with the

highest coal power plant capacity (Q. Liu et al., 2009). Supercritical plants have an efficiency of around 37% and ultra-supercritical 45% (Prakash et al., 2020), which corresponds to an energy improvement of 22%. Therefore, in subsequent steps (Section 4.2.2.2), we will consider that a 22% improvement gain in ultra-supercritical coal power plants depends on innovative SE technology deployment. This parameter is varied between 10% and 30% to see the sensitivity of the results with respect to it.

New thermal barrier coatings for gas turbines

Thermal barrier coatings (TBCs) are ceramic coatings applied to the surfaces of metallic parts (superalloys) in the hottest part of gas turbine engines, allowing for operation at higher gas temperatures (Clarke et al., 2012). The efficiency of gas turbines can be approximated by the Carnot efficiency (Equation 1) multiplied by a Carnot factor of 0.75 (Gülen, 2013). The efficiency is thus directly proportional to the inlet gas temperature entering the turbine section (T_{high} in Equation 1), and reaching a higher temperature leads to an increase in the efficiency, assuming that we increase the pressure ratio as well (T. Wang, 2017). Traditionally, 7 wt% yttria stabilized zirconia (YSZ) is the most commonly used TBC material due to its unique properties (low thermal conductivity and high thermal expansion); however, its applications are limited to 1200°C. The search of new coating materials applicable at temperatures above 1300°C is ongoing (Vaßen et al., 2010). Coating materials with pyrochlores structure $A_2B_2O_7$ have lower thermal conductivity than YSZ and provide excellent thermal stability. In terms of thermal conductivity, $La_2Zr_2O_7$ (LZ) is the most promising replacement for YSZ; however, its low thermal expansion coefficient leads to higher thermal stress. Thus, $Gd_2Zr_2O_7$ (GZ) is more compatible in terms of thermal expansion and offers a good compromise (Vaßen et al., 2010) allowing to reach a temperature of 1400°C (Bakan et al., 2014; Mahade, Zhou, et al., 2019). To estimate the improved efficiency of gas turbines using GZ, the efficiency was calculated based on Equation 4.1 and multiplied by the Carnot factor.

$$Carnot\ efficiency = 1 - \frac{T_{low}}{T_{high}} \tag{4.1}$$

Where : T_{low}: Lowest temperature in the cycle; the inlet of the compressor (in Kelvin)

T_{high}: Turbine inlet temperature (in Kelvin)

The efficiency of combined cycle gas turbines with YSZ as a TBC is around 60% (Moreno Ruiz et al., 2018), with a T_{high} of 1473 K, and a T_{low} close to ambient temperature (287 K). When using GZ as a TBC, T_{high} increases to 1673 K, while the ambient temperature stays the same. Based on Equation 1 multiplied by the Carnot factor, the efficiency would increase from 60% to 62% (an improvement of 3.5%) when shifting to GZ as a TBC. Consequently, we will model a 3.5% improvement gain from SE technology deployment in the innovative gas turbines in the subsequent steps. This parameter is subject to temperatures achieved, and thus is varied between 1.5% and 4%, corresponding to temperatures of 1300^{o}C and 1500^{o}C, respectively to see the sensitivity of the results with respect to it.

Hydrophobic coating for solar panels (self-cleaning)

Hydrophobicity is a characteristic of the surface with superior water-repellent properties and is usually quantified by the water contact angle (CA) and the sliding angle (SA). Surfaces with a CA>90^o are termed hydrophobic and those with a CA>150^o and SA<10^o are termed superhydrophobic (Tejero-Martin et al., 2019). Using hydrophobic coatings could achieve self-cleaning properties for surfaces by removing the dirt on the surface through rolling droplets of water on it. Solar photovoltaic panels can benefit from this property to improve their efficiency. Alamri et al. (2020) found that solar panels coated with hydrophobic SiO_2 nanomaterial had an improved efficiency of 5% compared to manually cleaned uncoated ones, and 15% compared to dusty panels with no cleaning. In our study, we used the average value of 10% to model the efficiency improvement when the panels are coated, and the extremes are used in the sensitivity analysis.

Icephobic and superhydrophobic coatings for wind turbines

Icephobic coatings can be used on surfaces to repel water droplets, delay ice nucleation and reduce ice adhesion, which is beneficial in wind turbines situated in cold regions because of passive anti-icing (Huang et al., 2019). Poly(tetrafluoroethylene) (PTFE) has been identified as a candidate icephobic coating for wind turbines, providing a contact angle of 145^o and slipping angle of 45^o (Karmouch et al., 2009). The durability and practicality of applying icephobic coatings has been a limiting factor of implementing them (Janjua et al., 2017), and accordingly we will use a superhydrophobic coating in our model. Superhydrophobicity, although not necessarily linked to

icephobicity (ibid.), can be used in anti-icing applications. Polyvinylidene fluoride (PVDF) was the only superhydrophobic coating tested as a candidate anti-icing coating for wind turbines (C. Peng et al., 2012), achieving a contact angle of 156°. The absence of data linking CA and SA to the amount of electric energy that can be saved by coating forces us to test the range provided in literature. Power losses due to ice accretion on the blades of wind turbines ranges between 0.005-50% (Parent & Ilinca, 2011). In this study, we will model the improvement in generation efficiency with the average of 25% by using PVDF superhydrophobic coating in northern climates, and this parameter will be varied between 0.005% and 50% in the sensitivity analysis.

Table 4.1 summarizes the energy efficiency improvements that depend on innovative surface engineering technologies for different energy conversion technologies. Due to the uncertainty of the relative efficiency improvement values, a sensitivity analysis is also performed (Appendix A, Figure A.6) for the range provided between parentheses.

Table 4.1 Efficiency improvements from applying innovative surface engineering technologies to different energy conversion technologies. The range in the parentheses is used in the sensitivity analysis. NiCrBSi: nickel chrome boron silicium; GZ: gadolinium zirconate; SiO_2: silicon dioxide; PVDF: polyvinylidene fluoride

Energy conversion technology	**SE technology**	**Coating material**	**Relative improvement in energy conversion attributed to SE**
Coal power plants	Thermal spray	NiCrBSi	22% (10-30%)
Gas turbines	Thermal spray	GZ	3.5% (1.5-4%)
Solar panels	Sol gel	SiO_2	10% (5-10%)
Wind turbines	paint	PVDF	25% (0.005%-50%)

4.2.2.2 Energy generation scenarios

Baseline electricity mix scenarios

Having identified the efficiency improvements from SE for each technology, the next step is applying this improvement on a large scale based on scenarios of evolution of the electricity mix. Prospective energy scenarios until 2100, in terms of the total amount of energy supplied from each energy conversion technology, were obtained from the MESSAGE integrated assessment model (Huppmann et al., 2019b), which includes 43 energy conversion technologies in 11 world regions and is available in open access. It operates in ten-year time steps between 2010 and 2100.

MESSAGE was used with three baseline shared socio-economic scenarios (O'Neill et al., 2017) representing the two extreme scenarios (SSP1: "sustainability" and SSP3: "regional rivalry") with the moderate one (SSP2: "middle of the road"). In addition to the baseline scenarios, policy scenarios are also included, which contain additional constraints to reach certain radiative forcing. In this study, the representative concentration pathways (RCPs) associated with policy scenarios limiting the temperature increase to 1.5 degrees and 2 degrees were included. In the policy scenarios, technologies with carbon capture and storage (CCS) are also available.

Vintage tracking through reverse calculation

In our model, innovative SE technologies are adopted mainly by newly built power plants, thus it is important to anticipate both the replacement of decommissioned plants and the expansions in the installed capacity that are implied by the different energy scenarios. In absence of information about the age-cohort of the energy infrastructure in different SSPs over different years, we estimated these constructions with a stock-driven model, thereby estimating the in-use stock (in our case, the energy capacity satisfying a specific demand) as suggested by Pauliuk et al. (2012). Assuming that gas turbines, wind turbines and solar panels have a fixed lifetime of 30 years and coal power plants 40 years (E. G. Hertwich et al., 2015; Turconi et al., 2013), the entire age-cohort would be decommissioned after 30 and 40 years, respectively. The model was run between the years 2020 and 2100, with a step of 10 years between each time series. In the outcomes of the MESSAGE model, no data is provided about the age-cohort of the energy infrastructure at t_0-1 (the year 2010 in our case). Accordingly, a normal distribution with a mean μ = 20 years old and a standard deviation σ = 10 years was taken to allocate the total energy capacity satisfying the demand into three age groups: 10, 20 and 30 years remaining. For coal power plants, with a lifetime of 40 years, μ was set to 25 years, and an additional age group of 40 years remaining is added. In the age-cohort table, this means that the capacity needed to supply the demand at t_0-1 was installed in the years 1990, 2000, and 2010 respectively (and 1980 for the coal power plants). For the coming years, a recursive procedure is repeated to fill the age-cohort; as the plants age (decommissioned), new ones are built to satisfy the increased demand. In some cases, the added capacity could be negative when the demand sharply reduces for some energy conversion technologies, so it is set to 0 instead (i.e., no new capacity is added that year), and the negative capacity is added to the age-

cohort of the oldest technology, indicating early decommissioning of older plants. More about the vintage tracking could be found in Appendix A.

Penetration of innovative surface engineering technologies in the energy sector

After identifying the vintage of the power plants, we modelled the penetration of SE enhanced coal power plants, gas turbines, solar panels and wind turbines building on three scenarios as per Table 4.2, consistent with the narratives given by the socio-economic pathways (SSPs) (O'Neill et al., 2017). For SSP1, the technology development and transfer are *rapid*, and the shift of energy conversion technologies is "directed away from fossil fuels, towards *efficiency* and renewables." In SSP2, the technology development is *medium* and *uneven*, the technology transfer is *slow*, and the change of energy conversion technologies has "some investment in renewables but continued reliance on fossil fuels." SSP3 has *slow* technology development and transfer, and a "*slow technology change*, directed toward domestic energy sources." In SSP1, retrofitting old plants by de-coating them and applying the new coating is assumed possible. In fact, gas turbine blades can be de-coated and recoated with minimum disruptions (Le Guevel et al., 2016). Besides, geographical constraints apply to the wind turbines, where innovative SE is used in northern countries where icing on the turbines increases downtimes in winter. In OECD, the proportion of wind turbines in cold climates is proxied by Canada and Sweden, the two cold regions with the highest capacities of wind turbines (6% of the OECD supply) (GWEC, 2020). In the reforming economies (e.g., Russia, Ukraine and Kazakhstan), all countries have subzero temperatures in the winter, and thus assumed to be cold climates. Accordingly, innovative SE is applied to all the energy supply in the reforming economies (REF)and 6% of the supply in the OECD. It is also assumed that 50% of the supplied energy from wind turbines occur in the winter.

Table 4.2 Linking the three assessed surface engineering deployment scenarios with the corresponding shared socio-economic pathway (SSP)

SE scenario	**Corresponding SSP**	**Description**
Pessimistic	SSP3	Innovative surface engineering technologies are applied only to 10% of newly deployed energy technologies.
Optimistic	SSP2	Innovative surface engineering technologies are applied to 80% of newly deployed energy technologies
Optimistic + Retrofit	SSP1	Innovative surface engineering technologies are applied to 100% of newly deployed energy technologies, with the possibility of applying them directly to 50% of in-stock technologies.

4.2.2.3 Environmental impacts

Having determined the rate of adoption of each energy conversion technology and the size of their market uptake (Section 4.2.2.2), we then turn to quantify the environmental consequences of this adoption. For that, a life cycle perspective is adopted to evaluate the environmental burdens and benefits of identified SE technologies. The potential burdens arise from the coating material and surface engineering processes, whereas the benefits are realized from the improved efficiency of energy conversion technologies as identified in Table 4.1. The inventory data for different coating techniques builds on proxy studies found in literature and documented in the Appendix A (Tables A.1-A.6). The inventory data of each energy conversion technology is based on the energy outputs of different scenarios in the IAM obtained from the model described in the previous section.

The IAM provides the inventory of direct emissions associated with each energy conversion technology, but indirect emissions associated with other life cycle stages (e.g., mining and manufacturing) are not provided. Accordingly, emissions provided by the IAM are not used to quantify the environmental impacts. To include all the emissions and their related potential impacts, the impact factors for each technology ($kgCO_2$-eq/kWh) are calculated using ecoinvent 3.5 (Wernet et al., 2016) and characterized with the "climate change, short term" midpoint indicator provided by IMPACTWorld+ (Default Recommended Midpoint 1.29) (Bulle et al., 2019) and corresponding to the Global Warming Potential with 100-year time horizon. To account for a

possible shift of impacts between different environmental categories, the areas of protection "ecosystem quality" and "human health" (both excluding the "climate change" endpoint results) were also calculated based on IMPACTWorld+ (Default Recommended Damage 1.47). The characterization factors for the energy supplied by power plants with a vintage adopting innovative surface engineering were reduced proportional to the energy efficiency gains (Table 4.1). To be consistent, the same database and impact assessment methods were used to calculate the impact of the coating process.

Our model also differentiates between the five geographical regions in the SSPs by proxying them to the country in that region with the highest production volume of an energy conversion technology in ecoinvent. The mapping of different technologies in MESSAGE with their equivalent flows in ecoinvent is available in Appendix (Table A.8). Since the data for carbon capture and storage (CCS) is not available in ecoinvent, it is assumed that the climate change potential is 75% less impactful for coal power plants, 55% less impactful for gas turbines and -10 times less impactful for biomass power plants (E. G. Hertwich et al., 2015). For the ecosystem quality and human health indicators, CCS technologies have a larger impact (ibid.), and the scaling factors used are provided in Appendix A.

The python code for our model, COATS (CO_2 Abatement Tied to Surface engineering), can be found here: https://github.com/mohamadkaddoura/COATSResults.

4.2.3 Results

4.2.3.1 Future energy supply

Figure 4.2 shows the energy supplied with SE-enhanced technologies replacing the one supplied with the baseline technology for the different SSPs. Energy supplied in absolute units (EJ) is provided on the y-axis on the left and in percentage with respect to the total energy supply on the right. The reference year is 2020, where 0% of the current energy conversion technologies operate with the innovative SE technologies. Results depend on the share of each energy conversion technology in the original SSPs, the age-cohort of those technologies and the adoption rates of innovative SE technologies according to the narratives described in Table 4.1.

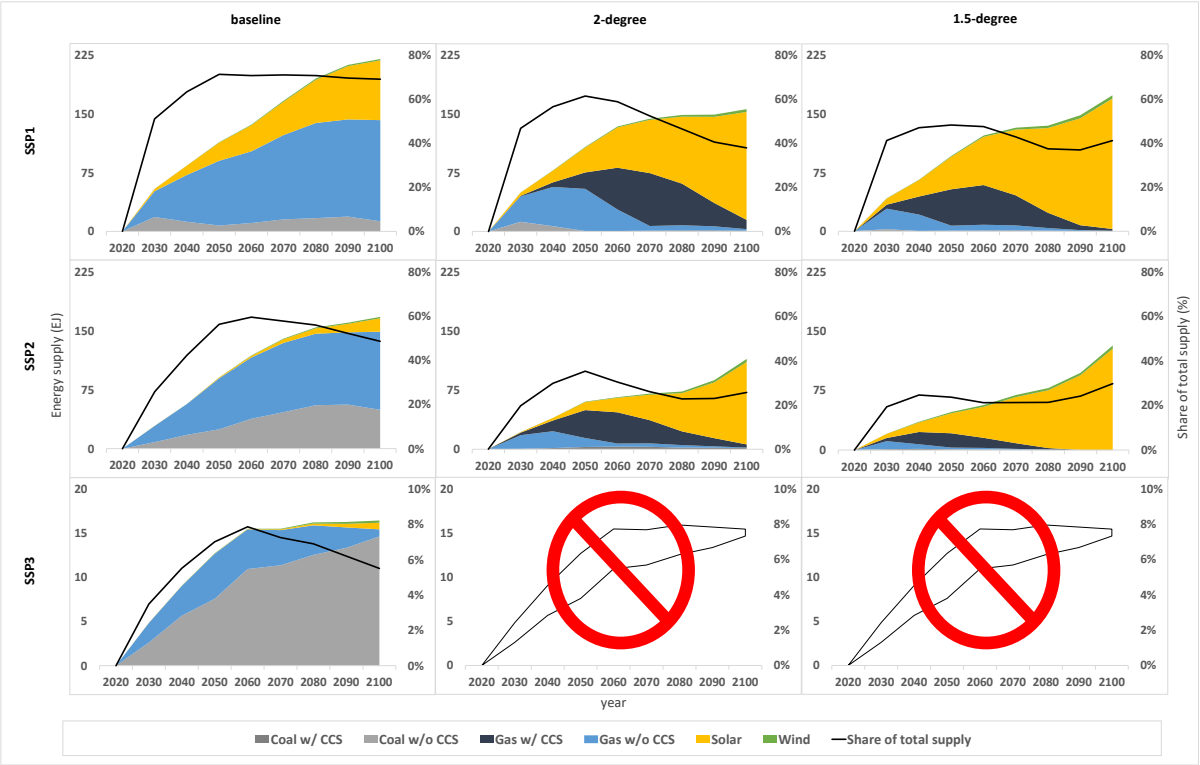

Figure 4.2 Energy supplied from innovative SE-enhanced energy conversion technologies replacing baseline ones for SSP1, SSP2, and SSP3 from 2020 to 2100 including the baseline scenario and the 1.5-degree and 2-degree policy scenarios. The left axis represents the energy supply replaced by innovative SE-enhanced energy conversion technologies (in EJ), and the right axis represents the share of the energy supplied by SE-enhanced technologies with respect to the total energy supply.

Thanks to the high adoption rates in SSP1, innovative SE would be applied to around 50% of the energy technologies in 2030 and saturating at around 70% by 2050 in the baseline scenario. Energy supplied by SE-enhanced gas turbines is the highest because most of the energy is supplied by gas turbines in the baseline SSP1, and SE is applied to 100% of the new plants. By the year 2100, energy supplied by the SE-enhanced wind turbines and solar panels represents a share that is almost half of that of gas turbines, while the share supplied by SE-enhanced coal power plants is negligible. In the policy scenarios of SSP1, more renewables are introduced, and CCS technologies become available. Solar panels become the dominant technology adopting SE, while the total share of technologies adopting innovative SE decreases to around 45% in 2100, because nuclear power

plants (around 20% in 2100) are forecasted to replace coal power plants and gas turbines, and SE is not applied to increase the efficiency of nuclear power plants in our model.

In SSP2 and SSP3 baseline scenarios, the share of energy supplied by SE-enhanced technologies steadily increases from 2020 to 2060 reaching 60% and 8%, respectively. After 2060, the year where all the energy conversion technologies in the age-cohort are "new" compared to the base year 2020, the energy supplied by newly deployed coal, gas, solar and wind plants will decrease relative to an increase of the energy supplied by other technologies where innovative SE is not applied (i.e., biomass, hydro and nuclear). Similar to SSP1, SE technologies are mostly applied to gas turbines in SSP2. However, more energy is supplied by SE-enhanced coal power plants and solar panels have a lower share. In SSP3, SE technologies are mostly applied to coal power plants, but in absolute values, the energy supplied by SE-enhanced coal power plants is lower than that in SSP1 (except for the year 2100) due to the lower adoption rates in SSP3. The policy scenarios for SSP2 follow the same trend as SSP1 (SE mainly applied to solar panels), whereas the policy scenarios can't be reached in SSP3 due to socio-economic conditions.

4.2.3.2 Environmental impacts

The climate change potential impact of each SSP scenario with and without SE is shown in Figure 4.3. The cumulative benefits (in terms of GHG mitigation) are represented by the area between the solid lines (where SE is not applied) and the dashed lines (where SE is applied) for each SSP scenario. For all the scenarios, the benefits are mainly from coal power plants, and to a lower extent, gas turbines.

In the baseline scenarios that exclude introduction of energy policies (the red, blue and light green curves), the lowest benefits are achieved in SSP3 (narrative with low adoption rates of the SE technologies). The greatest benefits are observed in SSP2, because although it has a lower adoption rate of SE than SSP1, it includes more coal power plants, where the improvements from SE are most realized. In SSP2, an annual reduction of 1.8 Gt CO2-eq is forecasted by 2050 and 3.4 Gt CO2-eq by 2100, corresponding to a 7% and 8.5% reduction of GHG emissions from the energy sector, respectively. An annual reduction of 1 Gt CO2-eq and 1.7 Gt CO2-eq is forecasted for SSP1 baseline scenario by 2050 and 2100, respectively, representing a 6% reduction of GHG emissions. Lower reductions are achieved in both SSP1 and SSP2 policy scenarios because the climate change

impacts are already lower relative to their respective baselines, and they include more renewables, which achieve less benefits from innovative SE technologies. Beyond GHG emissions, a net reduction is also achieved for ecosystem quality and human health (Figures A.3 and A.4 in Appendix A).

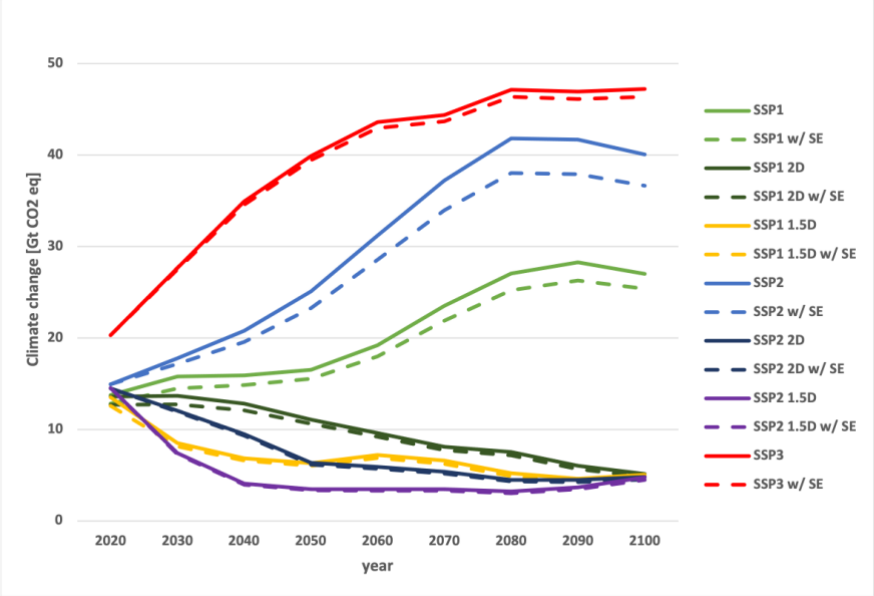

Figure 4.3 Prospective climate change potential impact from global electricity production based on different shared socio-economic pathways (SSPs) with (dashed lines) and without (solid lines) innovative surface engineering technologies. The red, blue and light green curves represent the baseline scenarios where no energy policies are introduced, and the 1.5D and 2D are policy mitigation scenarios corresponding to the 1.5 degree and 2 degree rising temperature targets in the Paris Agreement, respectively.

The climate change potential impacts from the coating process (including the production of the coating materials and other indirect upstream processes) are low compared to the benefits of the SE-enhanced energy conversion efficiency, and a net GHG reduction is always achieved (Figure 4.4). The impacts of the coating process are mainly from the production of NiCrBSi used in thermal spraying the boiler of the coal power plants. The same is true for the impacts on ecosystem quality and human health (Appendix A).

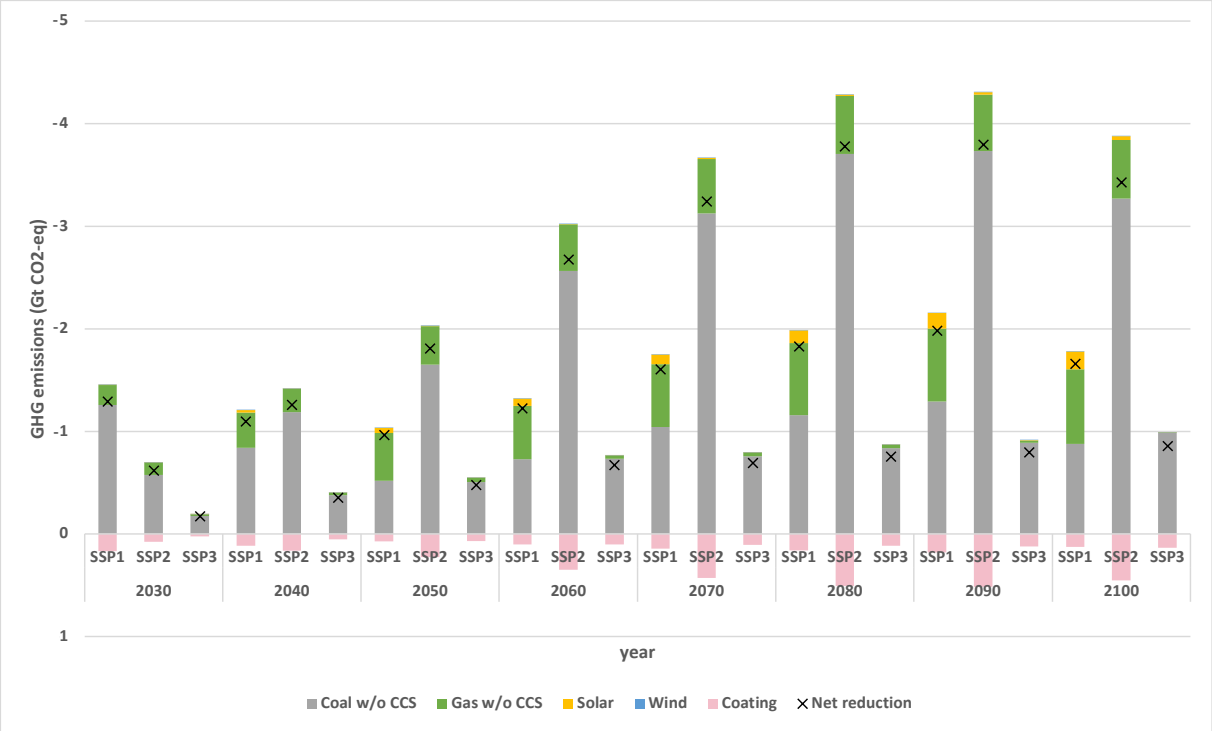

Figure 4.4 The contribution of surface engineering technologies on different energy production technologies to reducing CO2-eq emissions in different SSPs from 2030 to 2100.

The magnitude of environmental benefits is explained by three main factors: the share of energy supplied by each energy conversion technology (Figure 4.2), the efficiency improvement (Table 4.1) and the emission intensity of each technology without SE ($kgCO_2$-eq/kWh). For example, although for wind turbines the gain in energy efficiency is 25% compared to 5% in gas turbines, the emission from the former without SE is 14-25 gCO_2-eq/kWh vs. 550-1,000 gCO_2-eq/kWh for the latter. This corresponds to a reduction of 4-6 gCO_2-eq/kWh for wind turbines and 25-50 gCO_2-eq/kWh for gas turbines. This also explains the important contribution of SE in coal power plants in GHG reduction due to the scale of the initial emissions. Despite representing a low share of the overall energy supply in SSP1 and SSP2 (Figure 4.3), coal power plants gain significantly in energy efficiency (22%) when SE is applied, coupled with high emissions without SE (around 1,000gCO_2-eq/kWh).

4.2.4 Discussion and conclusions

4.2.4.1 Linking IAMs and LCA

This work illustrated how linking IAMs and LCA provides helpful insights about prospective environmental studies on large-scale adoption of novel technologies. The IAM forecasts future energy demands based on consistent socio-economic scenarios and constraints needed in prospective environmental models (Arvidsson et al., 2018; D. R. Cooper & Gutowski, 2020). LCA has been integrated to overcome two weaknesses of IAMs: (i) inclusion of the life cycle perspective of energy conversion technologies such as the infrastructure, being the key contributor to renewables and (ii) expanding the analysis of potential environmental impacts beyond the ones related to GHG emissions, such as ecosystem quality and human health. Besides, the LCA model of prospective SE processes includes the prospective life cycle inventory of the electricity supply obtained from our model.

This study contributes to a larger community effort to validate from the bottom-up (detailed engineering models) the feasibility and implications of macroscale scenarios (e.g., the ones in IAM) (Pauliuk et al., 2017). In this study, we point to the efficiency gains that hinge specifically on the progress of SE technologies, and how would they affect the global emissions provided by energy technologies in IAMs. This approach can be generalized so as to detail the physical and value-chain transformations necessary to enable the overall climate change mitigation effort and assess the likelihood of energy efficiency objectives in a reaching specific mitigation level.

4.2.4.2 Potential of SE in mitigation climate change

Surface engineering technologies have the potential of reducing GHG emissions in the energy sector by improving the energy efficiency. The reduced emissions come mainly from fossil-based technologies (coal power plants and gas turbines) because gains in energy efficiency are linked with reduction in fossil fuel consumption and thus high intensity GHG emissions. Similar or higher efficiency gains in renewable energy conversion technologies have lower influence on GHG mitigation, with such technologies having much lower GHG emission intensities compared to fossil fuels. Despite lower GHG mitigation potential for wind turbines and solar panels, the impact of the coating process remains smaller than the environmental benefits over the life cycle. Thus, such an

efficiency gain may contribute to helping these technologies reach market profitability and not require as much subsidy needed today to achieve decarbonization scenarios.

In the best-case scenario (SSP2-baseline), SE can contribute to an annual reduction of 1.8 $GtCO_2$-eq by 2050, representing a 7% reduction in the total GHG emissions from the energy sector. This falls short from the required 19 $GtCO_2$-eq annual reduction (75% reduction) required in the policy scenario to achieve the two-degree temperature increase target in the policy scenario. Still, the magnitude of the reductions achieved is comparable to the potential of other mitigation measures. CCS technologies that were in trial operation in 2009 captured and stored 3 $MtCO_2$-eq from power plants and could contribute to a 20% reduction in world emissions from energy in the future (Haszeldine, 2009). This suggests that SE technology deployment is essential to a portfolio of highly relevant mitigation options to address the climate problem.

Another benefit of SE in the energy sector, which was not included in this study, is when it is used to increase the durability of components. SE could be used to extend the lifetime of energy conversion technologies and would contribute to reduced emissions from the avoided production of primary materials in the construction phase. For coal and gas power plants, the global warming potential of constructing the plants is 0.14% and 0.25% of the total impact, respectively (Bulle et al., 2019; Wernet et al., 2016). Thus, extending the lifetime of the plants would have negligible benefits in term of GHG reduction compared to the potential gains in the operation phase. On the other hand, the impact of the infrastructure is around 100% of the total impact for solar panels and wind turbines (ibid.), and more benefits could be expected.

4.2.4.3 Limitations and future work

Despite its efficiency and simplicity in giving exploratory insights, it is important to take the approach proposed in this article with care, because it is subject to some uncertainties. The adoption rates of innovative SE technologies in energy conversion technologies for different SSPs were chosen to be compatible with the narratives of the SSPs. SSP3 is the most sensitive scenario to adoption rates, where a 4.8 $GtCO_2$-eq reduction between 2020 and 2100 could be achieved if the adoption rate increases by one percentage point (Appendix A, Table A.10). This could be improved in the future by looking into the maturity of the technologies and having a global parameter for technology developments in the SSPs. Besides, parameters used for vintage tracking through

reverse calculation (e.g., the fixed age of the power plants and the initial normal distribution of the age-cohort) adds some uncertainties in the results. Providing a detailed energy outcome from IAMs, split by age-cohorts, would make linking more reliable. The same applies for the efficiency gains estimated from literature, where the efficiency gains are qualitatively mentioned, but rarely quantified. A sensitivity analysis indicated a net benefit in terms of GHG mitigation from the SE technologies beyond 1% gains in energy efficiency (Appendix A, Figure A.5).

In addition, improving the efficiency of energy conversion technologies might steer the supply from some technologies to others as they become cheaper, which was not assessed in our study. The IAM is not optimized after implementing the efficiency gains, due to the absence of the parameters used in the modelling. It is, however, assumed that the improvement in efficiencies does not affect the price elasticities and the equilibrium of the IAM. Although for coal power plants the improvement in efficiency is significant (22%), making it competitive in terms of price; it was assumed that countries will still phase out this technology due to energy policies. The effect on the equilibrium of the model could be tested in future studies if the price parameters used for modelling the SSPs are provided.

Finally, although the model shows a GHG emissions mitigation potential of up to 8.5% by adopting innovative SE technologies in the energy sector, these benefits might be partly offset by a risk of lowering the recyclability potential for surface engineered materials. The material cycles and recycling are ignored in most IAMs (Pauliuk et al., 2017), which could be a limiting factor for adopting a new technology (D. R. Cooper & Gutowski, 2020). Despite the discussed uncertainties, linking IAM and LCA is sufficient for assessing prospective GHG mitigation scenarios in the energy sector.

CHAPTER 5 ARTICLE 2: ESTIMATING AND REDUCING DISSIPATIVE LOSSES IN THERMAL SPRAY: A PARAMETRIZED MATERIAL FLOW ANALYSIS APPROACH

Authors: Mohamad Kaddoura, Guillaume Mejeau-Bettez, Ben Amor, Dominique Poirier, and Manuele Margni

Submitted on November 21, 2023 and published on March 26, 2024 in the Journal of Cleaner Production, Volume 450, Issue 15 April 2024, eLocator: 141978, DOI: 10.1016/j.jclepro.2024.141978

5.1 Article presentation

The second article, which responds to specific objective 2, estimates the dissipative losses of thermal spray in the energy and transportation sectors in 2014. The focus of the article is to identify the life cycle stage in the coating process with the highest losses, and propose circular economy strategies specific to the sector.

The authors of this article are: Mohamad, Guillaume Majeau-Bettez, Ben Amor, Dominique Poirier and Manuele Margni. It was published in the Journal of Cleaner Production in March 2024. The content of the article was also presented at the International Conference on Resource Sustainability (icRS) in August 2023 (Guildford, UK) and the 11th International Conference on Industrial Ecology (ISIE) in July 2023. Supplementary material published with the article is available in Appendix B.

5.2 Manuscript

5.2.1 Introduction

Thermal spray, a family of surface engineering technologies, is used to improve the properties of surfaces and the characteristics of components to allow them to function in their desired environments (Vardelle et al., 2016). Those technologies have been vital in aircraft engine applications and gas turbines since the 1960s (Tucker Jr., 2013). While thermal spray increases the lifetime or energy efficiency of components, reducing their environmental impacts (Kaddoura et al., 2022), it is not without its drawbacks. One major drawback is the dissipative losses occurring throughout the life cycle of the component (Zimmermann, 2017). Dissipative losses are “losses of

material into the environment, other material flows, or permanent waste storage that result in concentrations in the receiving medium such that a recovery of these materials is technically or economically unfeasible" (Zimmermann & Gößling-Reisemann, 2013). In thermal spray applications, the majority of those dissipative losses occur at the coating stage (Zimmermann, 2017), where part of the sprayed powders do not adhere to the substrate (Nassar, 2017). The powder is collected and typically sent to waste management, where most of it is thought to end in landfills (Zimmermann, 2017).

Material flow analysis (MFA) has been the main tool used to track the flow of materials and the losses in different life cycle stages (Cullen & Cooper, 2022). Most of the MFA studies focused on materials that have large extraction rates, e.g., aluminum, copper, and iron (ibid), and have already been implemented on a global scale. However, metals used in small quantities for specialized applications are those of greatest concern due to their criticality (Graedel et al., 2015). The concept of metal criticality comes from the real or anticipated supply and demand imbalance. Graedel et al. (2015) characterized criticality according to three dimensions: supply risk, environmental implications and vulnerability to supply restrictions. Despite the importance of studying critical metals, MFAs for critical materials are still mainly performed for specific countries (e.g., China) with well-documented applications (Hu et al., 2022; Zheng et al., 2022), ignoring smaller applications and the global scale.

Studies assessing the dissipative losses of materials used in surface engineering are scarce, and when found rely on assumptions based on a limited set of literature and undisclosed communications with companies, and with a limited spatial coverage (Zimmermann, 2017). Due to the criticality of some of the coating materials, it is important to study their fate to guide the efforts in reducing the losses, taking into account the feasibility of these reduction measures. Knowing the criticality of metals can help decision makers in their strategy and research planning (Y. Jin et al., 2016). To our knowledge, only one MFA study was performed for yttria-stabilized zirconia (YSZ) used as a thermal barrier coating, with a limited spatial coverage of Germany (Zimmermann, 2017). Other studies added surface engineering as an application rather than the focus of the study. Nassar (2017) included physical vapor deposition (PVD), a surface engineering technology, as an application of tantalum when assessing its stocks and flows. The losses during spraying were assumed to be new scrap that is recovered and recycled, which might not be realistic

and would underestimate the real dissipative losses. Leal-Ayala et al. (2015) included wear applications for tungsten in general, without specifying the end products in which they are used, or whether they are used as coatings or not. While the mentioned MFA studies are helpful in quantifying the stocks of the material, they fall short in their applicability to specific contexts different from their original, limiting the scope of study. A parametrized model that captures the nature of the technology is thus needed to add flexibility in the models, which could then be readily adapted and iteratively expanded with more information.

In recent years, more calls for making sustainability science a cumulative effort are being heard (Pauliuk, 2020), with data transparency being key in achieving that goal (E. Hertwich et al., 2018; Pauliuk et al., 2015). In the context of critical material demand, Nguyen et al. (2018) called for efforts to build multi-tiered consumptions databases for trade networks of critical materials. With flexible parametrized models, and shared open databases, results could easily be updated to reflect the advancement in research. In thermal spray applications, knowing the amount of critical materials in components (e.g., Zr in combustion chambers and blades of gas turbine engines) and in the product (e.g., Zr in land-based gas turbines) is important to keep track of the material flows. With a transparent database, more robust circularity strategies could be recommended in the thermal spray field.

The applicability and benefits of circular economy have been well documented for large sectors (e.g., the manufacturing industry (Lieder & Rashid, 2016) and the automotive sector (Prochatzki et al., 2023)). A wide range of material efficiency strategies have been identified (Allwood & Cullen, 2012) and could theoretically be applicable to surface engineering applications. The strategies include using less metal by design, reducing yield losses, diverting manufacturing scrap, re-using old components, extending the lives of products, and reducing final demand. Secondary benefits of implementing circular economy strategies to mitigate the supply issues of critical materials includes reduced energy consumption, waste, pollution, and costs (Gaustad et al., 2018). In the thermal spray field, efforts are mainly focused on reducing yield losses by increasing deposition efficiency (Baik & Kim, 2008; Cai et al., 2015; Waldbillig & Kesler, 2011; Yang et al., 2022). Some studies also focused on recycling waste powders during spraying (Sarjas et al., 2012), where the achieved characteristics were comparable to new powders. Open loop-recycling is another feasible alternative, when specific desired characteristics of the coating material is of less

interest (e.g., using waste YSZ powders from thermal spray in ceramic tiles (Siligardi et al., 2017)). The applicability of different circularity strategies for thermal spray applications have thus been investigated in isolation, but a global assessment of all options on which to base strategic planning for the field is still missing.

The aim of this paper is to build a roadmap for the surface engineering community to transition to a circular economy. This is done through a parametrized model to quantify the dissipative losses of the main metals used in thermal spray (Cr, Co, Mg, Mo, Ni, W, Y and Zr) along the life cycle of coated components. The first objective is complemented with a second one aiming to evaluate the mitigation potential of several material efficiency strategies to reduce dissipative losses of these materials. The third objective will then assess potential co-benefits and trade-offs between material circularity and environmental efficiency.

5.2.2 Methods and data

To answer the research question, we developed the model called Dissipative Losses in Thermal Spray (DLiTS) using python to estimate dissipative losses using a set of parameters. The code is available on Github (https://github.com/mohamadkaddoura/DLiTS), and the input data is available in Appendix B. Figure 5.1 shows the general framework used in the model. The model starts by calculating the inventory of each coating material (section 5.2.2.1) based on the applications. The mass balance (section 5.2.2.2) is then achieved based the determinants of the dissipative losses. This is followed by scaling up the MFA to the estimated thermal spray global demand in 2014 (section 5.2.2.3), applying the material efficiency measures (section 5.2.3), and calculating the resulting environmental impacts (section 5.2.4). Details about each step are explained in the coming subsections.

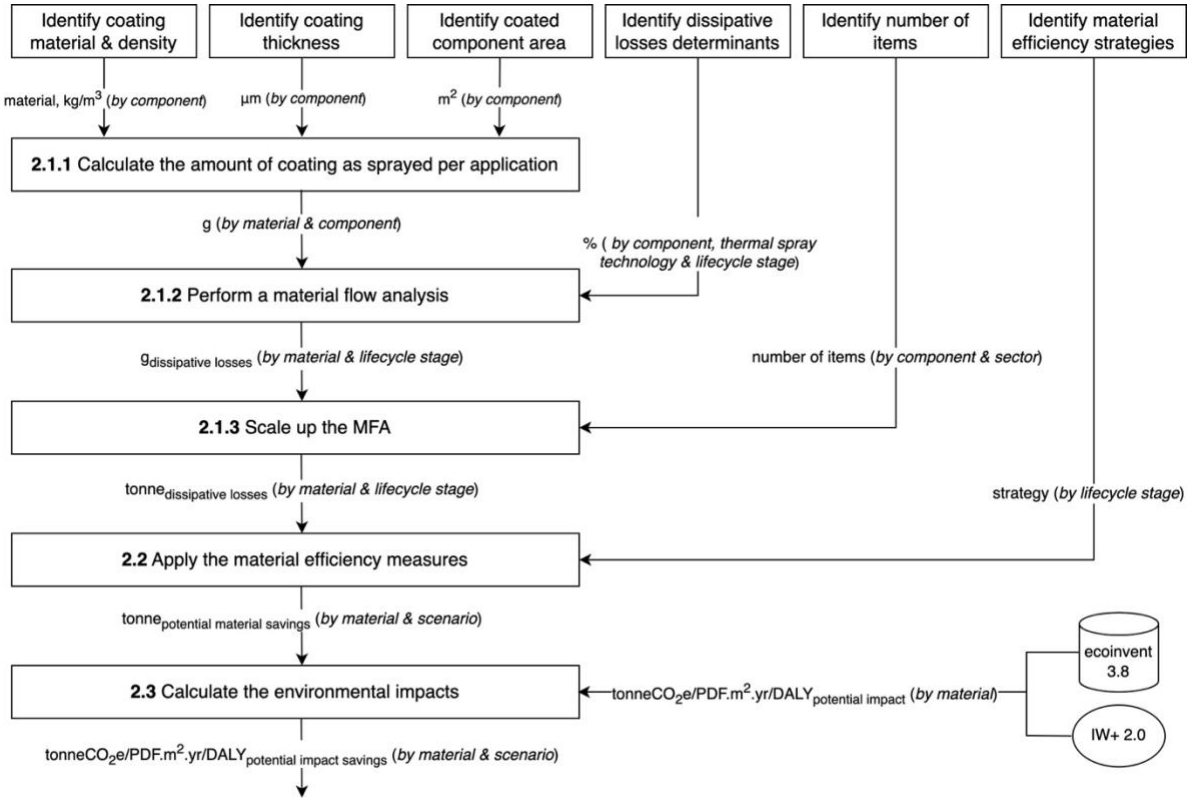

Figure 5.1 Overview of the methodology used to quantify the dissipative losses, investigate material efficiency measures, and calculate the environmental impacts. Pdf: potentially disappeared fraction; DALY: disability-adjusted life year; IW+: impact world plus.

5.2.2.1 Quantifying dissipative losses

Material flows and the corresponding dissipative losses were modelled using data from different sources, while ensuring the mass balance at each stage. The flows cover the ore extraction, material production, powder production, thermal spraying, end use applications, maintenance, and end-of-life. For the modelling, the end use applications were first quantified, and based on different parameters, dissipative losses were quantified for the upstream and downstream. The results were visually presented in the form of a Sankey diagram.

5.2.2.1.1 Thermal spray applications

Material flows and losses in thermal spray applications are seldom documented due to the small fraction of material used for coating compared to the substrate material, so comprehensive data

collection was challenging. The first step was to identify and gather data for the various thermal spray applications mainly from Tucker Jr. (2013), and complement the findings with estimates from interviews/surveys with thermal spray experts. The applications included in this study were in the energy sector (gas turbine, biomass boiler and hydropower blades) and the transportation sector (piton, piston rings, aircraft engine, and aircraft landing gear). Application in electrical and electronics, biomedical, infrastructures and other industries were excluded due to the limited literature on them, and their lower coating content compared to the energy and transportation sectors. The provided information about the applications usually contained the material used (Mo, YSZ, NiCrSi and WCCoCr), thermal spray technology (flame spray, atmospheric plasma spray and high velocity oxy-fuel), and the coating thickness. Table 5.1 summarizes the applications targeted in this study.

Table 5.1 Thermal spray applications studied with their material, technology, and thickness. APS: atmospheric plasma spray; FS: flame spray; HVOF: high-velocity oxy-fuel

Application	**Coating material**	**Thermal spray technology**	**Coating thickness (μm)**	**Coating mass (g/application)**
Gas turbine	YSZ	APS	950	1090
Biomass boiler	NiCrSi	HVOF	650	3253
Hydropower blade	WCCoCr	HVOF	300	377
Piston	NiCrSi	HVOF	400	34
Piston ring	Mo	FS	100	2.4
Aircraft engine	YSZ	APS	150	12656
Aircraft landing gear	WCCoCr	HVOF	75	2526

The final step was to calculate the amount of coating needed for each application (in g/vehicle, g/aircraft and g/MW). Data from literature and technical reports were used to get that information.

When the data was missing, we estimated the coated area and multiplied it by the thickness and density. For thermal barrier coating, the amount was found directly in literature (Zimmermann, 2017). Information about sources and calculations is in Table B.1 in Appendix B.

5.2.2.1.2 Dissipation losses and MFA

In our work, we follow the definition of Zimmermann and Gößling-Reisemann (2013) for dissipative losses. Dissipative losses were estimated mainly based on expert's judgements who helped identify the losses and complemented by literature. The dissipative losses were linked to identified key parameters, namely: mining efficiency (E_m), powder production efficiency (E_p), theoretical deposition efficiency ($E_{d,th}$), target deposition efficiency ($E_{d,ta}$), post-processing efficiency ($E_{d,pp}$), corrosion ratio (R_c), friction ratio (R_f), thermal fatigue ratio (R_{tf}), wear ratio (R_w), coating recycling rate (RR_c), maintenance recycling rate (RR_m), and EOL recycling rate (RR_{eol}). The definition of those parameters and the sources used for their values are detailed in Table B.2 in Appendix B. All parameters affecting the coating stage were modeled with probability distribution functions to account for their uncertainties. Most of the uncertainties were modelled with a uniform distribution as it was the easiest to provide by the experts, but when data was not available, pedigree matrices v 2.0 (Ciroth et al., 2016) were used as proxies. The pedigree matrix is used in LCA to transform qualitative data quality information to quantitative uncertainty distributions (lognormal distributions). This data was propagated through the model with 1,000 Monte Carlo simulations, and the variation of the overall dissipative losses were quantified. The data about uncertainties is available in SI2. For applications with maintenance during their lifetime, maintenance interval (I_m), component lifetime (LT_c), and product lifetime (LT_p) were used to know how much of the dissipative losses is happening at which time. This was helpful to estimate the amount of coating material removed during maintenance, which might potentially be collected and recycled. Based on these parameters, it was possible to determine the dissipative losses (L) through different lifecycle stages (indices: coat, use, recoat, main, eol) based on the following equations:

$$L_{coat} = \left(\frac{1}{\prod_{i=m,p,dth,dta,dpp} E_i} - 1\right) \times (1 - RR_c) \quad (5.1)$$

$$L_{use} = \left(\prod_{i=c,f,tf,w} R_i\right) \times \frac{LT_p}{I_m} \quad (5.2)$$

$$L_{recoat} = L_{coat} \times \left(\frac{LT_p}{I_m} - 1\right) \quad (5.3)$$

$$L_{main} = \left(1 - \prod_{i=c,f,tf,w} R_i\right) \times (1 - RR_m) \times \left(\frac{LT_p}{I_m} - \frac{LT_p}{LT_c}\right) \quad (5.4)$$

$$L_{eol} = \left(1 - \prod_{i=c,f,tf,w} R_i\right) \times (1 - RR_{eol}) \times \frac{LT_p}{LT_c} \quad (5.5)$$

5.2.2.1.3 Large scale

To analyze the large-scale volume of the dissipative losses, product scaling factor (S_p) and economy scaling factor (S_e) were used, and the total dissipative losses could be expressed as:

$$L_{total} = (L_{coat} + L_{use} + L_{recoat} + L_{main} + L_{eol}) \times S_p \times S_e \quad (5.6)$$

S_p was collected from different technical reports and peer reviewed articles (section 5.2.2.1.1). S_e data was more coherent since it was sourced from the same model; IEA ETP model (IEA, 2017). The ETP model includes data about the energy generation and the distance covered by different modes of transport for 2014, with some perspective scenarios (Tables B.3, B.4, and B.5 in Appendix B). Since the calculated material use (S_p) for different applications was mass per unit (vehicle, aircraft and TW), few more data was needed to convert them to the units used in the IEA ETP model (TWh, passenger kilometers, and tonne kilometers). The needed parameters and calculations are provided in Tables B.6, B.7, and B.8 in Appendix B. Our study focused on the flow of coating material entering the stock in 2014, while the ETP provides the total stock (including previous age-cohorts). To calculate the initial stock, we followed a similar approach to Pedneault et al. (2022), where we used the survival function of each cohort using the Weibel distribution with an average lifetime (gamma) depending on the application and shape parameter

(beta) as 6 (Held et al., 2021). This is then scaled up to the 2014 stock from the ETP, and finally reversed and adjusted with our timeline.

5.2.2.2 Evaluating the potential of material efficiency strategies in reducing material dissipative losses

Three material efficiency strategies were identified as relevant for thermal spray applications based on the life cycle stages where losses occur and the applicability of the strategies to surface engineering. The first strategy focuses on the reduction of the material losses during the coating stage by design. This could be achieved by optimizing the coating process and improving the deposition efficiency. The second strategy is extending the lifetime of coating on components, which would increase the material efficiency during the use phase by increasing the intervals between maintenance events. This could also be achieved by improving the coating parameters and structure (e.g., porosity, density, …). A third strategy aims to recycle the powder (either that used during spraying and collected in the form of dust or the stripping of components during maintenance and at the end-of-life). Those strategies were structured in different scenarios (Table 5.2). The likelihood of each scenario is provided as low or high by the author, based on indications from the provided sources.

Table 5.2 Description of the different material efficiency scenarios. BAU: business as usual; ME: material efficiency; EOL: end-of-life; acronyms of parameters are provided in Section 5.2.2.1.1

Scenario name	**Parameters**	**BAU**	**ME**	**Description**	**Likelihood [justification]**
S0 BAU	-	-	-	-Current coating practices and EOL recycling	-

Table 5.2 Description of the different material efficiency scenarios. BAU: business as usual; ME: material efficiency; EOL: end-of-life; acronyms of parameters are provided in Section 5.2.2.1.1 (cont'd).

S1 Dust recycling	RR_c	0%	90%	-Send collected dust during spraying to recycling (Sarjas et al., 2012)	Low [dust is collected, but recycling rate of the metals is low (Graedel et al., 2011) and the dust is highly contaminated and deformed (Eybel, 2023; Poirier, 2022; Tang, 2022)]
S2 Optimized coating process	$E_{d,th}$ (general)	40%	60%	-Optimized coating process parameters (Waldbillig & Kesler, 2011)	High [surface engineering research focuses on improved processes (Waldbillig & Kesler, 2011)]
	$E_{d,th}$ (gas turbine)	50%	60%		
	$E_{d,ta}$ (small component)	60%	73%	-Optimized nozzle diameter to stay more on the target (Baik & Kim, 2008) -Better tool path planning (Cai et al., 2015; Yang et al., 2022)	
	$E_{d,ta}$ (medium component)	80%	87%		
	$E_{d,ta}$ (large component)	100%	100%		

Table 5.2 Description of the different material efficiency scenarios. BAU: business as usual; ME: material efficiency; EOL: end-of-life; acronyms of parameters are provided in Section 5.2.2.1.1 (cont'd).

	$E_{d,pp}$	75%	90%	-In-situ monitoring of thickness buildup with feedback loop to adjust tool path and add material only where needed (Sampath et al., 2009; Zhou et al., 2022)	
S3 Extended durability	I_m	X years	2X years	-Extend the lifetime of coating with better characteristics (Luo et al., 2022)	High [commercial novel coatings claim to double the lifetime (Castolin Eutectic, 2015; Oerlikon, 2014)]
S4 Improved recycling - maintenance	RR_m	0%	80%	-Strip components at the maintenance and send it to recycling (Yousefzadeh, 2021)	Low [similar to S1, while the coating is stripped during maintenance (Nagy, 2023) the materials have low recycling rates and they have impurities]

Table 5.2 Description of the different material efficiency scenarios. BAU: business as usual; ME: material efficiency; EOL: end-of-life; acronyms of parameters are provided in Section 5.2.2.1.1 (cont'd and end).

S5 Improved recycling – EOL	RR_{eol}	0%	50%	-Strip components at the EOL and send it to recycling (Yousefzadeh, 2021)	Low [collection at EOL to strip is hard, similar to S1 (low recycling rate of coating materials, impurities)]
S6 Best case	All the above	-	-	-A combination of S1, S2, S3, S4 and S5	Low

5.2.2.3 Environmental impact

This section describes how to quantify the environmental impacts associated with the dissipative losses of each scenario (Section 5.2.2.1 and 5.2.2.2). A life cycle perspective is adopted to evaluate the environmental burdens of mining the materials that are finally dissipated. The impact score for each material (impact/kg_{mined}) are calculated using ecoinvent 3.8 (Wernet et al., 2016) and characterized with a comprehensive set of impact indicators from the IMPACTWorld+ v2.0 methods (Bulle et al., 2019) to account for a possible shift of impact between different environmental categories. The selected impact profile includes "climate change" (based on IPCC GWP100 factors), "ecosystem quality," and "human health" indicators. The latter two represent the aggregate impact scores of environmental issues contributing to the respective areas of protection. Table B.12 in Appendix B shows the ecoinvent processes used for different materials.

5.2.3 Results

The dissipative losses during the coating process are presented as a probability distribution function per 1 kg coated component for one use cycle in Figure 5.2. Pistons and piston rings have the highest

dissipative losses during coating (up to 8 kg lost per 1 kg adhered) because of their small size, where spraying outside the target is more frequent. The results do not include the maintenance stage, as they aim to assess the coating process of each component, and not the life cycle of the process itself. If maintenance was included, gas turbine would have more losses over the whole life cycle of the plant (Figure B.1 in Appendix B).

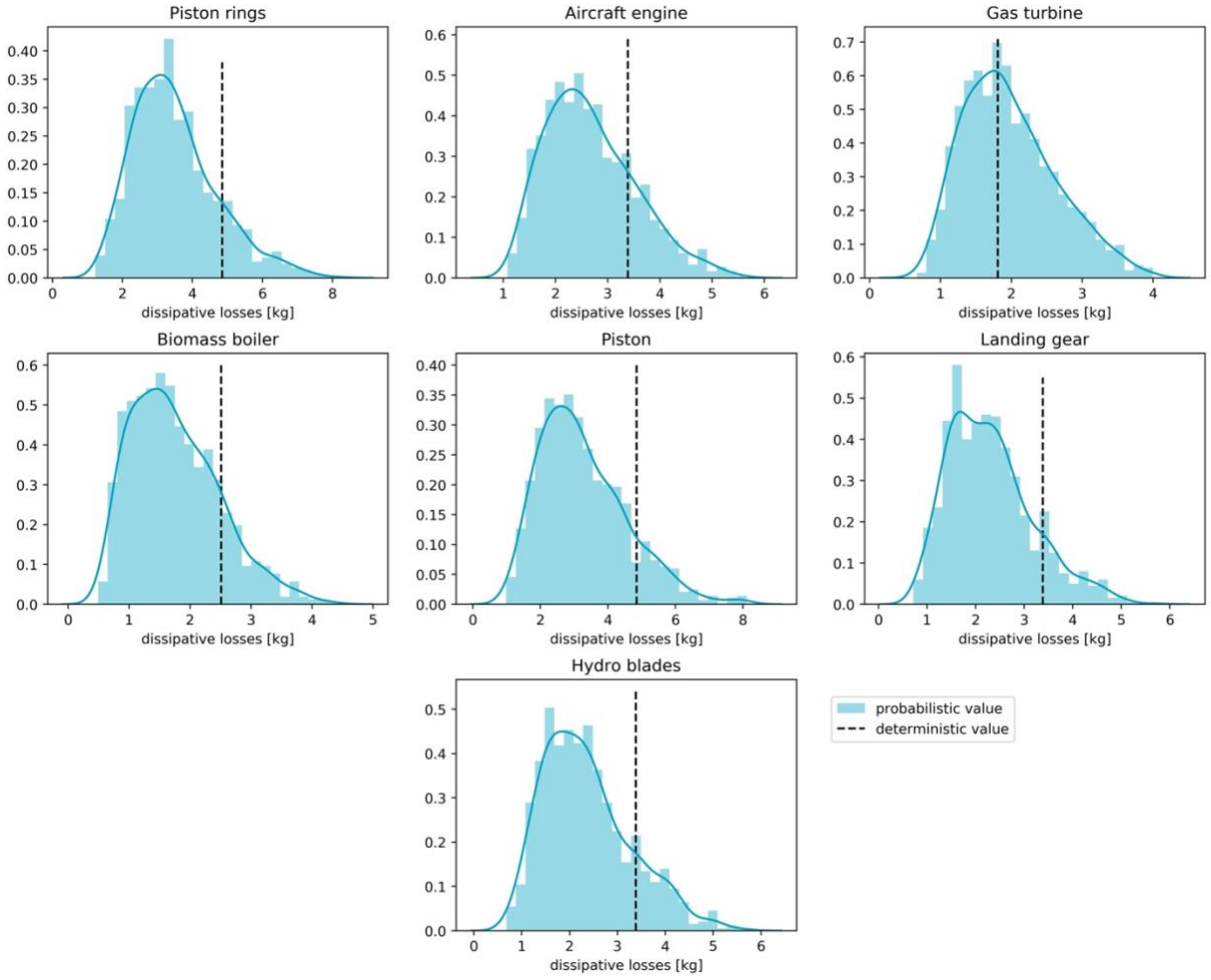

Figure 5.2 Probability distribution functions for the dissipative losses during the coating process per 1 kg coated for different applications

Scaling up the results, and including all the life cycle stages, Figure 5.3 shows the Sankey diagram of the material flows for thermal spray applications with 2014 data. This includes seven applications (pistons, piston rings, landing gears. Biomass boilers, hydropower plant blades, gas turbines, and aircraft engines), three thermal spray technologies (HVOF, APS, and FS) and four

coating powders (NiCrSi, YSZ, Mo, WCCoCr). Vehicle pistons require the highest amount of coating powder in their in-use stocks (3.26 ktonne of NiCrSi). Although the amount of coating adhering to pistons is small compared to other applications (34 g per piston), the large number of new vehicles entering the stock in 2014 justifies this high figure. This also makes HVOF the thermal spray technology with the largest share of powder use (19 ktonne of NiCrSi). The coating stage is responsible with the highest share of dissipative losses; around 15.5 ktonne of NiCrSi is lost at this stage in the form of powder dust. The remaining losses of NiCrSi occur at the EOL of pistons (3.3 ktonnes) and re-coating of biomass boilers (2.3 ktonnes).

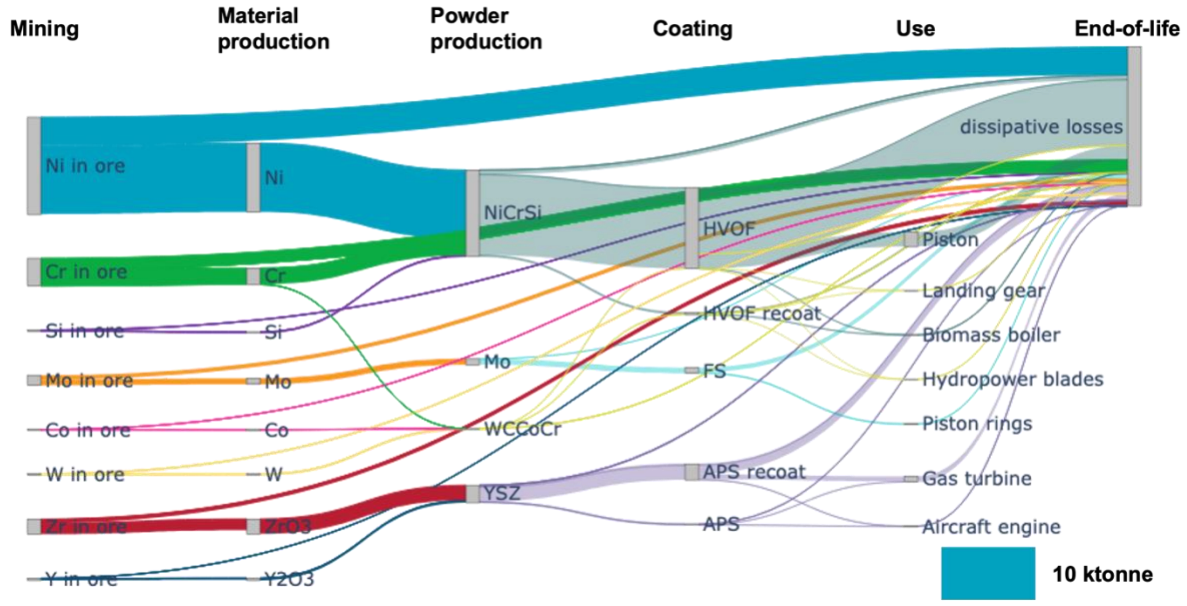

Figure 5.3 Sankey diagram showing the dissipative losses for different materials at different life cycle stages. HVOF: high-velocity oxy-fuel, APS: atmospheric plasma spray, FS: flame spray

Gas turbines are the second most demanding applications of coating materials (1.27 ktonne), where most of it comes from re-coating at the maintenance stage (1.21 ktonne). This is justified by the short maintenance interval for gas turbine (recoated every year). As a result, most of the YSZ dissipative losses happen in the recoating process (2.2 ktonne). A detailed dynamic representation for when in time do the dissipative losses occur for applications with maintenance is provided in Figure B.2 in Appendix B.

The dissipative losses during mining, material production and powder production are also shown in the Sankey diagram. Although of less interest to the objectives of this study, they offer an interesting comparison with the losses over the entire life cycle stages.

Figure 5.4 shows the benefits from different material efficiency scenarios for thermal spray applications (for demand scale as in 2014) in terms of dissipative losses and the associated environmental impacts. S2 (optimized coating process) is the scenario with the least dissipative losses because we focus on the coating phase (including re-coating) were most of the losses happen. A potential of 14.3 ktonnes reduction of Ni dissipative losses could be achieved, and total dissipative losses are reduced by 51%. Another scenario that focuses on the coating stage is S1 (powder recycling), were a reduction of around 46% is possible. This, however, is a scenario that is less likely to be implemented, as the recycling of powder is not mature yet. Scenarios focusing on improving the recycling after use (maintenance and EOL) have lower reduction potential, as most of the losses do not occur at this stage. The same applies to extending the lifetime of the coating, were this will only affect applications which undergo maintenance during their lifetime. When all the scenarios are combined, there is a potential of 78% decrease, but this is the least likely scenario. Contributions of each material to each application per scenario is available in Figure B.3 in Appendix B and of each application to each material in Figure B.4.

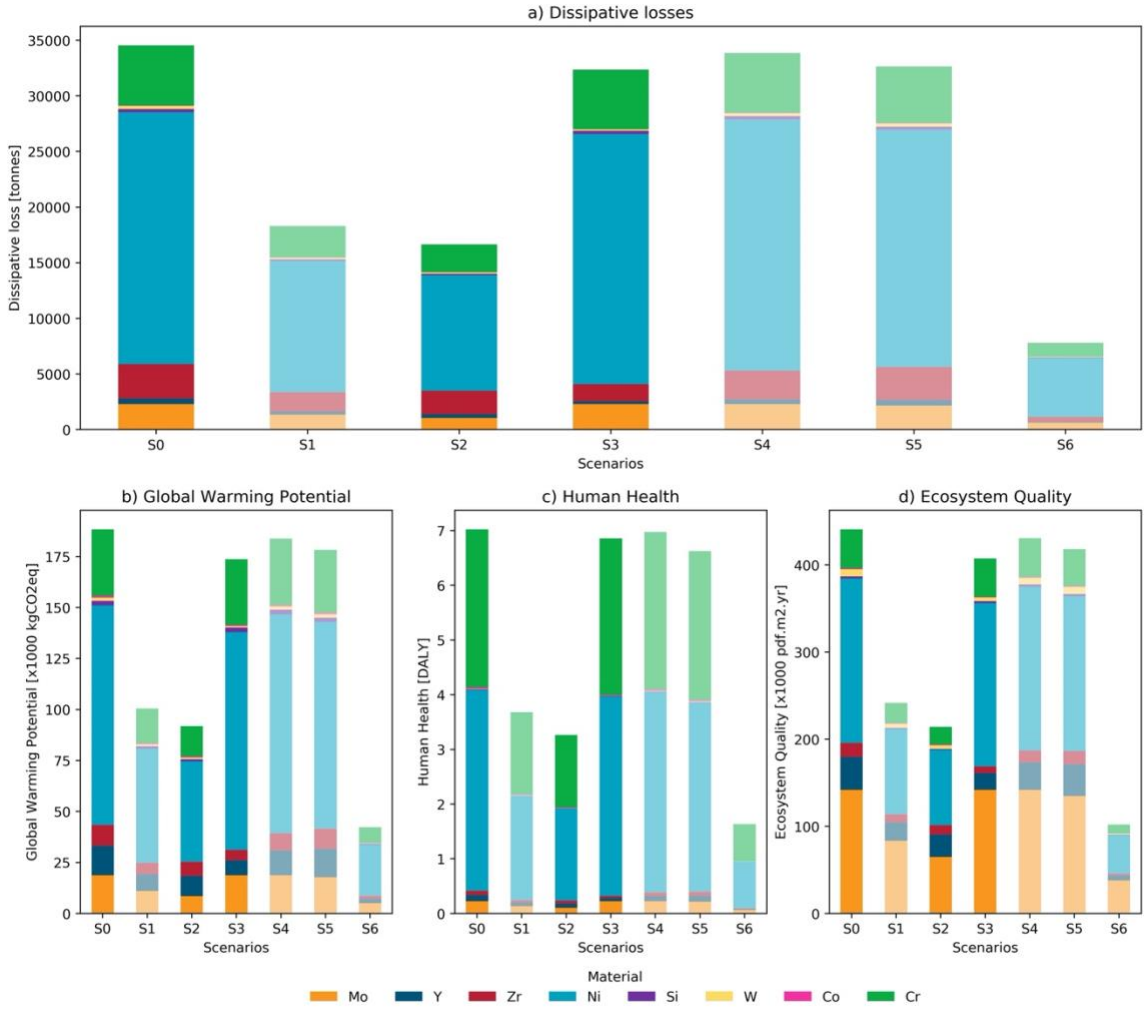

Figure 5.4 a) Dissipative losses of different material efficiency scenarios and the associated environmental impacts on b) global warming potential c) human health and d) ecosystem quality. Solid colors indicate a higher likeliness of a scenario based on Table 5.2. DALY: disability-adjusted life year, PDF.m^2.yr: potentially disappeared fraction of species over given area (m^2) during a given time (yr). The scenarios are for thermal spray applications in 2014 and described in Table 5.2.

Looking at the environmental impacts, the global warming potential (Figure 5.4, b) largely follows the trends in the dissipative losses. For human health (Figure 5.4, b), impacts from nickel remain the highest (because of their high dissipation), but chromium becomes almost as impactful, although it has a lower amount. In ecosystem quality (Figure 5.4, c), while the impacts from nickel are also the highest, molybdenum becomes problematic. There results suggest that a shift of burden might happen, and specific materials should have a priority when looking at material efficiency strategies.

5.2.4 Discussion

5.2.4.1 Key findings and validation

The dissipative losses of coatings on components are low in comparison to other engineering processes (around 40 ktonnes compared to 6.2 Mtonnes in the fabrication and manufacturing of aluminum products for example (Helbig et al., 2020)). However, the amount of material used per kg of coating is significant, which is consistent with Helbig et al. (2020). As this is the first attempt to quantify the dissipative losses along the major thermal spray applications, comparison with other studies is limited. To validate the results, the proportion of the losses in each life cycle stage could be compared with other individual applications, or the total amount of material used could be compared with MFAs of that material. For gas turbines, 58% of the losses occur during the coating process (including maintenance), a bit higher than the 43% reported by Zimmermann (2017). This is justified by including additional losses in our study (losses affected by target-efficiency and post-processing efficiency). This is also within the same range of other studies on surface engineering applications (18 to 81% losses of tantalum in PVD (Nassar, 2017)). Regarding the use of materials, in our study we found that 360 tonnes of tungsten is used for wear protection coating, compared to 8.3 ktonnes of tungsten used in wear applications in general (Leal-Ayala et al., 2015). The difference in the numbers could be due to that some wear applications like cutting tools might use tungsten as the base material, or other surface engineering methods (e.g., weld overlay) are used. This comparison was not possible with other materials, as available MFAs do not explicitly include coatings in the applications, and more granularity is needed in that regards.

5.2.4.2 Eco-design considerations

The results of the study are important in guiding the circularity of the surface engineering sector. A combination of different material strategies should be considered to reduce the dissipative losses in the thermal spray industry. The priority should be given based on the life cycle stages where the losses are the highest (i.e., the coating process). From an environmental perspective, specific materials should be prioritized (e.g., chromium for human health and molybdenum for ecosystem quality). While some fragmented efforts were conducted in terms of recycling coating powders (Sarjas et al., 2012; Siligardi et al., 2017), a more comprehensive strategy is still needed. Another consideration to think about is the feasibility of implementing the strategies. For recycling, it easier to collect the powder or dust during coating, and to a less extent the stripped powder during maintenance. At the EOL, this could not be feasible when there is no control on collecting the used components. The sector where the strategies are to be implemented could also add a barrier to implementation. For example, it is difficult in the aerospace industry to alter the coating parameters or use secondary materials, where it is highly standardized for safety issues (Eybel, 2023; Nagy, 2023).

5.2.4.3 Limitations, future outlooks, and applicability of the study

This study provides surface engineering researchers with an overview of the dissipative losses of their materials and guides them to improve their material efficiency. For surface engineering applications, data is scarce for all the life cycle stages, and expert judgements carrying some uncertainties were needed to fill the gaps. Including uncertainty analysis provided an understanding of how the lack of accurate data affects the results. For the future, we identified a need for improved data collection when it comes to different parameters affecting the coating process, and in particular the real deposition efficiency. With the provided parametrized model, results could be easily adapted when new data becomes available. Besides, assessing the dissipative losses of the coating material without considering the linkage to the substrate material cycle is a limitation of this study, because some coating materials could stay as impurities after recycling substrate materials. This could be assessed by identifying the substrate materials and checking which coating materials could be problematic. Another limitation is the inventory data in the end uses, where coating materials are usually omitted when providing the inventory of products. The estimations made from different

literature and technical reports were sufficient to give a good order of magnitude. In the future, a prospective study could be implemented, where future demand and prospective applications (e.g., cold spray for repair and additive manufacturing) could be included. In addition, including the environmental impacts of mining new materials could be added, where impacts are expected to increase with the increased exploitation of resources. This work can serve as the foundation for the elaboration of a sector-wide roadmap, as it provides an initial estimation of the stocks and dissipative losses, and a parametrized model that is ready to be adjusted. More efforts are needed in the data collection from different stakeholders involved in surface engineering, and a transparent database to support the collective work. A more robust and precise quantification of the dissipative losses allows for better circularity recommendations and decision-making support.

5.2.5 Conclusion

The dissipative losses in thermal spray applications are determined by different parameters, including deposition efficiency and various recycling rates. In this study, a methodology to quantify dissipative losses in surface engineering was provided, with a parametrized model that can be improved upon by the community as a way to collaboratively consolidate knowledge on opportunities to improve the sector's circular performance. Surface engineering was found to be highly dissipative as a ratio of the coated amount, but less apparent at a large-scale level. The coating process incurs the highest losses, where some of the deposited powder does not adhere to the substrate. The low recycling rates of specialized coating materials further contribute to the losses. Different material efficiency strategies could reduce these losses, where the optimal option is to improve the coating parameters and focus on recycling the powder/dust from coating process. More work is need in the field to collect more accurate data about the deposition efficiencies.

CHAPTER 6 ARTICLE 3: GLOBAL SENSITIVITY ANALYSIS REDUCES DATA COLLECTION EFFORTS IN LCA: A COMPARISON BETWEEN TWO ADDITIVE MANUFACTURING TECHNOLOGIES

Authors: Mohamad Kaddoura, Guillaume Mejeau-Bettez, Ben Amor, and Manuele Margni

Submitted on September 5, 2024 to the Journal of Cleaner Production.

6.1 Article presentation

The third article, which responds to specific objective 3, proposes a framework to prioritize data collection efforts when performing an LCA. The framework is based on global sensitivity analysis, a tool that has been used more recently by LCA researchers to identify parameters contributing to the highest variability of the impacts. We focus on the strength of the tool in identifying the parameters while systematically improving the data quality in the most cost-efficient way.

The authors of this article are: Mohamad, Guillaume Majeau-Bettez, Ben Amor and Manuele Margni. It was submitted to the Journal of Cleaner Production in September 2024. Supplementary material associated with the article is available in Appendix C.

6.2 Manuscript

6.2.1 Introduction

Assessing the environmental impacts of products and services is becoming important for manufacturers, users and governments (Fernandez-Feijoo et al., 2014). Life cycle assessment (LCA) is a well-established method to quantify the environmental impacts of products and services in a holistic way (ISO, 2006), and is widely used by researchers and practitioners in the area of sustainability assessment (Göran Finnveden et al., 2009). LCA is best suited for systems where sufficient information is available, as data collection is time intensive, especially in the inventory analysis phase (Laca et al., 2011; Zargar et al., 2022). The tool has an inherent problem with data availability due to several reasons. A typical product system includes thousands of processes that need to be described, and the high cost of primary data collection constrains the gathering of all

the information (Reinhard et al., 2016). Some data is also not easily measurable or proprietary to manufacturers, and sharing this information could damage the competitive advantage of a company (Kuczenski et al., 2017). Regionalization is another aspect when collecting data, where the inventory for one process (e.g., electricity) is different according to the region (Mutel & Hellweg, 2009), and might require some proxies.

In an effort to overcome the data availability problem in LCA, and reduce time and cost associated with it, simplified versions of LCA were developed (Gradin & Björklund, 2021). Screening and streamlined LCAs are the most common simplification approaches used. Screening LCAs are qualitative or semi-quantitative LCAs mainly used at an early development stage (Hochschorner & Finnveden, 2003) and were used for different applications (e.g., electric vehicles (Ellingsen et al., 2016)). While the aim of those studies is to take a full life cycle approach, the impacts are not necessarily quantified, and hotspots are highlighted instead. Streamlined LCAs are quantitative yet simplified studies (Hung et al., 2020) and were used to assess the impacts of vehicles (Arena et al., 2013). Those methods do not use the full potential of LCA by eliminating some processes and impact categories and relying on lower data quality. They are helpful in early-stage prognosis studies, but the simplifications included increases the risk of displacements and misguiding in the results. When a complete environmental profile is needed, those methods are not fit for purpose, and other ways to collect data in an efficient way are needed.

The main strategies used to model missing data in LCA can be classified into data-driven (e.g., artificial neural network), mechanistic (e.g., process simulation) and future inventory data (e.g., learning curves) approaches (Zargar et al., 2022). For data-driven methods, a limiting factor is the high domain knowledge requirement, particularly for those using machine learning models (ibid.). Another limitation is that missing data are estimated (e.g., estimating unit process data using similarity-based approach (Hou et al., 2018)), requiring having a training set of datasets, and for new technologies where it is not possible to have a proxy, it is not applicable. Mechanistic models are mainly applicable to chemical and biological processes, and the data uncertainty must be assessed separately (Zargar et al., 2022). Future inventory data modelling is performed in prospective LCA studies (e.g., by patent analysis (Spreafico et al., 2023)), but usually adds more variability and uncertainty to the results (Spreafico, 2024). Gathering costly primary data will remain essential in LCAs, as simplifications and estimates may not suffice. Given budget

limitations, it is crucial to follow approaches that are easily used by LCA practitioners and applicable across all product systems to prioritize data collection.

Reinhard et al. (2019) applied a contribution-based method to prioritise data collection in LCI databases. The principle is also applicable to products, where the inputs are ranked based on their contribution to the impact score, and the approach is commonly used by LCA practitioners. However, contribution analysis can be limited by its reliance on existing data, which might be wrong or of low quality, and results could possibly overlook potential hotspots. Another approach is based on the expected benefits (in terms of reduced uncertainty) per cost of getting the data by combining the value of information (VOI) with LCA (Marchese et al., 2018) which was applied to assess the impacts of electronic tablets. This approach, while accounting for the issue of data quality and uncertainty, demands information on the VOI, which themselves could be uncertain and costly. To overcome these challenges, uncertainty analysis offers a more comprehensive solution by accounting for the low quality of data through wider uncertainty ranges, and is less data intensive than the VOI approach, where no information on the cost of data is needed. Using the uncertainty of data to identify key issues for further investigation and reliability improvement has been suggested since the early days of LCA (Heijungs, 1996), but not widely adopted. This could be due to the perception of statistical approaches as complex by LCA experts, or the computational power needed at the time.

The main use of uncertainty analysis in LCA has been to assess the reliability of the results (Larsson Ivanov et al., 2019; Von Pfingsten et al., 2017; Zhai et al., 2021) and give more comprehensive information to decision-makers (Cao et al., 2019; Mendoza Beltran, Prado, et al., 2018; Romero-Gámez et al., 2017). To take a more active approach and reduce the uncertainty by increasing the quality of data, a global sensitivity analysis (GSA) could be used, which has been adopted by LCA practitioners and is increasingly being used (e.g., implemented in Activity Browser (Stefano Cucurachi et al., 2021) and available in easy-to-use codes (Puy et al., 2022)). GSA is used after stochastic methods (e.g., Monte Carlo analysis) to propagate the uncertainty and estimate how much each input contributes to the model's output variance. GSA has been used in both the life cycle inventory (Groen et al., 2017b; Jaxa-Rozen et al., 2021; Khang et al., 2017; Lacirignola et al., 2017; Zhao et al., 2021) and the life cycle impact assessment (S. Cucurachi et al., 2016) stages of the LCA. The goal of performing the GSA in those studies was to assess the robustness of the

study, contribute to decision-making, and provide simplified calculation models based on highest contributing parameters (Lacirignola et al., 2017). Patouillard et al. (2019) proposed a methodology to help LCA practitioners prioritize data collection for regionalization in life cycle impact assessment (LCIA) based on GSA, and applied it to biofuel production and land passenger transport. They highlighted the importance of setting the acceptable level of uncertainty and defining the uncertainty of the inputs. In the context of life cycle inventory (LCI), there is a lack of clear documentation of using GSA to prioritize data collection with consistent terminology and clear directions, despite it being suggested in literature. This would allow for easier implementation and better communication of the results, and the validity of the approach could be assessed.

The aim of this study is to propose a framework based on GSA to prioritize data collection efforts in LCA and reach conclusive results at a given confidence level while efficiently minimizing the work efforts. A case study comparing two additive manufacturing technologies is also provided to operationalize and test the framework.

6.2.2 Methods and data

6.2.2.1 Framework

In our framework, we propose not to start with complete and almost “blind” data collection phase as in a traditional LCA, but with a screening data collection, followed by uncertainty analysis to identify where to prioritize the data collection efforts (Figure 6.1). Chronometers are added at the steps where the time would change compared to a traditional LCA. Green shapes and arrows refer to revised steps based on the learnings of the study and are mentioned in the discussion later. The following subsections describe the details of each step in our framework.

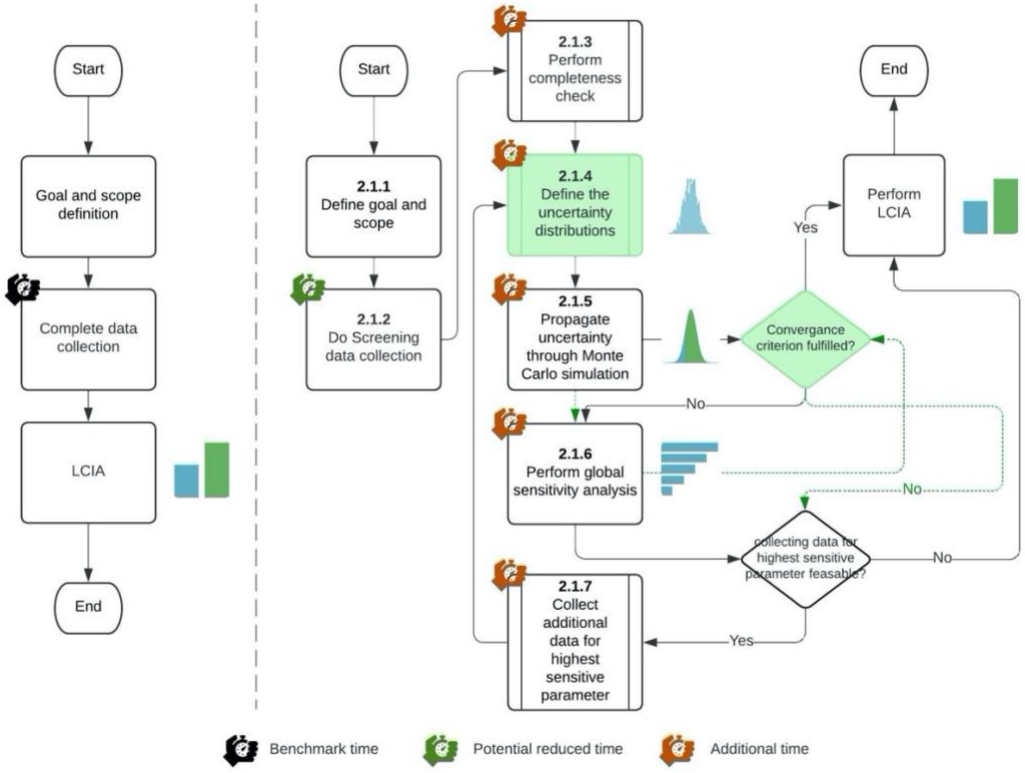

Figure 6.1 Overview of the proposed framework (right) compared to a traditional LCA (left). Green shapes refer to steps that are revised and dashed green arrows are steps with altered order in the revised methodology.

6.2.2.1.1 Goal and scope definition

We define the goal and scope of the study as specified by ISO 14044 for a traditional LCA (ISO, 2006). In a comparative study between two product systems (A and B) where this framework is applicable, the acceptable level of discrimination between them needs to be defined in this step, which we refer to as the convergence criterion. The latter is initially defined as the percentage of times the impact scores of A is lower than that of B during a defined set of Monte Carlo simulations. This can be seen as the confidence level that product A has lower environmental performance than product B given the uncertainties in the inventory data. The convergence criterion is based on the level of risk decision makers are comfortable with and the allocated resources to conduct the LCA.

6.2.2.1.2 Screening data collection

In this step, we identify the input processes and parameters defining the studied products and collect available data with minimum effort and without detailed and costly exploration. We follow the definition of Gradin and Björklund (2021) where screening "is applied in the inventory analysis steps, usually covering the entire life cycle with lower data quality." This could also be referred to as "desk-based" data collection strategy, where existing data source (e.g., product declarations) are used and roughly adapted (e.g., by extrapolation) when needed (Hischier et al., 2014).

6.2.2.1.3 Completeness check

Our framework builds on including as much inventory flows of the system as possible at the beginning, even if their quality is low. As there might be some truncation in the screening data collection, some methods could be used to fill those gaps. This could be done using input-output tables, information from LCAs of similar products (i.e., proxies) and applying the law of mass conservation (Huijbregts et al., 2001). When a study is done in the context of an industry, it is easier to have a sense check with experts in the field to ensure that most of the flows are included.

6.2.2.1.4 Defining the uncertainty distribution

A probability distribution function is applied to define the variability of all identified input parameters. As this is meant to be an initial screening modelling, in absence of specific information we suggest using a uniform distribution, which only requires a lower and upper bound value. This information is usually readily available in literature or could be estimated by experts. When no information is available, we recommend applying conservative lower and upper bounds. We recommend setting the lower bound to half the value and the upper bound to its double as suggested by Finnveden and Lindfors (1998) and Hedbrant and Sörme (2001). Other simplified sensitivity ranges (e.g., ±10%) might fail to highlight highly inaccurate input parameters with only modest influence (Huijbregts et al., 2001), leading us to propose the half/double approach. Such default values, however, should respect other limits of mass and energy conservation (e.g., not exceeding 100% if dealing with percentages). Uncertainty distributions should also be defined for the background data, which is usually already provided in the database. In ecoinvent for example, lognormal distribution is used to estimate the uncertainties from qualitative assessments using a

pedigree matrix (Ciroth et al., 2016). In our framework, we propose adding an additional uncertainty related to the discrepancy between the usually generic background dataset used (e.g., from ecoinvent) and the specific process used in the model. For example, the chromium steel dataset from ecoinvent comes with its own uncertainty irrespective of its use in a given LCA, and if this dataset is used as a rough proxy to represent a different specific steel alloy needed in the foreground of in an LCA, this discrepancy further introduces uncertainty. We refer to this additional uncertainty as the *applicability uncertainty* and propose using pedigree matrices to quantify it as a starting point.

6.2.2.1.5 Uncertainty propagation through Monte Carlo simulation

A random sample of each input parameter is first generated (based on the defined mean, lower bound, and upper bound) and simultaneously propagated through the LCA model. We used 1,000 Monte Carlo iterations for the case study below, but the number of iterations could be increased to obtain a representative frequency chart of the out variables. At each iteration, a value of the distribution of the parameter is chosen and used in the formula to get the distribution of the impact. Note that the same sampling of each parameter/process is used in calculating the LCA of A and the LCA of B and not independent sampling. For example, if steel is used in both A and B, the same impact of steel is allocated for A and B at each iteration. When all the iterations are done, we compare alternative A with B using a pairwise method, where the impact of each alternative is compared to the other for each Monte Carlo iteration. We represent this using equation (6.1):

$$\%\ (GWP_A > GWP_B) = \frac{\#_{i=1}^{N}\left(GWP_{i,A} - GWP_{i,B} > 0\right)}{N} \times 100 \qquad (6.1)$$

Where # is a counting function and N is the number of iterations (1,000 in our case). If the convergence criterion is achieved, the results of the LCA fulfill the objective of the LCA with no need to further iterate. Otherwise, more data collection will be required, and we move to the next step (Section 6.2.2.1.6).

6.2.2.1.6 Global Sensitivity analysis

Further data collection specifically targets the parameter that contributes the most to the variability of the impact score. We suggest using the first order Sobol' indices (Sobol, 2001) that calculate

quantitative indices allowing to rank the influence of each input parameter on the LCA results. We only consider the first order Sobol' index in this study assuming that the parameters are independent, but higher order Sobol' indices should be calculated when input parameters are correlated (Kevin Sinisterra-Solís et al., 2024; Wei et al., 2015). The GWP impact (or other impact categories) could be expressed as a function of different parameters as GWP = $f(p_1,p_2,\ldots,p_n)$. For a parameter p_i, the first order Sobol' index (SI_i) is calculated based on equation (6.2):

$$SI_i = \frac{V\left[E[GWP|p_i]\right]}{V[GWP]} \tag{6.2}$$

Where V is the variance and E is the expected value, both calculated based on the Monte Carlo results. More information on how the first order Sobol' index was calculated is available in Appendix C.

6.2.2.1.7 Additional data collection

Data collection will focus on the input parameter identified as the most contributor to the variability based on the GSA. But first, we should check if we have access to the data or if it is feasible to collect it within the allocated resources (e.g., from a budget and time constraints). If it is not feasible to collect higher quality data for the parameter / process with the highest SI, the parameter / process has to be flagged, and we move on to the parameter with the next highest SI. Otherwise, more accurate data need to be collected by e.g., lab experiments (Hischier et al., 2014), running process simulations (e.g., using ASPEN PLUS) (Ferdous et al., 2024), experts' interviews, or further literature review. This is referred to as the "lab-based" data collection strategy (Hischier et al., 2014). Using the updated data, we go back to step 2.1.4.

6.2.2.2 Case study of emerging surface engineering technology

To demonstrate the applicability of the suggested framework, a case study was carried out on two additive manufacturing technologies.

6.2.2.2.1 Goal and scope definition

The aim of the study is to compare the environmental impacts of cold spray additive manufacturing (CSAM) and wire arc additive manufacturing (WAAM) at a 95% confidence level. As no specific

additively manufactured product is assessed, this study is a cradle to gate study, where the use and end-of-life phases are excluded. The transportation is also excluded for simplicity. The functional unit is mass-based and defined as “manufacturing 1 kg of an additively manufactured ring steel component in Quebec, Canada in 2022”. The system boundaries associated with the functional unit is described in section 6.2.2.2.4. The modelling is done using a code written in Python and available on Github (https://github.com/mohamadkaddoura/GSAPDaC), with input data provided in Appendix C. The background data is based on the ecoinvent 3.8 database (Wernet et al., 2016) characterized by the IPCC 2013 global warming potential 100 years (GWP100a) characterization factors (IPCC, 2014). Other impact categories could be assessed by the framework, but only global warming potential is used here to demonstrate the applicability of the framework.

6.2.2.2.2 Screening data collection

The initial data was sourced from literature, where parameters relevant to each technology were determined. For WAAM, the inputs to the system are the welding wire (steel), shielding gas (argon), and electricity (in QC). The inputs for CSAM are feedstock powder (steel), carrier gas (nitrogen) and electricity (in QC). As the processes for powder production (atomization and annealing) are not available in ecoinvent, their parameters were included as well (Table 6.1).

Table 6.1 The parameters used to model CSAM and WAAM

Parameter	**Name**	**Amount**	**Unit**	**Source**
Wire arc				
Wire feed	wire_fr	1.5	kg/hr	(Bekker & Verlinden, 2018; Shah et al., 2023)
Shield gas flow rate	shi_gas_fr	15	L/min	(G.P. et al., 2017)
Wire arc power	power_wa	1.146	kW	(G.P. et al., 2017)
Casting losses	cast_loss	10	%	(Bekker & Verlinden, 2018)
Rolling losses	roll_loss	5	%	(Bekker & Verlinden, 2018)
Wire drawing losses	draw_loss	8	%	(Bekker & Verlinden, 2018)
Cold spray				
Powder feed rate	powder_fr	9	kg/hr	(Vuoristo, 2014)
Carrier gas flow rate	car_gas_fr	1.675	m^3/min	(Vuoristo, 2014)
Cold spray power	power_cs	32	kW	(Vuoristo, 2014)
Atomization electricity	elec_atom	0.75	kWh/kg	(Lavery et al., 2013)
Atomization gas	arg_atom	0.333	Kg/kg	(Lavery et al., 2013)
Atomization losses	atom_loss	5	%	(Lavery et al., 2013)
Annealing heat	heat_anneal	0.143	MJ/kg	(L et al., 2020)
Annealing losses	anneal_loss	0	%	(L et al., 2020)

6.2.2.2.3 Completeness check

Completeness check was done by discussing with domain experts in the industry, mainly from Polycontrols, a CSAM company in Canada. They confirmed that we included the main parameters, but also identified two missing parameters: the deposition efficiency and the post-processing losses. Both could have significant impacts on the results by affecting the electricity and gas supply, and the amount of feedstock needed that would be highly underestimated if we neglect those parameters. In fact, most of the losses of the material in thermal spray applications occur during the deposition phase due to low deposition efficiencies (Kaddoura et al., 2024). The values for those parameters were estimated with the help of experts and shown in Table 6.2.

Table 6.2 Additional parameters needed in the model

Parameter	**Name**	**Amount**	**Unit**
Wire arc			
Deposition efficiency	dep_eff_wa	85	%
Cold spray			
Deposition efficiency	dep_eff_cs	90	%
General			
Post-processing losses	post_proc_loss	10	%

Based on the collected parameters, the intermediary parameters (AM duration) and the processes (amount of material, gas, and electricity) are calculated according to the formulas given in Table 6.3. A parametrized model adds flexibility to the LCA (e.g., can change one parameter affecting a process rather than the amount of the process) and makes the data collection more precise and targeted. It would also allow to pinpoint exactly which parameter is contributing to the uncertainty.

Table 6.3 Formulas to calculate the amount of processes needed based on the defined parameters, where density_ar = 1.63 g/L, density_n = 3.1293 kg/m3 and coating_amount = 1 kg (based on the functional unit)

Parameter / process	**Name**	**Formula**	**Unit**
WAAM duration	duration_wa	$\frac{coating\_amount}{wire\_fr}$	hrs
CSAM duration	duration_cs	$\frac{coating\_amount}{powder\_fr}$	hrs
Wire	wire	$\frac{coating\_amount}{(1-cast\_loss)\times(1-roll\_loss)\times(1-draw\_loss)\times dep\_eff\_wa\times(1-post\_proc\_loss)}$	kg
Powder	powder	$\frac{coating\_amount}{(1-atom\_loss)\times(1-anneal\_loss)\times dep\_eff\_cs\times(1-post\_proc\_loss)}$	kg
Electricity for WA	elec_wa	$power\_wa \times duration\_wa$	kWh
Electricity for CS	elec_cs	$power\_cs \times duration\_cs$	kWh
Argon	arg_wa	$\frac{shi\_gas\_fr \times duration\_wa \times 60 \times density\_ar}{1000}$	kg
Nitrogen	nit_cs	$car\_gas\_fr \times duration\_cs \times 60 \times density\_n$	kg

6.2.2.2.4 Defining the uncertainty distribution

The identified parameters (Tables 6.1 and 6.2) were modelled with uniform pdfs as only the minimum and maximum values were found in literature (Table 6.4). For the shield gas flow rate, weld arc power, and post processing losses, no ranges were found, and the minimum and maximum were estimated as half and double the values to be as broad as possible. The deposition efficiencies' ranges were missing as well, but as identified by experts, both additive manufacturing technologies

are highly efficient, and the range was defined accordingly. Throughout the paper, results relating to those parameter uncertainties will be colored blue. The uncertainty of the background processes was obtained directly from the ecoinvent database as based on the lognormal distribution generated by the pedigree matrix of the corresponding input processes. Those are colored orange in the following section. The applicability uncertainty distribution was modelled based on the pedigree matrix approach (Table C.1 in Appendix C) and are colored green in the paper. The resulting pdfs are available in Appendix C (Figure C.2 and Figure C.3).

Table 6.4 The minimum and maximum of the uniform distribution for different parameters

Parameter	**min**	**max**	**Source**
wire_fr	1	2	(Bekker & Verlinden, 2018; Shah et al., 2023)
shi_gas_fr	7.5	30	estimated
power_wa	0.57	2.3	estimated
powder_fr	4.5	13.5	(Vuoristo, 2014)
car_gas_fr	0.85	2.5	(Vuoristo, 2014)
power_cs	17	47	(Vuoristo, 2014)
dep_eff_wa	0.8	1	estimated
dep_eff_cs	0.8	1	estimated
post_proc_loss	0.05	0.2	estimated

Figure 6.2 illustrates how different uncertainty distributions are applied across the different life cycle stages of CSAM. The orange boxes are the uncertainties based on the background data (pedigree matrix in ecoinvet). The green boxes represent the applicability uncertainty, which act as a scaling factor, and its distribution is based on our defined pedigree scores. Blue boxes are the foreground data, where the parameters affecting the input are shown, and are modeled using a

uniform distribution as described earlier. The flow diagram for WAAM is available in Appendix C (Figure C.1).

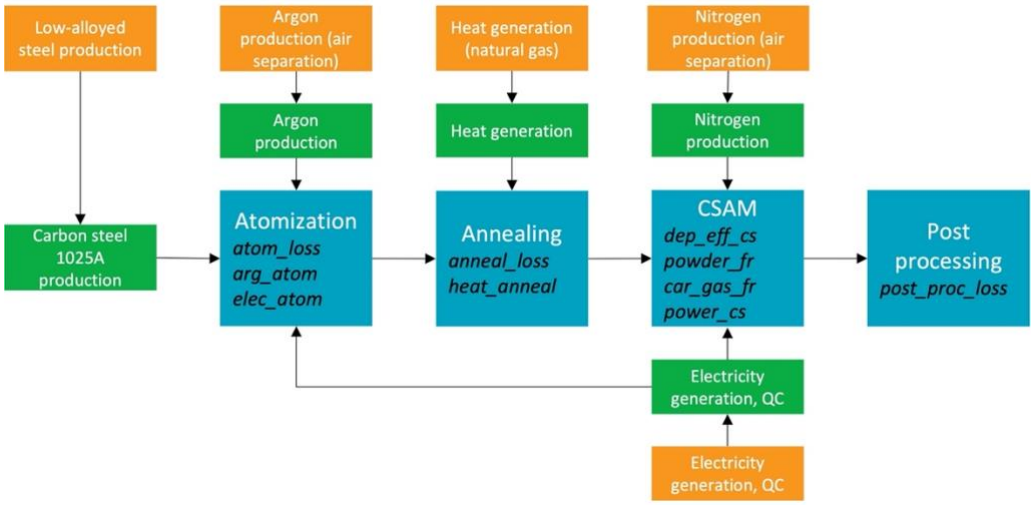

Figure 6.2 Flow chart showing where different uncertainties originate from. Blue boxes represent foreground data, green boxes applicability and orange boxes background data. CSAM: Cold Spray Additive Manufacturing, QC: Quebec.

6.2.3 Results

The results of the case study are presented hereby applying step by step the developed framework.

6.2.3.1 First iteration

Deterministic comparative LCA results showed that WAAM has a higher impact score (Global Warming Potential, GWP) than CSAM (2.44 and 1.71 kg CO_2-eq/f.u., respectively). More information about the deterministic results is available in Figure C.5 in Appendix C, as the focus of this study is on the probabilistic ones. Figure 6.3 (a) plots 1000 Monte Carlo iterations for the difference between the impact of WAAM and CSAM (GWP_{WAAM}-GWP_{CSAM}). Stochastic results showed a likelihood that GWP_{WAAM} was higher than GWP_{CSAM} in 93.6% of the runs (where the difference is positive). Since it is less than the convergence criterion defined in the goal and scope (95%), more data was needed to be collected to refine the results. To understand where the variability comes from, a GSA based on the first order Sobol' indices was performed (Figure 6.3, b) for the parameters (blue), background technology flows (green), and applicability of the

background technology flows (orange). The powder feed rate for the CSAM had the highest Sobol' index (0.18).

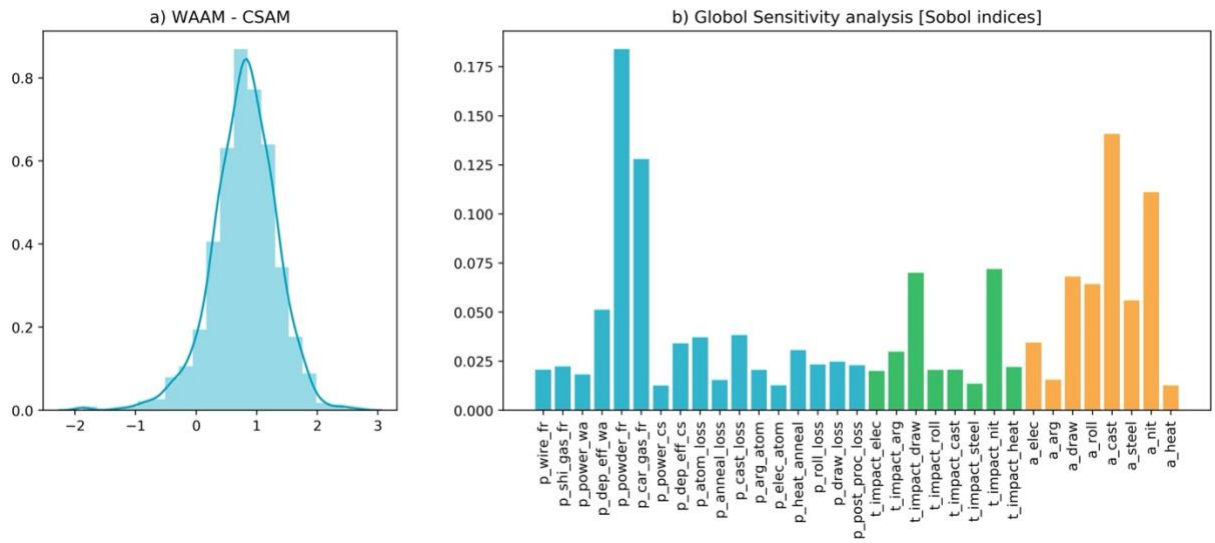

Figure 6.3 The results of the first iteration of the a) Monte Carlo analysis and b) Global Sensitivity Analysis. Blue bars are for parameters, green bars for technology (background processes) and orange bars are for applicability.

6.2.3.2 Second iteration

In this second iteration, targeted primary data were collected from Polycontrols for powder feed rate (1.5 kg/hr uniformly distributed between 1.2 and 1.8). Updated results reversed the conclusion; GWPWAAM became lower than GWPCSAM for 98.1% of the runs (Figure 6.4, a). This shift is explained by a significantly lower feed rate value from measured data collected at the company compared to the initial data gathered from literature. A lower feed rate (amount of powder less powder deposited per hour) requires more electricity to deposit the same amount of powder, thus increasing the impact of CSAM. The likelihood that GWPWAAM is lower than GWPCSAM (98.1%) was greater than the defined convergence criterion of 95%, suggesting that the results are conclusive. However, the carrier gas feed rate became the parameter contributing the most to the variability of the impact scores, with a first order Sobol' index of 0.35, more than 10 times higher than the others (Figure 6.4, b). According to the initial framework, the iteration should stop at this step. But as an exploratory phase, a third data collection round was performed to check if the results

of the Monte Carlo simulations were generating an adequate convergence criterion, or an early stop would lead to unreliable conclusions.

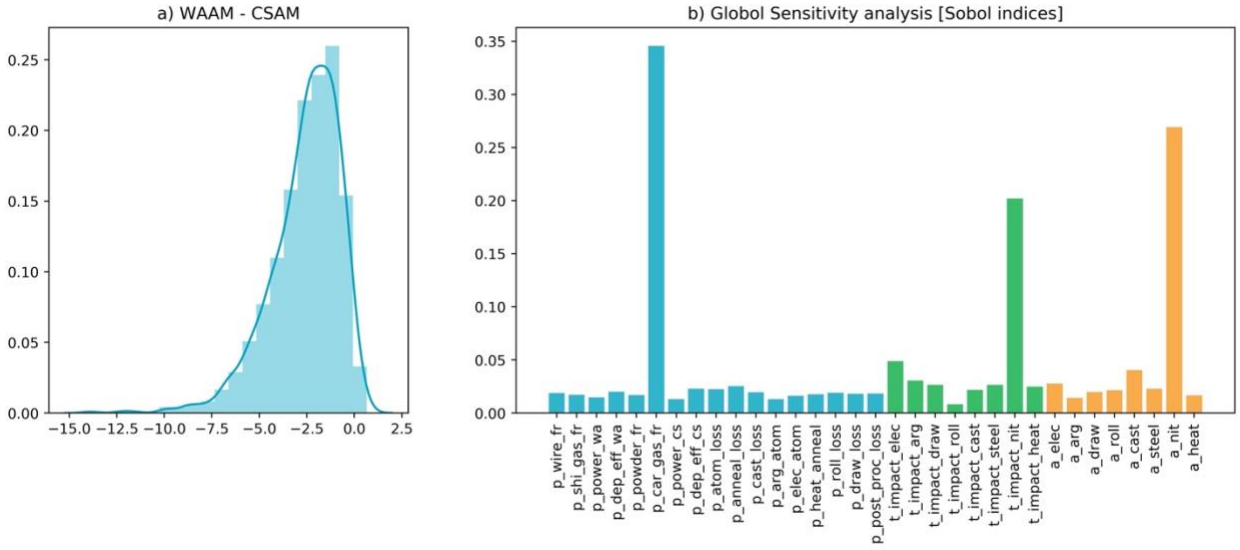

Figure 6.4 The results of the second iteration of the a) Monte Carlo analysis and b) Global Sensitivity Analysis. Blue bars are for parameters, green bars for technology (background processes) and orange bars are for applicability.

6.2.3.3 Third iteration

In this third iteration, primary data for the carrier gas flow rate were collected at Polycontrols (0.175 m^3/min uniformly distributed between 0.15 and 0.2) Updated results reversed the conclusion again; GWP_{WAAM} became higher than GWP_{CSAM} with a likelihood of 92.4% (Figure 6.5, a). This third iteration reduced the uncertainty range for the carrier gas flow rate by decreasing the upper and lower bound, meaning that less nitrogen is needed for the same duration of deposition and ultimately reducing the impact scores of CSAM. Since 92.4% was lower than the convergence criterion, additional data collection was needed. The steel casting applicability had the highest Sobol' index after this iteration at around 0.2 (Figure 6.5, b). However, because it corresponds to a background data (aluminum casting was used as a proxy), adjusting that flow to reflect the steel industry was out of allocated resources to this study, despite its importance. According to the framework, we focused the data collection on the parameter with the next highest Sobol' index, which is the power used for cold spray.

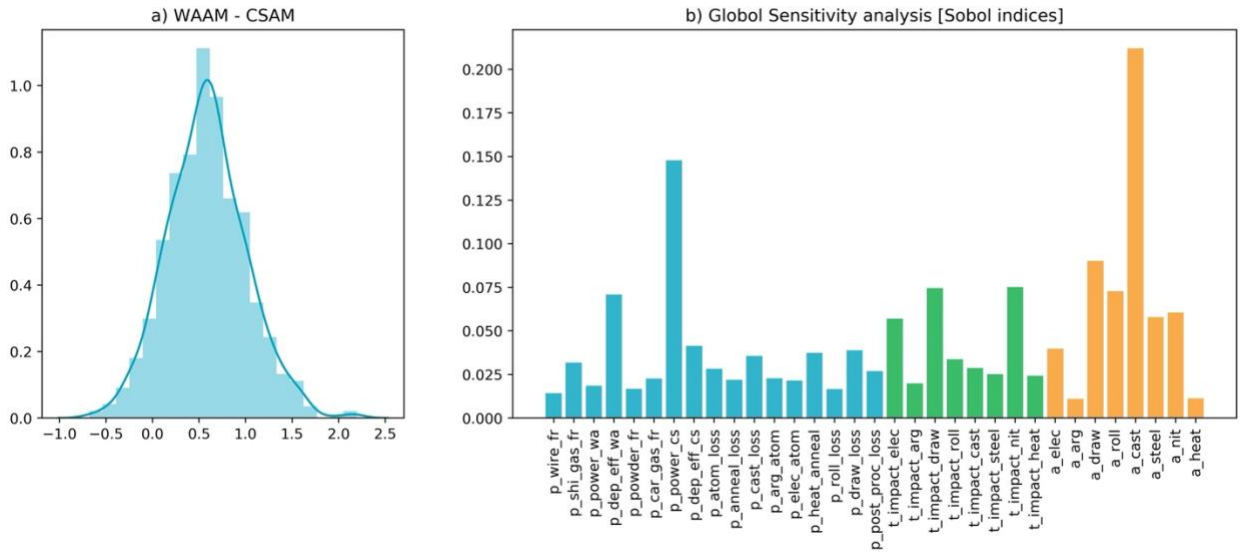

Figure 6.5 The results of the third iteration of the a) Monte Carlo analysis and b) Global Sensitivity Analysis. Blue bars are for parameters, green bars for technology (background processes) and orange bars are for applicability.

6.2.3.4 Final iteration

In the fourth iteration, primary data collection at Polycontrols was performed for the power used for the cold spray deposition (80.35 kW uniformly distributed between 43.05 and 106.85). The GWPWAAM became lower than GWPCSAM with a likelihood of 60.4% (Figure 6.6, a). At this point, the Sobol' indices for all the parameters were less than 0.1 (Figure 6.6, b). The Sobol' indices for some background technology flows and applicability uncertainties (green and orange bars) were still as twice higher than those of the parameters, but reducing their uncertainty was considered demanding in time and resources for a further iteration. For example, the Sobol' index of the ecoinvent process of electricity in Quebec is 0.08, where the uncertainty comes from the direct emissions of CO2 and N2O (Figure C.4 in Appendix C). Refining this data was beyond the control of Polycontrols, as it would have required a collaboration with the electricity supplier. Therefore, despite not reaching the 95% convergence criterion, the iterative process was ended and LCA results adopted to support internal decision making after the fourth and final iteration. The final deterministic results and the contribution analysis are available in Appendix C, Figure C.6.

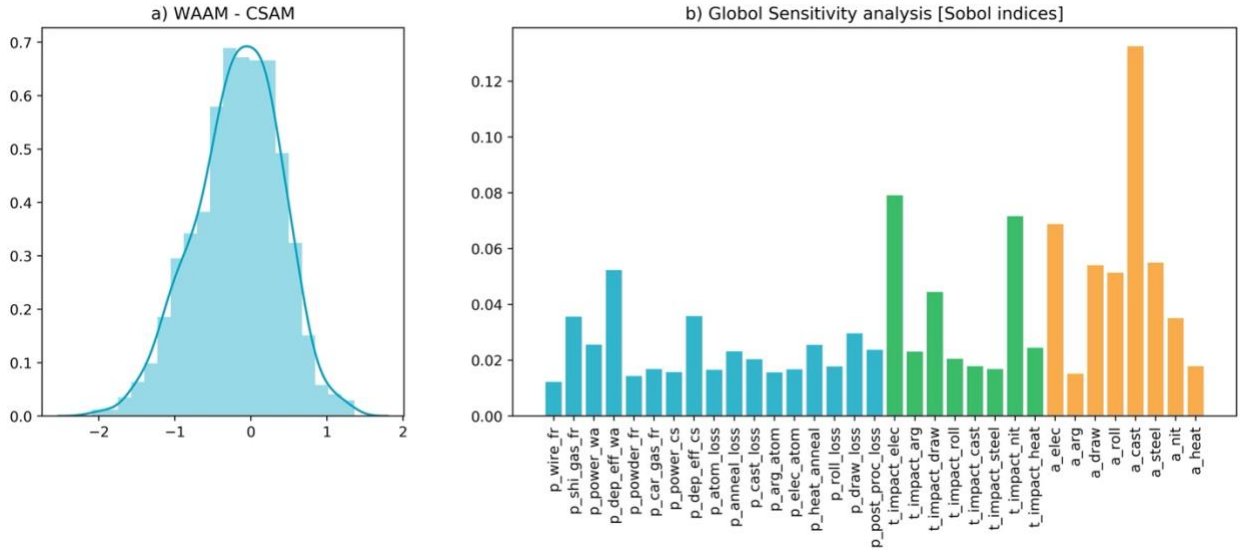

Figure 6.6 The results of the fourth iteration of the a) Monte Carlo analysis and b) Global Sensitivity Analysis. Blue bars are for parameters, green bars for technology (background processes) and orange bars are for applicability.

6.2.4 Discussion

GSA is mainly used in LCA to assess how robust and realistic the results are (Blanco et al., 2020), determine the main uncertainty drivers on the results (Kim et al., 2022), and empower reliable decision-making in LCA (Baaqel et al., 2023). We leverage the strengths of these applications to use GSA as a data collection guidance and reduce the effort needed to perform an LCA. We illustrated how to apply the framework to guide the data collection in a comparative LCA and showed how the results could change by targeting parameters with high variability. At the end of each iteration, comparing the results to the convergence criteria allows to test the robustness and reliability of the results in respect to requirements defined in the scoping phase of the study. Identifying the parameters contributing the highest to the variability of the results and prioritizing additional data collection around them ensures a systematic way to reduce uncertainty in the results. The case study validates how the framework achieves the targeted objective, and highlights some aspects (e.g., uncertainty range definition and convergence criteria) that need to be refined to improve the reliability of it. For simplicity, only GWP100 impacts were assessed, and a cradle-to-gate system boundary was chosen. Adding more impact categories and including the use and end of life phases is possible under the framework, requiring more knowledge on the application of the

product under study. Below we discuss the main learnings and recommendations to address those aspects.

Learning 1: The initial screening data might not be accurate, or its uncertainty range might be too narrow

The framework builds on the concept that the uncertainty range of the initial screening data would be wide enough and encompasses the real data (i.e., the high-quality primary data). As a common understanding, our hypothesis was that by improving the data quality in the additional data collection step, we narrow the range of the uncertainty and converge to the real data. However, this might not be the case, as results are highly influenced by the initial assumptions on the uncertainty ranges (Lacirignola et al., 2017). The uncertainty range of the screening data might be outside the range of the real (high-quality) data, and unless this variability is caught with the global sensitivity analysis, and thus improved, the results might be incorrect. This was the case of powder feed rate in our case study, and this lead to the change of the results (CSAM became worse than WAAM) after the first iteration. If the powder feed rate had not displayed such a high Sobol' Index, the result would have been misleading. Another instance which might lead to misleading results is if the uncertainty range is indeed close to the range of the real (high quality) value, but its uncertainty range is narrow. This could lead to that parameter being missed in the GSA and might lead us to stop the iterations earlier than expected while the value still needs improvement. Thus, defining the uncertainty range should be done with caution, and more rules and guidelines are needed to avoid prematurely ending the iterations. As a general rule, we recommend having the uncertainty range as wide as possible when few data are available, even if it means more iterations are needed. Figure 6.7 illustrates such situations where defining the screening data might lead to misleading results. The blue distribution represents the real data (that could also be a deterministic value). The green distribution is what we expected the screening data to look like when the framework was designed, where it is wide enough and incorporates the real data. The orange distributions are likely situations one might end up defining the distribution of the screening data and lead to misleading results.

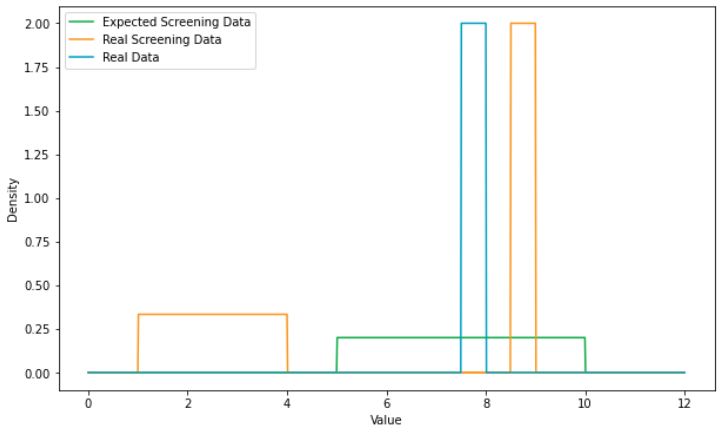

Figure 6.7 Hypothetical illustration of uniform probability distribution functions for the expected screening data, real screening data and real data.

Learning 2: Probability that the impact of A is larger than that of B in a Monte Carlo analysis as a convergence criterion needs to be complemented with a GSA.

Another vital step in the framework is defining the iteration convergence criteria. Initially, the criterion was defined as the probability that one product has a higher impact than the other through a Monte Carlo simulation (Figure 6.8, left). As demonstrated in the case study, misleading conclusions were drawn at the end of the second iteration despite achieving a probability of 98%, and only corrected after looking at the GSA results. This is the case when one of the parameters contributed highly to the uncertainty (as demonstrated by the GSA), but its real value was outside the uncertainty range initially defined in the screening data collection. Alternatively, one could define the convergence criterion as a maximum level of Sobol' index that all parameters should be below (e.g., 0.1 in Figure 6.8). It is not clear how this threshold should be chosen in the context of an LCA, but in other applications for example, parameters with a Sobol' index greater than 0.1 are considered highly sensitive (Wan et al., 2015). This could also include only foreground data if this is what practitioners have control on or extend to include the background data. We recommend defining such a criterion to complement the likelihood one rather than replace it, as each gives us different indications. Another criterion that could be explicitly defined is the time or cost needed to obtain high quality data (e.g., value of information used by Marchese et al. (2018)) for each parameter (the x ticks in Figure 6.8), and how do they compare to the remaining time or budget allocated to the study (the dashed line in Figure 6.8).

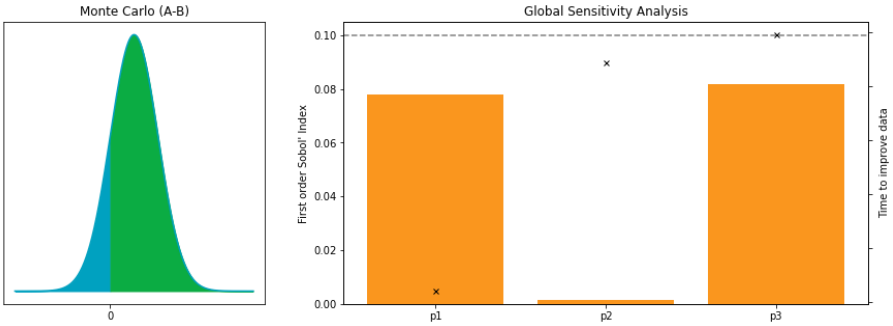

Figure 6.8 Hypothetical illustration of various convergence criteria. To the left is Monte Carlo analysis and to the right is Global Sensitivity Analysis complemented with time requirement

Learning 3: Using uncertainty analysis might not necessarily reduce time

Hypothetically, acquiring high quality data for fewer parameters would reduce the time to perform the study, but that is not necessarily true. As demonstrated by the case study, high quality data are collected iteratively in a serial effort (i.e., one data point collected after the other) following our approach, while in a traditional LCA data is collected in parallel. Therefore, depending on the number of iterations, the overall time might be longer (Figure 6.9). The billable time (e.g., wages for engineers providing the data), on the other hand, is likely to be reduced. That is because most of the time needed for the data collection, as we experienced in the case study, was calendar time. We define calendar time as time that do not incur any cost, which is mainly idle waiting time (e.g., waiting for an answer from an expert, waiting to reserve a lab for an experiment, etc …). For some studies, where the deadline is the constraint (rather than the budget), calendar time would be important. Note that additional time for the screening data collection and the Monte Carlo / GSA calculations could add more time to our proposed framework, but is considered negligible compared to the time to collect high quality primary data.

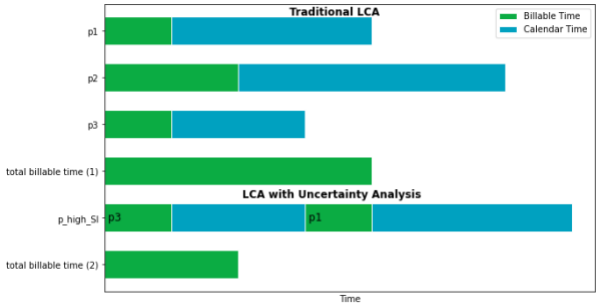

Figure 6.9 Hypothetical illustration of the time (billable and calendar) taken to perform a traditional LCA compared with an LCA using uncertainty analysis to guide data collection. p stands for parameter and p_high_SI stands for the parameter with the highest Sobol' Index.

6.2.5 Conclusion

In this study we proposed a framework to prioritize data collection in comparative LCAs using global sensitivity analysis (GSA). While GSA was proposed for other applications of LCA, it is perceived as demanding for practitioners, and with a structured framework, we hope this would increase its adoption. GSA ranks the parameters influencing LCA inventory data based on their contribution to the variability of the output, enabling practitioners to focus data collection efforts on high contributing ones while minimizing the time needed to reach conclusive results. A case study comparing two additive manufacturing technologies demonstrated its applicability. The framework, however, needs to be handled with caution, as the results are highly influenced by the initial definition of the uncertainty distributions of the data collected through a screening approach. More specifically we brought out that extreme care is needed when defining and using probabilistic values instead of deterministic ones, and we call practitioners for more uncertainty data inclusion when sharing inventory data. In addition, choosing the convergence criteria for conclusive results based on uncertainty propagation techniques such as Monte Carlo alone is not enough. We recommend complementing it with the definition of a maximum Sobol' index criterion not to be exceeded. Despite that, the framework gives higher clarity of communication between practitioners and decision-makers, who need to understand the level of confidence of the results and choose the risk levels they are satisfied with given the resource constraints.

CHAPTER 7 GENERAL DISCUSSION

7.1 Contributions of the thesis

The general objective of the thesis is to anticipate and assess the impacts of surface engineering on the environment and the material use at various scales of adoption, which was achieved by answering different specific objectives. The results where communicated with three scientific articles covering different elements of the research (Figure 7.1). Article 1 assess the prospective impact of large-scale adoption of novel surface engineering technologies on the environment. Article 2 quantifies the dissipative losses of surface engineering technologies in a retrospective manner and suggest material efficiency strategies to reduce those losses. Article 3 tries to reduce the time for such studies to make it easier to perform eco-design changes by suggesting a framework reducing the data collection needed.

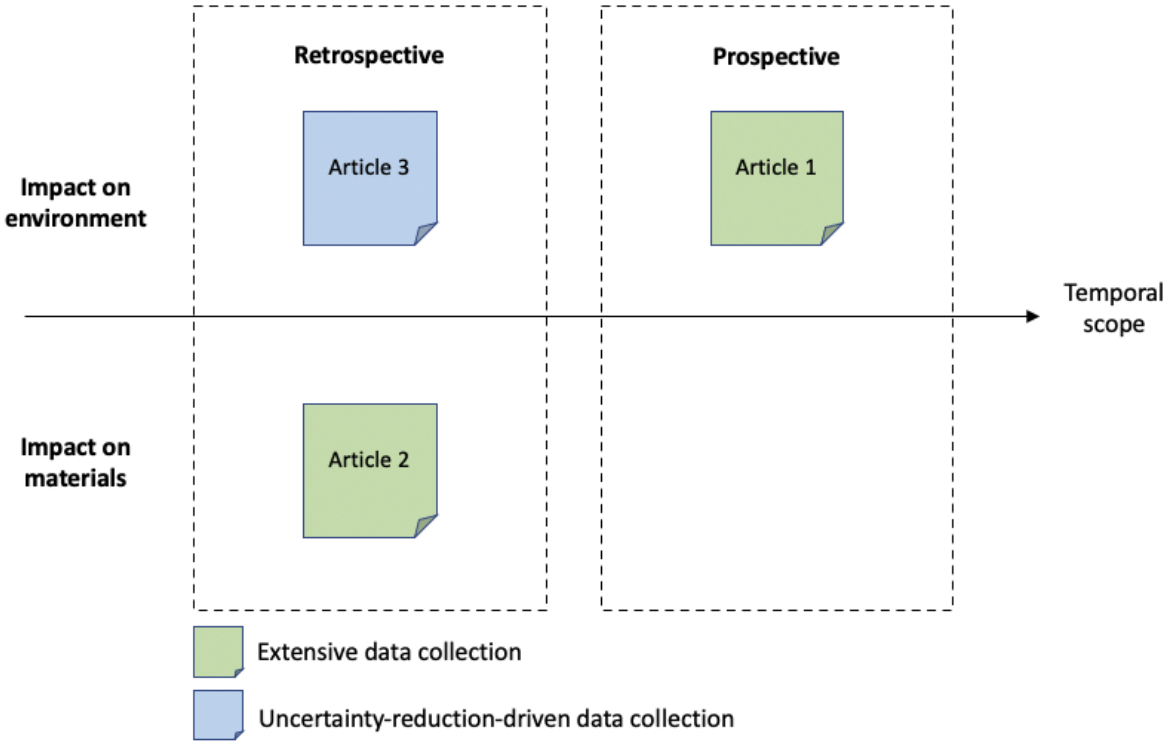

Figure 7.1 Scope of the articles

Following is a description of how specific objectives were achieved and their scientific contribution:

Specific objective 1: Evaluate the environmental impacts of prospective large-scale adoption of novel surface engineering technologies.

This objective was achieved by the results of the first article (Chapter 4), where the adoption of novel surface engineering technologies in the energy sector were modeled based on scenarios describing different socio-economic pathways. Literature review identified novel applications of surface engineering technologies in the energy sector leading to improved efficiency. SSPs where used to scale-up the potential impacts and benefits, and to define future scenarios. Applying innovative SE technologies to the energy sector has the potential of reducing annual CO2-eq emissions by 1.8 Gt in 2050 and 3.4 Gt in 2100 in an optimistic socio-economic pathway scenario. This corresponds to 7% and 8.5% annual reduction in the energy sector (compared to the baseline energy generation in MESSAGE SSP1) in 2050 and 2100, respectively. The mitigation potential of applying innovative SE technologies highly depends on the energy technology, the socio-economic pathways, and the implementation of stringent GHG mitigation policies. Due to their high carbon intensity, fossil-based technologies showed a higher GHG mitigation potential compared to renewables. Besides, GHG emissions related to the SE processes are largely offset by the GHG savings of the energy conversion technologies where the innovative SE technologies are applied. The main contributions achieved by this article are:

- **Quantifying the potential of surface engineering technologies in reducing GHG emissions:** LCA studies on surface engineering technologies are focused on the impacts of the coating process (Fiameni et al., 2021; Igartua et al., 2020; J. Liu et al., 2021). We try to quantify the indirect climatic environmental benefits (e.g., due to improved efficiency) of applying them on different products. Understanding how different characteristics of the coating would lead to a reduction of emissions helps surface engineering scientists design greener processes.
- **Linking LCA to IAM:** We propose a method to link the results of IAMs (future energy generations by each energy technology) with the impacts from LCA (endpoints from ecoinvent) in the domain of prospective modelling. This has been suggested recently to

model background data in prospective LCA studies (Mendoza Beltran, Cox, et al., 2018). In our model, we go further to use the output of the models and estimate the changes in stocks each year, allowing for a better modelling of adoption rates. We also demonstrated how to feedback the energy efficiency gains in the future due coating process to the impacts of the background data, reducing the environmental impact of the energy intensive coating process.

- **Programming the COATS model:** Our model is available on github for other researchers to use. This could be especially helpful for surface engineering researchers to account for future energy savings from novel developed surface engineering technologies in the energy sector. The model could also be used for other applications that improve the energy efficiency of energy generation technologies.

Specific objective 2: Quantify the dissipative losses associated with surface engineering technologies and suggest circular economy strategies to reduce them.

This objective was achieved in article 2 (Chapter 5), where we quantified the stocks of coating materials in the economy, and the associated material dissipative losses incurred during the life cycle of coated components. The energy and transportation sectors where modelled due to the availability of data, and a bottom-up approach was taken as no high level on the use of materials in coating in sectors is available. We used the IEA ETP model as it includes both the energy and transportation sectors, ensuring that the results are consistent. Results show that the coating process is the most contributing life cycle stage (up to 39% of the losses). Improving the deposition efficiency, recovering the unadhered and stripping the components at their end-of-life are key material efficiency strategies to reduce the material losses (up to 50%). On a same weight basis, piston and piston rings have the highest dissipative losses, where up to 8 kg of coating material is lost per 1 kg coated. This amounts to 19 kt of NiCrSi lost from pistons in the automotive industry. The following are the contributions of the second article:

- **Systematic way to estimate dissipative losses in surface engineering:** We identify the parameters that affect the losses and documented their values. For example, we differentiate between theoretical deposition efficiency usually communicated in literature and target

deposition efficiency. This allowed us to have a parametrized model, ensuring the transparency, usability and transferability of the inventory data (J. S. Cooper et al., 2012).

- **Circular economy strategies specific to the surface engineering sector:** While the literature on the circular economy is abundant (Allwood & Cullen, 2012), most of the strategies are generic, hindering their implementation in specific applications. This is not the case for large sectors, where specific strategies are usually recommended (e.g., manufacturing industry (Lieder & Rashid, 2016) and automotive sector (Prochatzki et al., 2023)). We recommend strategies that are specific to the surface engineering domain, which should help in designing new technologies while ensuring less material is lost.
- **Programming the DLiST model:** Out model is available on Github, where it is possible to assess new applications and materials used in surface engineering. This could also be used to update the results if better data becomes available on the parameters, and better inventory data for coated components are shared.

Specific objective 3: Develop a methodology to steer the efforts of data collection in LCA using uncertainty analysis.

This objective was achieved in article 3, where we propose a framework to prioritize data collection in LCA using global sensitivity analysis (GSA). This starts with a screening life cycle inventory analysis systematically informing all input parameters with uncertainty ranges. Monte Carlo analysis is then used to propagate the uncertainty through the model. This is followed by a GSA using Sobol' indices to rank different input parameters based on their contribution to the variability of the results. A case study comparing cold spray and wire arc additive manufacturing illustrates how to operationalize the framework. Learnings from the case study highlight the importance of defining the uncertainty ranges and the convergence criterion, where more work is needed in that domain. The main contributions of this article are:

- **Systematic methodology to use GSA in guiding data collection efforts:** The main use of uncertainty analysis in LCA has been to assess the reliability of the results (Larsson Ivanov et al., 2019; Von Pfingsten et al., 2017; Zhai et al., 2021). Our framework builds on this to leverage the strength of global sensitivity analysis in ranking input parameters based on their contribution to the variability of the output, prioritizing data collection for the highest

contributors. Providing the framework makes the method more systematic and applicable, where guidance is given at each step, and modifying any step would be easier.

- **Introducing the concept of available (time) resources and acceptable risk level in LCA:** In our framework, we deal with LCA as any study undertaken by companies, where there is a trade-off between available resources and the tolerated risk level in decision-making. This is introduced by adding two decision actions: checking the convergence criteria and checking if there are available resources to improve the data. If the convergence criterion (within the acceptable risk level of decision-makers) is achieved, there is no need for additional time-consuming data collection. Similarly, if the cost of collecting additional data is higher than the allocated budget, results should be communicated at lower confidence levels while flagging the uncertainty of the data used.
- **Programming the GSAPDaC model:** We shared our model used to do the assessment on Github, which allows for similar studies to be done by modifying the input files. This should reduce the barrier of entry for practitioners who are new to uncertainty analysis and improve the adoption of the methodology in the field.

7.2 Limitations of the thesis

While we achieved the objectives of the research through the three articles, some limitation that we faced are highlighted below.

The use of fixed adoption rates

In the prospective LCA model of novel surface engineering technologies, we used fixed adoption rates (e.g., 10%, 80% and 100%) depending on the scenario. A more precise representation could involve learning curves based on the technology readiness level (TRL) of the technologies (Buyle et al., 2019; van der Giesen et al., 2020). With a lack of literature around leaning curves in the surface engineering domain, using fixed rates are justifiable when we are trying to assess different scenarios, as long as each rate is in line with the scenario narrative.

Soft linking efficiency improvements to IAM

In our modelling, we used the outcomes of the IAM to estimate the benefits of the efficiency improvements achieved by implementing the novel surface engineering technologies. This means

that the results do not reflect any changes in the dynamics and interactions in the system. Adding new technologies might affect the optimization in the IAM (e.g., if the electricity from gas turbines with the novel coatings are more expensive than other technologies, less energy will be generated from gas turbines, which is not reflected in our model). For example, an extension of the MESSAGE IAM was modelled for Brazil to assess the impacts of CCS technologies (Nogueira et al., 2014). In that study, the fuel prices were included to account for the economic competition between the technological alternatives. Due to the lack of prices data and other parameters in the IAM model, we were not able to modify and rerun the model. We assume that the prices are not largely affected as small amounts of coatings are needed, and the energy production outcomes of the IAM would still be valid.

Excluding the impact of the substrate materials from the MFA

When assessing the dissipative losses, we only performed the MFA on the coating materials. But this is part of a larger system, where the substrate (the material to be coated) should also be assessed. That is because some coating materials act as impurities in the substrates, and result in material, quality and dilution losses in open-loop recycling systems (Nakajima et al., 2016), leading to dissipative losses of those materials as well. The scope of our studies was the coating materials, and the impact on the substrate should be added in the MFA of the substrate materials.

Assessing dissipative losses at an inventory level

In our assessment, the dissipative losses were quantified at an inventory level. However, the impact of those losses is not the same for all the materials, as some are more scarce or critical than others, and this could be reflected in the impact category. Current resource dissipation indicator methods in LCA are underdeveloped (Greffe et al., 2023) and often provide nonconclusive outcomes due to different methodological choices (Schrijvers et al., 2020). Communicating our results at an inventory level makes it possible to get the results of any impact method we want based on the purpose of the study.

Defining the uncertainty ranges as uniform distribution

In our framework to reduce data collection using uncertainty analysis, we used uniform distributions to model the uncertainty of the input parameters. Other distributions like triangular, normal and lognormal are also common in LCA (Igos et al., 2019) and might better illustrate the

uncertainty, but would require more time to collect such data. This is a limitation of the inventory data where they are shared as deterministic values. The aim of our framework was to reduce the time needed to collect data and choosing uniform (while wide) distribution would achieve that without risking missing uncertain parameters. Other ways to model uncertainty with less available data could be using the pedigree matrix (Ciroth et al., 2016) to generate lognormal uncertainty distributions, but it is more of a quality measure.

7.3 Future research

Investigate the unexploited links between the three subobjectives

Starting with the low hanging fruits, there are some links between the subobjective that have not been fully investigated due to time constraints (red dashed lines in Figure 3.1). For example, the outcomes of the uncertainty-based LCA, which is well adapted to novel technologies, could be scaled up using IAM and following our methodology for objective 1. This allows us to anticipate how will novel technologies (e.g., cold spray additive manufacturing) contribute to the sustainability transition. Besides, the background data for the uncertainty-based LCA was modelled retrospectively, but using IAM to model the variability of background data could be done. Finally, an uncertainty-based MFA could also be done to reduce time efforts in studies focusing on material use and losses.

Assess the impacts of surface engineering in extending the lifetime of components

While our study focused on the reduced GHG emissions in the energy sector due to improvements in the energy efficiency, the other benefit that SE brings is extending the lifetime of components. This would lead to less primary materials mined and less components manufactured, reducing the environmental impacts. We already discussed some lifetime extension measures in the second article (Chapter 5) that can serve as a starting point. For example, cold spray is highly used in repairing large components like aircraft engines (Dayı & Kılıçay, 2024) and cutting tools are usually coated with tungsten to reduce wear and extend their lifetime (Qinqiang Wang et al., 2021).

Use the methods on other sectors

The focus of this study was the assessing the impacts of surface engineering on the environment and the material flows. The methods we propose are applicable to other sectors or domain with

similar properties. This include specialized industrial applications that are not large enough to be considered as sectors in available industrial ecology tools (e.g., unlike transportation and energy sectors in IAMs and EEIO). The data for such domains is usually scarce, and bottom-up approaches as we suggested are needed. Example sectors could be machining, additive manufacturing, heat treatment, nanotechnology and robotics.

Better communication of uncertainty of inventory data in industrial ecology

A recurring theme in all the articles in this thesis is the lack of high-quality inventory data and the high uncertainty covering them (for both LCA and MFA). While we iterate on the importance of including the uncertainty and its effect on the results, uncertainty data is rarely shared with the inventory data. Most of the uncertainty of background data in ecoinvent is estimated based on the pedigree matrix (Ciroth et al., 2016), and might not be the best way to describe it. More work needs to be done to streamline and encourage the communication of uncertainty data. This could be by having more standards or rules of thumb that would make it easier to include them.

CHAPTER 8 CONCLUSION AND RECOMMANDATIONS

Surface engineering technologies are essential in most products to ensure they operate under the desired conditions and improve their performance. Novel technologies and materials are developed and adopted continuously, usually contributing to the growing decarbonization efforts. This thesis provides the tools to surface engineering researchers to address the sustainability aspects in the development stages, ensuring the benefits of novel technologies do not come at the expense of increased GHG emissions or material losses. This is done through utilizing LCA and MFA to assess the environmental impacts and impacts on materials, respectively. The two approaches where integrated with IAMs to add the large-scale and prospective nature of the assessment. The main contributions of this research are:

- **Potential of surface engineering in reducing GHG emissions in the future:** By combining LCA with different SSP scenarios, it was possible to estimate the GHG emission reduction from using novel surface engineering applications. This allows us to anticipate applications with the most reduction potential and prioritize future eco-design efforts accordingly.
- **Understanding the material dissipative losses associated with surface engineering:** Using MFA, it was possible to understand the life cycle stages associated with the highest dissipative losses of coated components and pinpoint the most used materials. This allowed us to recommend circular economy strategies that are relevant to the surface engineering domain.
- **Prioritizing data collection in LCA:** A framework to prioritize data collection in LCA using GSA was presented. This reduces the barrier of entry to perform an LCA and encourages more researchers in other domains to implement it. We also highlight methodological choices when defining uncertainty ranges and convergence criteria to improve the framework.

Some limitations and constraints were faced when applying the methods. The main limitation was the limited data about the inventory of SE technologies. This was solved by including the uncertainty in the MFA and basing the suggested simplified LCA study on it. Another issue that emerged was the use of uniform distribution to define the uncertainties, which was acceptable given that the range is wide enough to account the uncertainty. Despite that, the following recommendations are suggested:

- **Adopt novel coating materials in the energy sector:** Novel coating materials can improve the energy efficiency in different energy generation technologies. The impact associated with the coating process is usually less than the benefits achieved in terms of less GHG emissions, justifying the large-scale adoption.
- **Optimize the coating process and improve the recycling of coating materials:** The priority should be given to reducing the material losses, which mostly occur during the coating process, by optimizing this process. When this is not possible, especially for smaller parts, the powder dust lost during the coating process, which is already collected, should be recycled, as its direct reuse is not possible due to physical changes during the spraying process.
- **Prioritize data collection in LCA using uncertainty analysis:** Focus the data collection efforts on the parameters contributing the most to the variability of the results ensures reaching high confidence results in less time. GSA is a powerful tool to rank the parameters based on their contribution to the variability which should be used more often, especially in LCA studies of early-stage technologies.

The outcomes of this thesis are mainly directed to the surface engineering community, but the methodological part of it is general to the industrial ecology field.

REFERENCES

Adrianto, L. R., van der Hulst, M. K., Tokaya, J. P., Arvidsson, R., Blanco, C. F., Caldeira, C., Guillén-Gonsálbez, G., Sala, S., Steubing, B., Buyle, M., Kaddoura, M., Navarre, N. H., Pedneault, J., Pizzol, M., Salieri, B., van Harmelen, T., & Hauck, M. (2021). How can LCA include prospective elements to assess emerging technologies and system transitions? The 76th LCA Discussion Forum on Life Cycle Assessment, 19 November 2020. *International Journal of Life Cycle Assessment*, *26*(8), 1541–1544. https://doi.org/10.1007/s11367-021-01934-w

Alamri, H. R., Rezk, H., Abd-Elbary, H., Ziedan, H. A., & Elnozahy, A. (2020). Experimental investigation to improve the energy effciency of solar PV panels using hydrophobic SiO2 nanomaterial. *Coatings*, *10*(5). https://doi.org/10.3390/COATINGS10050503

AlFarra, H. J., & Abu-Hijleh, B. (2012). The potential role of nuclear energy in mitigating CO 2 emissions in the United Arab Emirates. *Energy Policy*, *42*, 272–285. https://doi.org/10.1016/j.enpol.2011.11.084

Allwood, J. M., Ashby, M. F., Gutowski, T. G., & Worrell, E. (2011). Material efficiency: A white paper. *Resources, Conservation and Recycling*, *55*(3), 362–381. https://doi.org/10.1016/j.resconrec.2010.11.002

Allwood, J. M., & Cullen, J. M. (2012). Sustainable Materials: With Both Eyes Open. In *Sustainable Materials: With Both Eyes Open* (1st ed.). UIT Cambridge Limited. https://www.uselessgroup.org/publications/book/chapters

Alonso, E., Sherman, A. M., Wallington, T. J., Everson, M. P., Field, F. R., Roth, R., & Kirchain, R. E. (2012). Evaluating rare earth element availability: A case with revolutionary demand from clean technologies. *Environmental Science and Technology*, *46*(6), 3406–3414. https://doi.org/10.1021/es203518d

Amoak, D., Luginaah, I., & McBean, G. (2022). Climate Change, Food Security, and Health: Harnessing Agroecology to Build Climate-Resilient Communities. *Sustainability (Switzerland)*, *14*(21). https://doi.org/10.3390/su142113954

Andrae, A. S. G., Zou, G., & Liu, J. (2004). LCA Case Studies LCA of Electronic Products. *Int J*

LCA, *9*(1), 45–52. https://doi.org/10.1007/BF02978535

Arena, M., Azzone, G., & Conte, A. (2013). A streamlined LCA framework to support early decision making in vehicle development. *Journal of Cleaner Production*, *41*, 105–113. https://doi.org/10.1016/j.jclepro.2012.09.031

Arvidsson, R., Kushnir, D., Molander, S., & Sandén, B. A. (2016). Energy and resource use assessment of graphene as a substitute for indium tin oxide in transparent electrodes. *Journal of Cleaner Production*, *132*, 289–297. https://doi.org/10.1016/j.jclepro.2015.04.076

Arvidsson, R., Sandén, B. A., & Svanström, M. (2023). Prospective, Anticipatory and Ex-Ante – What's the Difference? Sorting Out Concepts for Time-Related LCA. *SETAC Europe 33th Annual Meeting*, 2.

Arvidsson, R., Tillman, A. M., Sandén, B. A., Janssen, M., Nordelöf, A., Kushnir, D., & Molander, S. (2018). Environmental Assessment of Emerging Technologies: Recommendations for Prospective LCA. *Journal of Industrial Ecology*, *22*(6), 1286–1294. https://doi.org/10.1111/jiec.12690

Ashby, M. (2009). *Materials and the environment: eco-informed material choice*. Elsevier.

Azevedo, J. M. C., CabreraSerrenho, A., & Allwood, J. M. (2018). Energy and material efficiency of steel powder metallurgy. *Powder Technology*, *328*, 329–336. https://doi.org/10.1016/j.powtec.2018.01.009

Baaqel, H. A., Bernardi, A., Hallett, J. P., Guillén-Gosálbez, G., & Chachuat, B. (2023). Global Sensitivity Analysis in Life-Cycle Assessment of Early-Stage Technology using Detailed Process Simulation: Application to Dialkylimidazolium Ionic Liquid Production. *ACS Sustainable Chemistry and Engineering*, *11*(18), 7157–7169. https://doi.org/10.1021/acssuschemeng.3c00547

Baba, N. B., Omar, M. M. A., & Zin, N. A. M. (2014). Thermal properties of NiCrSiB coating on piston engine. *Advanced Materials Research*, *974*(June), 71–75. https://doi.org/10.4028/www.scientific.net/AMR.974.71

Badina, C. (2023). *Personal communication with Carmen Badina of EDF. Email, 14 March 2023*.

Baik, J. S., & Kim, Y. J. (2008). Effect of nozzle shape on the performance of high velocity oxygen-fuel thermal spray system. *Surface and Coatings Technology*, *202*(22–23), 5457–5462. https://doi.org/10.1016/j.surfcoat.2008.06.061

Baiocco, G., Salvi, D., & Ucciardello, N. (2024). Sustainable coating solutions: a comparative life cycle analysis of electrophoretic deposition and electroplating for graphene-reinforced anti-wear coatings. *International Journal of Advanced Manufacturing Technology*, *130*(7–8), 3341–3354. https://doi.org/10.1007/s00170-023-12796-x

Bakan, E., Mack, D. E., Mauer, G., & Vaßen, R. (2014). Gadolinium zirconate/YSZ thermal barrier coatings: Plasma spraying, microstructure, and thermal cycling behavior. *Journal of the American Ceramic Society*, *97*(12), 4045–4051. https://doi.org/10.1111/jace.13204

Balaguru, K., Xu, W., Chang, C. C., Leung, L. R., Judi, D. R., Hagos, S. M., Wehner, M. F., Kossin, J. P., & Ting, M. (2023). Increased U.S. coastal hurricane risk under climate change. *Science Advances*, *9*(14), 1–11. https://doi.org/10.1126/sciadv.adf0259

Baranda, M., Mayo, C., Diaz, R., Rodriguez, R., & Pérez, F. J. (2024). Comparative environmental assessment of coated ferritic steels suited to steam turbines of coal-fired supercritical and ultra-supercritical power plants. *Journal of Cleaner Production*, *443*(September 2023). https://doi.org/10.1016/j.jclepro.2024.141226

Bauer, C., Buchgeister, J., Hischier, R., Poganietz, W. R., Schebek, L., & Warsen, J. (2008). Towards a framework for life cycle thinking in the assessment of nanotechnology. *Journal of Cleaner Production*, *16*(8–9), 910–926. https://doi.org/10.1016/j.jclepro.2007.04.022

Bekker, A. C. M., & Verlinden, J. C. (2018). Life cycle assessment of wire + arc additive manufacturing compared to green sand casting and CNC milling in stainless steel. *Journal of Cleaner Production*, *177*, 438–447. https://doi.org/10.1016/j.jclepro.2017.12.148

Beltran, A. M., Cox, B., Mutel, C., & Vuuren, D. P. Van. (2018). *When the Background Matters Using Scenarios from Integrated Assessment Models in Prospective Life Cycle Assessment*. *24*(1). https://doi.org/10.1111/jiec.12825

Berger, M., Sonderegger, T., Alvarenga, R., Bach, V., Cimprich, A., Dewulf, J., Frischknecht, R., Guinée, J., Helbig, C., Huppertz, T., Jolliet, O., Motoshita, M., Northey, S., Peña, C. A.,

Rugani, B., Sahnoune, A., Schrijvers, D., Schulze, R., Sonnemann, G., … Young, S. B. (2020). Mineral resources in life cycle impact assessment: part II – recommendations on application-dependent use of existing methods and on future method development needs. *International Journal of Life Cycle Assessment*, *25*(4), 798–813. https://doi.org/10.1007/s11367-020-01737-5

Bewilogua, K., Bräuer, G., Dietz, A., Gäbler, J., Goch, G., Karpuschewski, B., & Szyszka, B. (2009). Surface technology for automotive engineering. *CIRP Annals - Manufacturing Technology*, *58*(2), 608–627. https://doi.org/10.1016/j.cirp.2009.09.001

Beylot, A., Dewulf, J., Greffe, T., Muller, S., & Blengini, G. A. (2024). Mineral resources depletion, dissipation and accessibility in LCA: a critical analysis. *International Journal of Life Cycle Assessment*, *29*(5), 890–908. https://doi.org/10.1007/s11367-023-02278-3

Bianco, I., Panepinto, D., Blengini, G. A., Onofrio, M., & Zanetti, M. (2020). Inventory and life cycle assessment of an Italian automotive painting process. *Clean Technologies and Environmental Policy*, *22*(1), 247–258. https://doi.org/10.1007/s10098-019-01780-3

Blanco, C. F., Cucurachi, S., Guinée, J. B., Vijver, M. G., Peijnenburg, W. J. G. M., Trattnig, R., & Heijungs, R. (2020). Assessing the sustainability of emerging technologies: A probabilistic LCA method applied to advanced photovoltaics. *Journal of Cleaner Production*, *259*. https://doi.org/10.1016/j.jclepro.2020.120968

Brunner, P. H., & Rechberger, H. (2004). *Practical handbook of material flow analysis*. CRC press.

Bulle, C., Margni, M., Patouillard, L., Boulay, A. M., Bourgault, G., De Bruille, V., Cao, V., Hauschild, M., Henderson, A., Humbert, S., Kashef-Haghighi, S., Kounina, A., Laurent, A., Levasseur, A., Liard, G., Rosenbaum, R. K., Roy, P. O., Shaked, S., Fantke, P., & Jolliet, O. (2019). IMPACT World+: a globally regionalized life cycle impact assessment method. *International Journal of Life Cycle Assessment*, *24*(9), 1653–1674. https://doi.org/10.1007/s11367-019-01583-0

Buyle, M., Audenaert, A., Billen, P., Boonen, K., & Van Passel, S. (2019). The future of ex-ante LCA? Lessons learned and practical recommendations. *Sustainability (Switzerland)*, *11*(19), 1–24. https://doi.org/10.3390/su11195456

Caduff, M., Huijbregts, M. A. J., Koehler, A., Althaus, H. J., & Hellweg, S. (2014). Scaling Relationships in Life Cycle Assessment: The Case of Heat Production from Biomass and Heat Pumps. *Journal of Industrial Ecology*, *18*(3), 393–406. https://doi.org/10.1111/jiec.12122

Cai, Z., Liang, H., Quan, S., Deng, S., Zeng, C., & Zhang, F. (2015). Computer-Aided Robot Trajectory Auto-generation Strategy in Thermal Spraying. *Journal of Thermal Spray Technology*, *24*(7), 1235–1245. https://doi.org/10.1007/s11666-015-0282-7

Cao, R., Leng, Z., Yu, H., & Hsu, S. C. (2019). Comparative life cycle assessment of warm mix technologies in asphalt rubber pavements with uncertainty analysis. *Resources, Conservation and Recycling*, *147*(April), 137–144. https://doi.org/10.1016/j.resconrec.2019.04.031

Castolin Eutectic. (2015). *Boiler Coating*.

Charpentier Poncelet, A., Loubet, P., Helbig, C., Beylot, A., Muller, S., Villeneuve, J., Laratte, B., Thorenz, A., Tuma, A., & Sonnemann, G. (2022). Midpoint and endpoint characterization factors for mineral resource dissipation: methods and application to 6000 data sets. *International Journal of Life Cycle Assessment*, *27*(9–11), 1180–1198. https://doi.org/10.1007/s11367-022-02093-2

Chebaeva, N., Lettner, M., Wenger, J., Schöggl, J. P., Hesser, F., Holzer, D., & Stern, T. (2021). Dealing with the eco-design paradox in research and development projects: The concept of sustainability assessment levels. *Journal of Cleaner Production*, *281*. https://doi.org/10.1016/j.jclepro.2020.125232

Ciacci, L., Harper, E. M., Nassar, N. T., Reck, B. K., & Graedel, T. E. (2016). Metal Dissipation and Inefficient Recycling Intensify Climate Forcing. *Environmental Science and Technology*, *50*(20), 11394–11402. https://doi.org/10.1021/acs.est.6b02714

Ciroth, A., Muller, S., Weidema, B., & Lesage, P. (2016). Empirically based uncertainty factors for the pedigree matrix in ecoinvent. *International Journal of Life Cycle Assessment*, *21*(9), 1338–1348. https://doi.org/10.1007/s11367-013-0670-5

Clarke, D. R., Oechsner, M., & Padture, N. P. (2012). Thermal-barrier coatings for more efficient gas-turbine engines. *MRS Bulletin*, *37*(10), 891–898. https://doi.org/10.1557/mrs.2012.232

Construction, N. S. (2023). *Denmark introduces CO2 limit for new constructions - Buildings' Life*

Cycle Assessments gain ground in the Nordics. https://www.nordicsustainableconstruction.com/news/2023/january/denmark-introduces-co2-limit-for-new-constructions

Cooper, D. R., & Gutowski, T. G. (2020). Prospective Environmental Analyses of Emerging Technology: A Critique, a Proposed Methodology, and a Case Study on Incremental Sheet Forming. *Journal of Industrial Ecology*, *24*(1), 38–51. https://doi.org/10.1111/jiec.12748

Cooper, J. S., Noon, M., & Kahn, E. (2012). Parameterization in Life Cycle Assessment inventory data: Review of current use and the representation of uncertainty. *International Journal of Life Cycle Assessment*, *17*(6), 689–695. https://doi.org/10.1007/s11367-012-0411-1

Cox, B., Mutel, C. L., Bauer, C., Mendoza Beltran, A., & Van Vuuren, D. P. (2018). Uncertain Environmental Footprint of Current and Future Battery Electric Vehicles. *Environmental Science and Technology*, *52*(8), 4989–4995. https://doi.org/10.1021/acs.est.8b00261

Crippa, M., Oreggioni, G., Guizzardi, D., Muntean, M., Schaaf, E., Lo Vullo, E., Solazzo, E., Monforti-Ferrario, F., Olivier, J., & Vignati, E. (2019). *Fossil CO2 & GHG emissions of all world countries: 2019 report* (Issue October). https://doi.org/10.2760/687800

Cucurachi, S., Borgonovo, E., & Heijungs, R. (2016). A Protocol for the Global Sensitivity Analysis of Impact Assessment Models in Life Cycle Assessment. *Risk Analysis*, *36*(2), 357–377. https://doi.org/10.1111/risa.12443

Cucurachi, Stefano, Blanco, C. F., Steubing, B., & Heijungs, R. (2021). Implementation of uncertainty analysis and moment-independent global sensitivity analysis for full-scale life cycle assessment models. *Journal of Industrial Ecology*, 1–18. https://doi.org/10.1111/jiec.13194

Cucurachi, Stefano, Van Der Giesen, C., & Guinée, J. (2018). Ex-ante LCA of Emerging Technologies. *Procedia CIRP*, *69*(May), 463–468. https://doi.org/10.1016/j.procir.2017.11.005

Cullen, J. M., & Cooper, D. R. (2022). Material Flows and Efficiency. *Annual Review of Materials Research*, *52*, 525–559. https://doi.org/10.1146/annurev-matsci-070218-125903

Dayı, S. C., & Kılıçay, K. (2024). Repairing Al7075 surface using cold spray technology with

different metal/ceramic powders. *Surface and Coatings Technology*, *489*(July), 131124. https://doi.org/10.1016/j.surfcoat.2024.131124

Dearnley, P. A. (2017). *Introduction to surface engineering*. Cambridge University Press.

Deng, Y., Chen, W., Li, B., Wang, C., Kuang, T., & Li, Y. (2020). Physical vapor deposition technology for coated cutting tools: A review. *Ceramics International*, *46*(11), 18373–18390. https://doi.org/10.1016/j.ceramint.2020.04.168

EC. (2014). *2030 climate & energy framework*.

EC. (2020). *COMMUNICATION FROM THE COMMISSION TO THE EUROPEAN PARLIAMENT, THE COUNCIL, THE EUROPEAN ECONOMIC AND SOCIAL COMMITTEE AND THE COMMITTEE OF THE REGIONS Stepping up Europe's 2030 climate ambition Investing in a climate-neutral future for the benefit of our* . https://eur-lex.europa.eu/legal-content/EN/TXT/?uri=CELEX:52020DC0562

Ellingsen, L. A. W., Hung, C. R., Majeau-Bettez, G., Singh, B., Chen, Z., Whittingham, M. S., & Strømman, A. H. (2016). Nanotechnology for environmentally sustainable electromobility. *Nature Nanotechnology*, *11*(12), 1039–1051. https://doi.org/10.1038/nnano.2016.237

Elshkaki, A., & Graedel, T. E. (2013). Dynamic analysis of the global metals flows and stocks in electricity generation technologies. *Journal of Cleaner Production*, *59*, 260–273. https://doi.org/10.1016/j.jclepro.2013.07.003

Elshkaki, A., & Shen, L. (2019). Energy-material nexus: The impacts of national and international energy scenarios on critical metals use in China up to 2050 and their global implications. *Energy*, *180*, 903–917. https://doi.org/10.1016/j.energy.2019.05.156

Encinas-Sánchez, V., Batuecas, E., Macías-García, A., Mayo, C., Díaz, R., & Pérez, F. J. (2018). Corrosion resistance of protective coatings against molten nitrate salts for thermal energy storage and their environmental impact in CSP technology. *Solar Energy*, *176*(September), 688–697. https://doi.org/10.1016/j.solener.2018.10.083

Espinosa, N., García-Valverde, R., Urbina, A., & Krebs, F. C. (2011). A life cycle analysis of polymer solar cell modules prepared using roll-to-roll methods under ambient conditions. *Solar Energy Materials and Solar Cells*, *95*(5), 1293–1302.

https://doi.org/10.1016/j.solmat.2010.08.020

Espinosa, N., García-Valverde, R., Urbina, A., Lenzmann, F., Manceau, M., Angmo, D., & Krebs, F. C. (2012). Life cycle assessment of ITO-free flexible polymer solar cells prepared by roll-to-roll coating and printing. *Solar Energy Materials and Solar Cells*, *97*, 3–13. https://doi.org/10.1016/j.solmat.2011.09.048

Eybel, R. (2023). *Personal communication with Roger Eybel of Safran. Phone call, 24 January 2023*.

Ferdous, J., Bensebaa, F., Hewage, K., Bhowmik, P., & Pelletier, N. (2024). Use of process simulation to obtain life cycle inventory data for LCA: A systematic review. *Cleaner Environmental Systems*, *14*(March), 100215. https://doi.org/10.1016/j.cesys.2024.100215

Fernandez-Feijoo, B., Romero, S., & Ruiz, S. (2014). Effect of Stakeholders' Pressure on Transparency of Sustainability Reports within the GRI Framework. *Journal of Business Ethics*, *122*(1), 53–63. https://doi.org/10.1007/s10551-013-1748-5

Fernández Astudillo, M., Vaillancourt, K., Pineau, P. O., & Amor, B. (2019). Human Health and Ecosystem Impacts of Deep Decarbonization of the Energy System. *Environmental Science and Technology*, *53*(23), 14054–14062. https://doi.org/10.1021/acs.est.9b04923

Fiameni, S., Battiston, S., Castellani, V., Barison, S., & Armelao, L. (2021). Implementing sustainability in laboratory activities: A case study on aluminum titanium nitride based thin film magnetron sputtering deposition onto commercial laminated steel. *Journal of Cleaner Production*, *285*, 124869. https://doi.org/10.1016/j.jclepro.2020.124869

Finnveden, Göran, Hauschild, M. Z., Ekvall, T., Guinée, J., Heijungs, R., Hellweg, S., Koehler, A., Pennington, D., & Suh, S. (2009). Recent developments in Life Cycle Assessment. *Journal of Environmental Management*, *91*(1), 1–21. https://doi.org/10.1016/j.jenvman.2009.06.018

Finnveden, Gran, & Lindfors, L.-G. (1998). Letters to the Editor Data Quality of Life Cycle Inventory D a t a - Rules of Thumb. *Int. J. LCA*, *3*(2), 65–66.

Fishman, T., & Graedel, T. E. (2019). Impact of the establishment of US offshore wind power on neodymium flows. *Nature Sustainability*, *2*(4), 332–338. https://doi.org/10.1038/s41893-019-0252-z

Fotovvati, B., Namdari, N., & Dehghanghadikolaei, A. (2019). On Coating Techniques for Surface Protection: A Review. *Journal of Manufacturing and Materials Processing*, *3*(1), 28. https://doi.org/10.3390/jmmp3010028

Fricko, O., Havlik, P., Rogelj, J., Klimont, Z., Gusti, M., Johnson, N., Kolp, P., Strubegger, M., Valin, H., Amann, M., Ermolieva, T., Forsell, N., Herrero, M., Heyes, C., Kindermann, G., Krey, V., McCollum, D. L., Obersteiner, M., Pachauri, S., … Riahi, K. (2017). The marker quantification of the Shared Socioeconomic Pathway 2: A middle-of-the-road scenario for the 21st century. *Global Environmental Change*, *42*, 251–267. https://doi.org/10.1016/j.gloenvcha.2016.06.004

Friedlingstein, P., Andrew, R. M., Rogelj, J., Peters, G. P., Canadell, J. G., Knutti, R., Luderer, G., Raupach, M. R., Schaeffer, M., Van Vuuren, D. P., & Le Quéré, C. (2014). Persistent growth of CO2 emissions and implications for reaching climate targets. *Nature Geoscience*, *7*(10), 709–715. https://doi.org/10.1038/NGEO2248

Furberg, A., & Arvidsson, R. (2024). Life Cycle Assessment of Synthetic Nanodiamond and Diamond Film Production. *ACS Sustainable Chemistry and Engineering*, *12*(1), 365–374. https://doi.org/10.1021/acssuschemeng.3c05854

Furberg, A., Arvidsson, R., & Molander, S. (2021). A practice-based framework for defining functional units in comparative life cycle assessments of materials. *Journal of Industrial Ecology*, 1–13. https://doi.org/10.1111/jiec.13218

G.P., R., Kamaraj, M., & Bakshi, S. R. (2017). Hardfacing of AISI H13 tool steel with Stellite 21 alloy using cold metal transfer welding process. *Surface and Coatings Technology*, *326*, 63–71. https://doi.org/10.1016/j.surfcoat.2017.07.050

García, V., Margallo, M., Aldaco, R., Urtiaga, A., & Irabien, A. (2013). Environmental sustainability assessment of an innovative Cr (III) passivation process. *ACS Sustainable Chemistry and Engineering*, *1*(5), 481–487. https://doi.org/10.1021/sc3001355

Gaustad, G., Krystofik, M., Bustamante, M., & Badami, K. (2018). Circular economy strategies for mitigating critical material supply issues. *Resources, Conservation and Recycling*, *135*(August 2017), 24–33. https://doi.org/10.1016/j.resconrec.2017.08.002

Gibon, T., & Hahn Menacho, Á. (2023). Parametric Life Cycle Assessment of Nuclear Power for Simplified Models. *Environmental Science and Technology*, *57*(38), 14194–14205. https://doi.org/10.1021/acs.est.3c03190

Gradin, K. T., & Björklund, A. (2021). The common understanding of simplification approaches in published LCA studies—a review and mapping. *International Journal of Life Cycle Assessment*, *26*(1), 50–63. https://doi.org/10.1007/s11367-020-01843-4

Graedel, T. E., & Allenby, B. R. (2010). *Industrial ecology and sustainable engineering* (Internatio). Pearson Education Inc.

Graedel, T. E., Allwood, J., Birat, J. P., Buchert, M., Hagelüken, C., Reck, B. K., Sibley, S. F., & Sonnemann, G. (2011). What do we know about metal recycling rates? *Journal of Industrial Ecology*, *15*(3), 355–366. https://doi.org/10.1111/j.1530-9290.2011.00342.x

Graedel, T. E., Barr, R., Chandler, C., Chase, T., Choi, J., Christoffersen, L., Friedlander, E., Henly, C., Jun, C., Nassar, N. T., Schechner, D., Warren, S., Yang, M. Y., & Zhu, C. (2012). Methodology of metal criticality determination. *Environmental Science and Technology*, *46*(2), 1063–1070. https://doi.org/10.1021/es203534z

Graedel, T. E., Harper, E. M., Nassar, N. T., Nuss, P., Reck, B. K., & Turner, B. L. (2015). Criticality of metals and metalloids. *Proceedings of the National Academy of Sciences of the United States of America*, *112*(14), 4257–4262. https://doi.org/10.1073/pnas.1500415112

Grandell, L., Lehtilä, A., Kivinen, M., Koljonen, T., Kihlman, S., & Lauri, L. S. (2016). Role of critical metals in the future markets of clean energy technologies. *Renewable Energy*, *95*, 53–62. https://doi.org/10.1016/j.renene.2016.03.102

Greffe, T., Margni, M., & Bulle, C. (2023). An instrumental value-based framework for assessing the damages of abiotic resources use in life cycle assessment. *International Journal of Life Cycle Assessment*, *28*(1), 53–69. https://doi.org/10.1007/s11367-022-02107-z

Groen, E. A., Bokkers, E. A. M., Heijungs, R., & de Boer, I. J. M. (2017a). Methods for global sensitivity analysis in life cycle assessment. *International Journal of Life Cycle Assessment*, *22*(7), 1125–1137. https://doi.org/10.1007/s11367-016-1217-3

Groen, E. A., Bokkers, E. A. M., Heijungs, R., & de Boer, I. J. M. (2017b). Methods for global

sensitivity analysis in life cycle assessment. *International Journal of Life Cycle Assessment*, *22*(7), 1125–1137. https://doi.org/10.1007/s11367-016-1217-3

Guan, D., Meng, J., Reiner, D. M., Zhang, N., Shan, Y., Mi, Z., Shao, S., Liu, Z., Zhang, Q., & Davis, S. J. (2018). Structural decline in China's CO2 emissions through transitions in industry and energy systems. *Nature Geoscience*, *11*(8), 551–555. https://doi.org/10.1038/s41561-018-0161-1

Guarino, S., Ucciardello, N., Venettacci, S., & Genna, S. (2017). Life cycle assessment of a new graphene-based electrodeposition process on copper components. *Journal of Cleaner Production*, *165*, 520–529. https://doi.org/10.1016/j.jclepro.2017.07.168

Gülen, S. C. (2013). Modern gas turbine combined cycle. *Turbomachinery International*, *54*(6), 31–35.

GWEC. (2020). Global Wind Report 2019. In *Wind Energy Technology*.

Haapala, K. R., Tiwari, S. K., & Paul, B. K. (2009). An environmental analysis of nanoparticle-assisted diffusion brazing. *Proceedings of the ASME International Manufacturing Science and Engineering Conference 2009, MSEC2009*, *1*, 145–153. https://doi.org/10.1115/MSEC2009-84308

Habib, K., Hansdóttir, S. T., & Habib, H. (2020). Critical metals for electromobility: Global demand scenarios for passenger vehicles, 2015–2050. *Resources, Conservation and Recycling*, *154*(November 2019), 104603. https://doi.org/10.1016/j.resconrec.2019.104603

Hart, N., Brandon, N., & Shemilt, J. (2000). Environmental evaluation of thick film ceramic fabrication techniques for solid oxide fuel cells. *Materials and Manufacturing Processes*, *15*(1), 47–64. https://doi.org/10.1080/10426910008912972

Haszeldine, R. S. (2009). Carbon Capture and Storage: How Green Can Black Be? *Science*, *325*(September), 1647–1652. https://doi.org/10.1126/science.1172246

Hawkins, T. R., Singh, B., Majeau-Bettez, G., & Strømman, A. H. (2013). Comparative Environmental Life Cycle Assessment of Conventional and Electric Vehicles. *Journal of Industrial Ecology*, *17*(1), 53–64. https://doi.org/10.1111/j.1530-9290.2012.00532.x

Hedbrant, J., & Sörme, L. (2001). Data Vagueness and Uncertainties in Urban Heavy-Metal Data Collection. *Water, Air, and Soil Pollution: Focus*, *1*, 43–53. http://dx.doi.org/10.1023/A:1017591718463

Heijungs, R. (1996). Identification of key issues for further investigation in improving the reliability of life-cycle assessments. *Journal of Cleaner Production*, *4*(3–4), 159–166. https://doi.org/10.1016/S0959-6526(96)00042-X

Helbig, C., Thorenz, A., & Tuma, A. (2020). Quantitative assessment of dissipative losses of 18 metals. *Resources, Conservation and Recycling*, *153*(October 2019), 104537. https://doi.org/10.1016/j.resconrec.2019.104537

Held, M., Rosat, N., Georges, G., Pengg, H., & Boulouchos, K. (2021). Lifespans of passenger cars in Europe: empirical modelling of fleet turnover dynamics. *European Transport Research Review*, *13*(1). https://doi.org/10.1186/s12544-020-00464-0

Hertwich, E. G., Gibon, T., Bouman, E. A., Arvesen, A., Suh, S., Heath, G. A., Bergesen, J. D., Ramirez, A., Vega, M. I., & Shi, L. (2015). Integrated life-cycle assessment of electricity-supply scenarios confirms global environmental benefit of low-carbon technologies. *Proceedings of the National Academy of Sciences of the United States of America*, *112*(20), 6277–6282. https://doi.org/10.1073/pnas.1312753111

Hertwich, E., Heeren, N., Kuczenski, B., Majeau-Bettez, G., Myers, R. J., Pauliuk, S., Stadler, K., & Lifset, R. (2018). Nullius in Verba1: Advancing Data Transparency in Industrial Ecology. *Journal of Industrial Ecology*, *22*(1), 6–17. https://doi.org/10.1111/jiec.12738

Hidalgo, V. H., Varela, F. J. B., Menéndez, A. C., & Martínez, S. P. (2001). A comparative study of high-temperature erosion wear of plasma-sprayed NiCrBSiFe and WC-NiCrBSiFe coatings under simulated coal-fired boiler conditions. *Tribology International*, *34*(3), 161–169. https://doi.org/10.1016/S0301-679X(00)00146-8

Hischier, R., Achachlouei, M. A., & Hilty, L. M. (2014). Evaluating the sustainability of electronic media: Strategies for life cycle inventory data collection and their implications for LCA results. *Environmental Modelling and Software*, *56*, 27–36. https://doi.org/10.1016/j.envsoft.2014.01.001

Hochschorner, E., & Finnveden, G. (2003). Evaluation of two simplified lca methods. *The International Journal of Life Cycle Assessment*, *8*(3), 119–128. http://link.springer.com/10.1007/BF02978456

Holmberg, K., & Matthews, A. (2009). *Coatings Tribology. Properties, Mechanisms, Techniques and Applications in Surface Engineering* (B. Briscoe (ed.); Second). Elsevier.

Holmberg, Kenneth, Andersson, P., & Erdemir, A. (2012). Global energy consumption due to friction in passenger cars. *Tribology International*, *47*, 221–234. https://doi.org/10.1016/j.triboint.2011.11.022

Holmberg, Kenneth, & Erdemir, A. (2019). The impact of tribology on energy use and CO2 emission globally and in combustion engine and electric cars. *Tribology International*, *135*(January), 389–396. https://doi.org/10.1016/j.triboint.2019.03.024

Holmberg, Kenneth, & Matthews, A. (2009). *Coatings Tribology: Properties, Mechanisms, Techniques and Applications in Surface Engineering*. https://books.google.com/books?id=SuTrD-AHpyUC&pgis=1

Hou, P., Cai, J., Qu, S., & Xu, M. (2018). Estimating Missing Unit Process Data in Life Cycle Assessment Using a Similarity-Based Approach. *Environmental Science and Technology*, *52*(9), 5259–5267. https://doi.org/10.1021/acs.est.7b05366

Hu, X., Luo, F., Lin, J., Wang, M., & Li, X. (2022). Dynamic material flow analysis of titanium sponge in China: 2000–2019. *Journal of Cleaner Production*, *371*(June), 133704. https://doi.org/10.1016/j.jclepro.2022.133704

Huang, X., Tepylo, N., Pommier-Budinger, V., Budinger, M., Bonaccurso, E., Villedieu, P., & Bennani, L. (2019). A survey of icephobic coatings and their potential use in a hybrid coating/active ice protection system for aerospace applications. *Progress in Aerospace Sciences*, *105*(July 2018), 74–97. https://doi.org/10.1016/j.paerosci.2019.01.002

Huijbregts, M. A. J., Norris, G., Bretz, R., Ciroth, A., Maurice, B., Von Bahr, B., Weidema, B., & De Beaufort, A. S. H. (2001). Framework for modelling data uncertainty in life cycle inventories. *International Journal of Life Cycle Assessment*, *6*(3), 127–132. https://doi.org/10.1007/BF02978728

Hulme, M. (2016). 1.5 °C and climate research after the Paris Agreement. *Nature Climate Change*, *6*(3), 222–224. https://doi.org/10.1038/nclimate2939

Hung, C. R., Ellingsen, L. A. W., & Majeau-Bettez, G. (2020). LiSET: A Framework for Early-Stage Life Cycle Screening of Emerging Technologies. *Journal of Industrial Ecology*, *24*(1), 26–37. https://doi.org/10.1111/jiec.12807

Hunt, K. M. R., & Menon, A. (2020). The 2018 Kerala floods: a climate change perspective. *Climate Dynamics*, *54*(3–4), 2433–2446. https://doi.org/10.1007/s00382-020-05123-7

Huppmann, D., Gidden, M., Fricko, O., Kolp, P., Orthofer, C., Pimmer, M., Kushin, N., Vinca, A., Mastrucci, A., Riahi, K., & Krey, V. (2019a). The MESSAGEix Integrated Assessment Model and the ix modeling platform (ixmp): An open framework for integrated and cross-cutting analysis of energy, climate, the environment, and sustainable development. *Environmental Modelling and Software*, *112*(November 2018), 143–156. https://doi.org/10.1016/j.envsoft.2018.11.012

Huppmann, D., Gidden, M., Fricko, O., Kolp, P., Orthofer, C., Pimmer, M., Kushin, N., Vinca, A., Mastrucci, A., Riahi, K., & Krey, V. (2019b). The MESSAGEix Integrated Assessment Model and the ix modeling platform (ixmp): An open framework for integrated and cross-cutting analysis of energy, climate, the environment, and sustainable development. *Environmental Modelling and Software*, *112*(March 2018), 143–156. https://doi.org/10.1016/j.envsoft.2018.11.012

Ichou, H., Arrousse, N., Berdimurodov, E., & Aliev, N. (2024). Exploring the Advancements in Physical Vapor Deposition Coating: A Review. *Journal of Bio- and Tribo-Corrosion*, *10*(1), 1–14. https://doi.org/10.1007/s40735-023-00806-0

IEA. (2017). Energy Technology Perspectives 2017. In *International Energy Agency (IEA) Publications*. https://doi.org/10.1787/energy_tech-2014-en

IEA. (2019). *World Energy Outlook 2019*. https://www.iea.org/reports/world-energy-outlook-2019

Igartua, A., Mendoza, G., Fernandez, X., Zabala, B., Alberdi, A., Bayon, R., & Aranzabe, A. (2020). Surface treatments solutions to green tribology. *Coatings*, *10*(7).

https://doi.org/10.3390/coatings10070634

Igos, E., Benetto, E., Meyer, R., Baustert, P., & Othoniel, B. (2019). How to treat uncertainties in life cycle assessment studies? *International Journal of Life Cycle Assessment*, *24*(4), 794–807. https://doi.org/10.1007/s11367-018-1477-1

IPCC. (2014). Climate Change 2014 Mitigation of Climate Change. In *Climate Change 2014 Mitigation of Climate Change*. https://doi.org/10.1017/cbo9781107415416

IPCC. (2022). *Climate Change 2022: Impacts, Adaptation and Vulnerability*. Cambridge University Press.

ISO. (2006). *ISO 14040:2006 Environmental management - Life cycle assessment - Principles and framework.* https://www.iso.org/standard/37456.html

Janjua, Z. A., Turnbull, B., Choy, K. L., Pandis, C., Liu, J., Hou, X., & Choi, K. S. (2017). Performance and durability tests of smart icephobic coatings to reduce ice adhesion. *Applied Surface Science*, *407*, 555–564. https://doi.org/10.1016/j.apsusc.2017.02.206

Jaxa-Rozen, M., Pratiwi, A. S., & Trutnevyte, E. (2021). Variance-based global sensitivity analysis and beyond in life cycle assessment: an application to geothermal heating networks. *International Journal of Life Cycle Assessment*, *26*(5), 1008–1026. https://doi.org/10.1007/s11367-021-01921-1

Jin, D., Yang, F., Zou, Z., Gu, L., Zhao, X., Guo, F., & Xiao, P. (2016). A study of the zirconium alloy protection by Cr3C2-NiCr coating for nuclear reactor application. *Surface and Coatings Technology*, *287*, 55–60. https://doi.org/10.1016/j.surfcoat.2015.12.088

Jin, Y., Kim, J., & Guillaume, B. (2016). Review of critical material studies. *Resources, Conservation and Recycling*, *113*, 77–87. https://doi.org/10.1016/j.resconrec.2016.06.003

Kaddoura, M., Majeau-Bettez, G., Amor, B., Moreau, C., & Margni, M. (2022). Investigating the role of surface engineering in mitigating greenhouse gas emissions of energy technologies: An outlook towards 2100. *Sustainable Materials and Technologies*, *32*, e00425. https://doi.org/10.1016/j.susmat.2022.e00425

Kaddoura, M., Majeau-Bettez, G., Amor, B., Poirier, D., & Margni, M. (2024). Estimating and

reducing dissipative losses in thermal spray: A parametrized material flow analysis approach. *Journal of Cleaner Production*, *450*, 141978. https://doi.org/10.1016/j.jclepro.2024.141978

Karka, P., Papadokonstantakis, S., & Kokossis, A. (2022). Digitizing sustainable process development: From ex-post to ex-ante LCA using machine-learning to evaluate bio-based process technologies ahead of detailed design. *Chemical Engineering Science*, *250*, 117339. https://doi.org/10.1016/j.ces.2021.117339

Karmouch, R., Coudé, S., Abel, G., & Ross, G. G. (2009). Icephobic PTFE coatings for wind turbines operating in cold climate conditions. *2009 IEEE Electrical Power and Energy Conference, EPEC 2009*, 0–5. https://doi.org/10.1109/EPEC.2009.5420897

Kawahara, Y. (2016). An overview on corrosion-resistant coating technologies in biomass/waste-to-energy plants in recent decades. *Coatings*, *6*(3). https://doi.org/10.3390/coatings6030034

Keech, P. G., Vo, P., Ramamurthy, S., Chen, J., Jacklin, R., & Shoesmith, D. W. (2014). Design and development of copper coatings for long term storage of used nuclear fuel. *Corrosion Engineering Science and Technology*, *49*(6), 425–430. https://doi.org/10.1179/1743278214Y.0000000206

Kevin Sinisterra-Solís, N., Sanjuán, N., Ribal, J., Estruch, V., Clemente, G., & Rozakis, S. (2024). Developing a composite indicator to assess agricultural sustainability: Influence of some critical choices. *Ecological Indicators*, *161*(October 2023). https://doi.org/10.1016/j.ecolind.2024.111934

Khang, D. S., Tan, R. R., Uy, O. M., Promentilla, M. A. B., Tuan, P. D., Abe, N., & Razon, L. F. (2017). Design of experiments for global sensitivity analysis in life cycle assessment: The case of biodiesel in Vietnam. *Resources, Conservation and Recycling*, *119*, 12–23. https://doi.org/10.1016/j.resconrec.2016.08.016

Kim, A., Mutel, C. L., Froemelt, A., & Hellweg, S. (2022). Global Sensitivity Analysis of Background Life Cycle Inventories. *Environmental Science & Technology*. https://doi.org/10.1021/acs.est.1c07438

Koch, G., Varney, J., Thompson, N., Moghissi, O., Gould, M., & Payer, J. (2016). *International measures of prevention, application, and economics of corrosion technologies study*.

http://impact.nace.org/documents/Nace-International-Report.pdf

Kuczenski, B., Sahin, C., & El Abbadi, A. (2017). Privacy-preserving aggregation in life cycle assessment. *Environment Systems and Decisions*, *37*(1), 13–21. https://doi.org/10.1007/s10669-016-9620-7

Kumar, A., Boy, J., Zatorski, R., & Stephenson, L. D. (2005). Thermal spray and weld repair alloys for the repair of cavitation damage in turbines and pumps: A technical note. *Journal of Thermal Spray Technology*, *14*(2), 177–182. https://doi.org/10.1361/10599630523737

Kumar, D., Palanisamy, S., Krishnan, K., & Alam, M. M. (2023). Life Cycle Assessment of Cold Spray Additive Manufacturing and Conventional Machining of Aluminum Alloy Flange. *Metals*, *13*(10). https://doi.org/10.3390/met13101684

Kwon, D. S., Cho, J. H., & Sohn, S. Y. (2017). Comparison of technology efficiency for CO2 emissions reduction among European countries based on DEA with decomposed factors. *Journal of Cleaner Production*, *151*, 109–120. https://doi.org/10.1016/j.jclepro.2017.03.065

L, G. S., Queirós, G. W., Salazar, J. M. G. De, & Criado, A. J. (2020). *Comparative Life Cycle Analysis (LCA) Study on Two Wear-Resistant Boron Steels : RAEX450 and 30MnB5*. *9*, 2–4. https://doi.org/10.37421/jme.2020.9.551

Laca, A., Herrero, M., & Díaz, M. (2011). Life Cycle Assessment in Biotechnology. In *Comprehensive Biotechnology, Second Edition* (Second Edi, Vol. 2). Elsevier B.V. https://doi.org/10.1016/B978-0-08-088504-9.00140-9

Lacirignola, M., Blanc, P., Girard, R., Pérez-López, P., & Blanc, I. (2017). LCA of emerging technologies: addressing high uncertainty on inputs' variability when performing global sensitivity analysis. *Science of the Total Environment*, *578*, 268–280. https://doi.org/10.1016/j.scitotenv.2016.10.066

Lakatos, I., Titrik, Á., & Orbán, T. (2011). Data Determination of an Internal Combustion Engine for Model Set-Up. *Hungarian Journal of Industry and Chemistry*, *39*(1), 35–40.

Lanzi, E., Verdolini, E., & Haščič, I. (2011). Efficiency-improving fossil fuel technologies for electricity generation: Data selection and trends. *Energy Policy*, *39*(11), 7000–7014. https://doi.org/10.1016/j.enpol.2011.07.052

Larsson Ivanov, O., Honfi, D., Santandrea, F., & Stripple, H. (2019). Consideration of uncertainties in LCA for infrastructure using probabilistic methods. *Structure and Infrastructure Engineering*, *15*(6), 711–724. https://doi.org/10.1080/15732479.2019.1572200

Lask, J., Kam, J., Weik, J., Kiesel, A., Wagner, M., & Lewandowski, I. (2021). A parsimonious model for calculating the greenhouse gas emissions of miscanthus cultivation using current commercial practice in the United Kingdom. *GCB Bioenergy*, *13*(7), 1087–1098. https://doi.org/10.1111/gcbb.12840

Lavery, N. P., Jarvis, D. J., Brown, S. G. R., Adkins, N. J., & Wilson, B. P. (2013). Life cycle assessment of sponge nickel produced by gas atomisation for use in industrial hydrogenation catalysis applications. *International Journal of Life Cycle Assessment*, *18*(2), 362–376. https://doi.org/10.1007/s11367-012-0478-8

Le Guevel, Y., Grégoire, B., Bouchaud, B., Bilhé, P., Pasquet, A., Thiercelin, M., & Pedraza, F. (2016). Influence of the oxide scale features on the electrochemical descaling and stripping of aluminide coatings. *Surface and Coatings Technology*, *292*, 1–10. https://doi.org/10.1016/j.surfcoat.2016.03.019

Leal-Ayala, D. R., Allwood, J. M., Petavratzi, E., Brown, T. J., & Gunn, G. (2015). Mapping the global flow of tungsten to identify key material efficiency and supply security opportunities. *Resources, Conservation and Recycling*, *103*, 19–28. https://doi.org/10.1016/j.resconrec.2015.07.003

Leiden, A., Brand, P., Cerdas, F., Thiede, S., & Herrmann, C. (2020). *Transferring life cycle engineering to surface engineering*. *90*, 557–562. https://doi.org/10.1016/j.procir.2020.02.132

Li, Q., Vogt, M. R., Wang, H., Monticelli, C., & Zanelli, A. (2024). Life cycle assessment of roll-to-roll produced chemical vapor deposition graphene transparent electrodes towards copper foil recycling. *Journal of Cleaner Production*, *468*(July), 143068. https://doi.org/10.1016/j.jclepro.2024.143068

Li, W., Yang, K., Yin, S., Yang, X., Xu, Y., & Lupoi, R. (2018). Solid-state additive manufacturing and repairing by cold spraying: A review. *Journal of Materials Science and Technology*,

34(3), 440–457. https://doi.org/10.1016/j.jmst.2017.09.015

Lieder, M., & Rashid, A. (2016). Towards circular economy implementation: A comprehensive review in context of manufacturing industry. *Journal of Cleaner Production*, *115*, 36–51. https://doi.org/10.1016/j.jclepro.2015.12.042

Lifset, R. J., Eckelman, M. J., Harper, E. M., Hausfather, Z., & Urbina, G. (2012). Metal lost and found: Dissipative uses and releases of copper in the United States 1975-2000. *Science of the Total Environment*, *417–418*, 138–147. https://doi.org/10.1016/j.scitotenv.2011.09.075

Liu, J., Wang, L., Li, F., Li, Y., Ran, X., Kong, L., & Fu, Y. (2021). Evaluation and improvement of the greenness of plasma spraying through life cycle assessment and grey relational analysis. *International Journal of Life Cycle Assessment*, *26*(8), 1586–1606. https://doi.org/10.1007/s11367-021-01910-4

Liu, Q., Shi, M., & Jiang, K. (2009). New power generation technology options under the greenhouse gases mitigation scenario in China. *Energy Policy*, *37*(6), 2440–2449. https://doi.org/10.1016/j.enpol.2009.02.044

Lloyd, S. M., & Ries, R. (2007). Characterizing, propagating, and analyzing uncertainty in life-cycle assessment: A survey of quantitative approaches. *Journal of Industrial Ecology*, *11*(1), 161–179. https://doi.org/10.1162/jiec.2007.1136

Louwen, A., van Sark, W. G. J. H. M., Schropp, R. E. I., Turkenburg, W. C., & Faaij, A. P. C. (2015). Life-cycle greenhouse gas emissions and energy payback time of current and prospective silicon heterojunction solar cell designs. *Prog. Photovolt: Res. Appl.*, *23*(10), 1406–1428. https://doi.org/10.1002/pip.2540

Luderer, G., Pehl, M., Arvesen, A., Gibon, T., Bodirsky, B. L., de Boer, H. S., Fricko, O., Hejazi, M., Humpenöder, F., Iyer, G., Mima, S., Mouratiadou, I., Pietzcker, R. C., Popp, A., van den Berg, M., van Vuuren, D., & Hertwich, E. G. (2019). Environmental co-benefits and adverse side-effects of alternative power sector decarbonization strategies. *Nature Communications*, *10*(1), 1–13. https://doi.org/10.1038/s41467-019-13067-8

Luo, L., Chen, Y., Zhou, M., Shan, X., Lu, J., & Zhao, X. (2022). Progress update on extending the durability of air plasma sprayed thermal barrier coatings. *Ceramics International*, *48*(13),

18021–18034. https://doi.org/10.1016/j.ceramint.2022.04.044

Mahade, S., Curry, N., Björklund, S., Markocsan, N., & Nylén, P. (2015). Thermal conductivity and thermal cyclic fatigue of multilayered Gd2Zr2O7/YSZ thermal barrier coatings processed by suspension plasma spray. *Surface and Coatings Technology*, *283*, 329–336. https://doi.org/10.1016/j.surfcoat.2015.11.009

Mahade, S., Curry, N., Jonnalagadda, K. P., Peng, R. L., Markocsan, N., & Nylén, P. (2019). Influence of YSZ layer thickness on the durability of gadolinium zirconate/YSZ double-layered thermal barrier coatings produced by suspension plasma spray. *Surface and Coatings Technology*, *357*(October 2018), 456–465. https://doi.org/10.1016/j.surfcoat.2018.10.046

Mahade, S., Zhou, D., Curry, N., Markocsan, N., Nylén, P., & Vaßen, R. (2019). Tailored microstructures of gadolinium zirconate/YSZ multi-layered thermal barrier coatings produced by suspension plasma spray: Durability and erosion testing. *Journal of Materials Processing Technology*, *264*(April 2018), 283–294. https://doi.org/10.1016/j.jmatprotec.2018.09.016

Månberger, A., & Stenqvist, B. (2018). Global metal flows in the renewable energy transition: Exploring the effects of substitutes, technological mix and development. *Energy Policy*, *119*(January), 226–241. https://doi.org/10.1016/j.enpol.2018.04.056

Manca, M., Cannavale, A., De Marco, L., Aricò, A. S., Cingolani, R., & Gigli, G. (2009). Durable superhydrophobic and antireflective surfaces by trimethylsilanized silica nanoparticles-based sol-gel processing. *Langmuir*, *25*(11), 6357–6362. https://doi.org/10.1021/la804166t

Mansoor, S., Farooq, I., Kachroo, M. M., Mahmoud, A. E. D., Fawzy, M., Popescu, S. M., Alyemeni, M. N., Sonne, C., Rinklebe, J., & Ahmad, P. (2022). Elevation in wildfire frequencies with respect to the climate change. *Journal of Environmental Management*, *301*(September 2021), 113769. https://doi.org/10.1016/j.jenvman.2021.113769

Marchese, D. C., Bates, M. E., Keisler, J. M., Alcaraz, M. L., Linkov, I., & Olivetti, E. A. (2018). Value of information analysis for life cycle assessment: Uncertain emissions in the green manufacturing of electronic tablets. *Journal of Cleaner Production*, *197*, 1540–1545. https://doi.org/10.1016/j.jclepro.2018.06.113

MatWeb. (2023a). *Molybdenum, Mo, Recrystallized*.

https://www.matweb.com/search/DataSheet.aspx?MatGUID=20341f89fd8e43f1995b4b9a2a8d9dbe

MatWeb. (2023b). *Sandvik Kanthal Nicrosil Thermocouple wire*.

MatWeb. (2023c). *Tungsten Carbide, WC*.

Meijer, A., Huijbregts, M. A. J., Schermer, J. J., & Reijnders, L. (2003). Life-cycle assessment of photovoltaic modules: Comparison of mc-Si, InGaP and InGaP/mc-Si solar modules. *Progress in Photovoltaics: Research and Applications*, *11*(4), 275–287. https://doi.org/10.1002/pip.489

Mendoza Beltran, A., Cox, B., Mutel, C., van Vuuren, D. P., Font Vivanco, D., Deetman, S., Edelenbosch, O. Y., Guinée, J., & Tukker, A. (2018). When the Background Matters: Using Scenarios from Integrated Assessment Models in Prospective Life Cycle Assessment. *Journal of Industrial Ecology*, *00*(0), 1–16. https://doi.org/10.1111/jiec.12825

Mendoza Beltran, A., Cox, B., Mutel, C., van Vuuren, D. P., Font Vivanco, D., Deetman, S., Edelenbosch, O. Y., Guinée, J., & Tukker, A. (2020). When the Background Matters: Using Scenarios from Integrated Assessment Models in Prospective Life Cycle Assessment. *Journal of Industrial Ecology*, *24*(1), 64–79. https://doi.org/10.1111/jiec.12825

Mendoza Beltran, A., Prado, V., Font Vivanco, D., Henriksson, P. J. G., Guinée, J. B., & Heijungs, R. (2018). Quantified Uncertainties in Comparative Life Cycle Assessment: What Can Be Concluded? *Environmental Science and Technology*, *52*(4), 2152–2161. https://doi.org/10.1021/acs.est.7b06365

Merlo, A., Duminica, F., Daniel, A., & Léonard, G. (2023). Techno-Economic Analysis and Life Cycle Assessment of High-Velocity Oxy-Fuel Technology Compared to Chromium Electrodeposition. *Materials*, *16*(10). https://doi.org/10.3390/ma16103678

Merlo, A., & Léonard, G. (2021). Magnetron sputtering vs. Electrodeposition for hard chrome coatings: A comparison of environmental and economic performances. *Materials*, *14*(14). https://doi.org/10.3390/ma14143823

Miyamoto, N. (2013). Automotive Coatings and Applications. In *Thermal Spray Technology* (Vol. 5A, pp. 298–305). ASM International. https://doi.org/10.31399/asm.hb.v05a.a0005740

Moign, A., Vardelle, A., Themelis, N. J., & Legoux, J. G. (2010). Life cycle assessment of using powder and liquid precursors in plasma spraying: The case of yttria-stabilized zirconia. *Surface and Coatings Technology*, *205*(2), 668–673. https://doi.org/10.1016/j.surfcoat.2010.07.015

Momber, A. W., & Marquardt, T. (2018). Protective coatings for offshore wind energy devices (OWEAs): a review. *Journal of Coatings Technology and Research*, *15*(1), 13–40. https://doi.org/10.1007/s11998-017-9979-5

Moreno Ruiz, E., Valsasina, L., Brunner, F., Symeonidis, A., FitzGerald, D., Treyer, K., Bourgault, G., & Wernet, G. (2018). *Documentation of changes implemented in ecoinvent database v3.5. Ecoinvent, Zürich, Switzerland. 5*, 1–97.

Moss, R. L., Tzimas, E., Kara, H., Willis, P., & Kooroshy, J. (2013). The potential risks from metals bottlenecks to the deployment of Strategic Energy Technologies. *Energy Policy*, *55*, 556–564. https://doi.org/10.1016/j.enpol.2012.12.053

Mutel, C. L., & Hellweg, S. (2009). Regionalized life cycle assessment: Computational methodology and application to inventory databases. *Environmental Science and Technology*, *43*(15), 5797–5803. https://doi.org/10.1021/es803002j

Nadolny, K., Kapłonek, W., Sutowska, M., Sutowski, P., Myśliński, P., Gilewicz, A., & Warcholiński, B. (2021). Moving towards sustainable manufacturing by extending the tool life of the pine wood planing process using the AlCrBN coating. *Sustainable Materials and Technologies*, *28*. https://doi.org/10.1016/j.susmat.2021.e00259

Nagy, D. (2023). *Personal communication with Douglas Nagy of Liburdi. Phone call, 20 January 2023*.

Nakajima, K., Takeda, O., Miki, T., Matsubae, K., & Nagasaka, T. (2016). Recycling and Dissipation of Metals: Distribution of Elements in the Metal, Slag, and Gas Phases During Metallurgical Processing. *Metal Sustainability: Global Challenges, Consequences, and Prospects*, 453–466. https://doi.org/10.1002/9781119009115.ch19

Nassar, N. T. (2017). Shifts and trends in the global anthropogenic stocks and flows of tantalum. *Resources, Conservation and Recycling*, *125*(July), 233–250.

https://doi.org/10.1016/j.resconrec.2017.06.002

Nassar, N. T., Lederer, G. W., Brainard, J. L., Padilla, A. J., & Lessard, J. D. (2021). Rock-to-Metal Ratio: A Foundational Metric for Understanding Mine Wastes. *Environmental Science and Technology*. https://doi.org/10.1021/acs.est.1c07875

Nguyen, R. T., Fishman, T., Zhao, F., Imholte, D. D., & Graedel, T. E. (2018). Analyzing critical material demand: A revised approach. *Science of the Total Environment*, *630*, 1143–1148. https://doi.org/10.1016/j.scitotenv.2018.02.283

Nogueira De Oliveira, L. P., Rodriguez Rochedo, P. R., Portugal-Pereira, J., Hoffmann, B. S., Aragão, R., Milani, R., De Lucena, A. F. P., Szklo, A., & Schaeffer, R. (2016). Critical technologies for sustainable energy development in Brazil: Technological foresight based on scenario modelling. *Journal of Cleaner Production*, *130*, 12–24. https://doi.org/10.1016/j.jclepro.2016.03.010

Nogueira, L. P. P., Frossard Pereira de Lucena, A., Rathmann, R., Rua Rodriguez Rochedo, P., Szklo, A., & Schaeffer, R. (2014). Will thermal power plants with CCS play a role in Brazil's future electric power generation? *International Journal of Greenhouse Gas Control*, *24*, 115–123. https://doi.org/10.1016/j.ijggc.2014.03.002

NRC. (2008). *Minerals, Critical Materials And the U.S. Economy*.

NTM. (2023a). *Air emissions calculations*. https://www.transportmeasures.org/en/wiki/manuals/air/air-methods/calculating-emissions-air-transports/

NTM. (2023b). *passenger Occupancy*. https://www.transportmeasures.org/en/wiki/manuals/10-road-passenger-car-transport/10-7-passenger-occupancy/

NTM. (2023c). *Vehicle type characteristics and default load factors*.

O'Neill, B. C., Kriegler, E., Ebi, K. L., Kemp-Benedict, E., Riahi, K., Rothman, D. S., van Ruijven, B. J., van Vuuren, D. P., Birkmann, J., Kok, K., Levy, M., & Solecki, W. (2017). The roads ahead: Narratives for shared socioeconomic pathways describing world futures in the 21st century. *Global Environmental Change*, *42*, 169–180. https://doi.org/10.1016/j.gloenvcha.2015.01.004

Oerlikon. (2014). *Solutions Flash: Robust coating solutions for hydropower turbines extend operating life and maintain efficiency* (Issue October). https://www.oerlikon.com/ecoma/files/SF-0023.1_HydroTurbineCoatingSolutions_EN.pdf?download=true

Owsianiak, M., van Oers, L., Drielsma, J., Laurent, A., & Hauschild, M. Z. (2022). Identification of dissipative emissions for improved assessment of metal resources in life cycle assessment. *Journal of Industrial Ecology*, *26*(2), 406–420. https://doi.org/10.1111/jiec.13209

Pacala, S., & Socolow, R. (2004). Stabilization Wedges: Solving the Climate Problem for the Next 50 Years with Current Technologies. *Science*, *305*(August), 968–972. https://doi.org/10.1126/science.1100103

Padey, P., Girard, R., Le Boulch, D., & Blanc, I. (2013). From LCAs to simplified models: A generic methodology applied to wind power electricity. *Environmental Science and Technology*, *47*(3), 1231–1238. https://doi.org/10.1021/es303435e

Panwar, N. L., Kaushik, S. C., & Kothari, S. (2011). Role of renewable energy sources in environmental protection: A review. *Renewable and Sustainable Energy Reviews*, *15*(3), 1513–1524. https://doi.org/10.1016/j.rser.2010.11.037

Parent, O., & Ilinca, A. (2011). Anti-icing and de-icing techniques for wind turbines: Critical review. *Cold Regions Science and Technology*, *65*(1), 88–96. https://doi.org/10.1016/j.coldregions.2010.01.005

Patouillard, L., Collet, P., Lesage, P., Tirado Seco, P., Bulle, C., & Margni, M. (2019). Prioritizing regionalization efforts in life cycle assessment through global sensitivity analysis: a sector meta-analysis based on ecoinvent v3. *International Journal of Life Cycle Assessment*, *24*(12), 2238–2254. https://doi.org/10.1007/s11367-019-01635-5

Pauliuk, S. (2020). Making sustainability science a cumulative effort. *Nature Sustainability*, *3*(1), 2–4. https://doi.org/10.1038/s41893-019-0443-7

Pauliuk, S., Arvesen, A., Stadler, K., & Hertwich, E. G. (2017). Industrial ecology in integrated assessment models. *Nature Climate Change*, *7*(1), 13–20. https://doi.org/10.1038/nclimate3148

Pauliuk, S., Majeau-Bettez, G., Mutel, C. L., Steubing, B., & Stadler, K. (2015). Lifting Industrial Ecology Modeling to a New Level of Quality and Transparency: A Call for More Transparent Publications and a Collaborative Open Source Software Framework. *Journal of Industrial Ecology*, *19*(6), 937–949. https://doi.org/10.1111/jiec.12316

Pauliuk, S., Wang, T., & Müller, D. B. (2012). Moving toward the circular economy: The role of stocks in the Chinese steel cycle. *Environmental Science and Technology*, *46*(1), 148–154. https://doi.org/10.1021/es201904c

Pedneault, J., Majeau-Bettez, G., Krey, V., & Margni, M. (2021). What future for primary aluminium production in a decarbonizing economy? *Global Environmental Change*, *69*, 102316. https://doi.org/https://doi.org/10.1016/j.gloenvcha.2021.102316

Pedneault, J., Majeau-Bettez, G., Pauliuk, S., & Margni, M. (2022). Sector-specific scenarios for future stocks and flows of aluminum: An analysis based on shared socioeconomic pathways. *Journal of Industrial Ecology*, *26*(5), 1728–1746. https://doi.org/10.1111/jiec.13321

Pehl, M., Arvesen, A., Humpenöder, F., Popp, A., Hertwich, E. G., & Luderer, G. (2017). Understanding future emissions from low-carbon power systems by integration of life-cycle assessment and integrated energy modelling. *Nature Energy*, *2*(12), 939–945. https://doi.org/10.1038/s41560-017-0032-9

Peng, C., Xing, S., Yuan, Z., Xiao, J., Wang, C., & Zeng, J. (2012). Preparation and anti-icing of superhydrophobic PVDF coating on a wind turbine blade. *Applied Surface Science*, *259*, 764–768. https://doi.org/10.1016/j.apsusc.2012.07.118

Peng, S., Li, T., Li, M., Guo, Y., Shi, J., Tan, G. Z., & Zhang, H. (2019). An integrated decision model of restoring technologies selection for engine remanufacturing practice. *Journal of Cleaner Production*, *206*, 598–610. https://doi.org/10.1016/j.jclepro.2018.09.176

Piccinno, F., Hischier, R., Seeger, S., & Som, C. (2016). From laboratory to industrial scale: a scale-up framework for chemical processes in life cycle assessment studies. *Journal of Cleaner Production*, *135*, 1085–1097. https://doi.org/10.1016/j.jclepro.2016.06.164

Pini, M., González, E. I. C., Neri, P., Siligardi, C., & Ferrari, A. M. (2017). Assessment of environmental performance of TiO 2 nanoparticles coated self-cleaning float glass. *Coatings*,

7(1), 1–16. https://doi.org/10.3390/coatings7010008

Poirier, D. (2022). *Personal communication with Dominique Poirier of National Research Council (NRC) of Canada. Phone call, 21 December 2022*.

Pollack, M. (2018). Replacement for Hard Chrome Plating on Aircraft Landing Gear. *Thermal Spray Technology*, *5*, 296–297. https://doi.org/10.31399/asm.hb.v05a.a0005739

Posset, U., Harsch, M., Rougier, A., Herbig, B., Schottner, G., & Sextl, G. (2012). Environmental assessment of electrically controlled variable light transmittance devices. *RSC Advances*, *2*(14), 5990–5996. https://doi.org/10.1039/c2ra20148h

Prakash, V., Ghosh, S., & Kanjilal, K. (2020). Costs of avoided carbon emission from thermal and renewable sources of power in India and policy implications. *Energy*, *200*(February), 117522. https://doi.org/10.1016/j.energy.2020.117522

Preston, B. L., Westaway, R. M., & Yuen, E. J. (2011). Climate adaptation planning in practice: An evaluation of adaptation plans from three developed nations. In *Mitigation and Adaptation Strategies for Global Change* (Vol. 16, Issue 4). https://doi.org/10.1007/s11027-010-9270-x

Prochatzki, G., Mayer, R., Haenel, J., Schmidt, A., Götze, U., Ulber, M., Fischer, A., & Arnold, M. G. (2023). A critical review of the current state of circular economy in the automotive sector. *Journal of Cleaner Production*, *425*(April), 138787. https://doi.org/10.1016/j.jclepro.2023.138787

Puy, A., Saltelli, A., Piano, S. Lo, & Levin, S. A. (2022). sensobol: An R Package to Compute Variance-Based Sensitivity Indices. *Journal of Statistical Software*, *102*(5). https://doi.org/10.18637/jss.v102.i05

Raftery, A. E., Zimmer, A., Frierson, D. M. W., Startz, R., & Liu, P. (2017). Less than 2 °c warming by 2100 unlikely. *Nature Climate Change*, *7*(9), 637–641. https://doi.org/10.1038/nclimate3352

Rech, S., Trentin, A., Vezzù, S., Vedelago, E., Legoux, J. G., & Irissou, E. (2014). Different Cold Spray Deposition Strategies: Single- and Multi-layers to Repair Aluminium Alloy Components. *Journal of Thermal Spray Technology*, *23*(8), 1237–1250. https://doi.org/10.1007/s11666-014-0141-y

Reinhard, J., Mutel, C. L., Wernet, G., Zah, R., & Hilty, L. M. (2016). Contribution-based prioritization of LCI database improvements: Method design, demonstration, and evaluation. *Environmental Modelling and Software*, *86*, 204–218. https://doi.org/10.1016/j.envsoft.2016.09.018

Reinhard, J., Wernet, G., Zah, R., Heijungs, R., & Hilty, L. M. (2019). Contribution-based prioritization of LCI database improvements: the most important unit processes in ecoinvent. *International Journal of Life Cycle Assessment*, *24*(10), 1778–1792. https://doi.org/10.1007/s11367-019-01602-0

Ridgeway, N. B. (2016). *Thermal barrier coating with improved adhesion* (Patent No. US20160215382A1). US Patent.

Roes, A. L., Tabak, L. B., Shen, L., Nieuwlaar, E., & Patel, M. K. (2010). Influence of using nanoobjects as filler on functionality-based energy use of nanocomposites. *Journal of Nanoparticle Research*, *12*(6), 2011–2028. https://doi.org/10.1007/s11051-009-9819-3

Romero-Gámez, M., Antón, A., Leyva, R., & Suárez-Rey, E. M. (2017). Inclusion of uncertainty in the LCA comparison of different cherry tomato production scenarios. *International Journal of Life Cycle Assessment*, *22*(5), 798–811. https://doi.org/10.1007/s11367-016-1225-3

Roy, P., Mohanty, A. K., & Misra, M. (2023). Prospects of carbon capture, utilization and storage for mitigating climate change. *Environmental Science: Advances*, *2*(3), 409–423. https://doi.org/10.1039/d2va00236a

Rúa Ramirez, E., Silvello, A., Torres Diaz, E., Tornese, F., Gnoni, M. G., & Garcia Cano, I. (2024). A comparison of cold spray, atmospheric plasma spray and high velocity oxy fuel processes for WC-Co coatings deposition through LCA and LCCA. *Heliyon*, *10*(19), e38961. https://doi.org/10.1016/j.heliyon.2024.e38961

Rúa Ramirez, Edwin, Silvello, A., Torres Diaz, E., Vaz, R. F., & Cano, I. G. (2024). A Comparative Study of the Life Cycle Inventory of Thermally Sprayed WC-12Co Coatings. *Metals*, *14*(4). https://doi.org/10.3390/met14040431

Sampath, S., Srinivasan, V., Valarezo, A., Vaidya, A., & Streibl, T. (2009). Sensing, control, and in situ measurement of coating properties: An integrated approach toward establishing

process-property correlations. *Journal of Thermal Spray Technology*, *18*(2), 243–255. https://doi.org/10.1007/s11666-009-9314-5

Sánchez-Cruces, E., Barrera-Calva, E., Lavanderos, K., & González, F. (2014). Life cycle analysis (LCA) of solar selective thin films by electrodeposition and by sol-gel techniques. *Energy Procedia*, *57*(186), 2812–2818. https://doi.org/10.1016/j.egypro.2014.10.314

Sangal, S., Singhal, M. K., & Saini, R. P. (2018). Hydro-abrasive erosion in hydro turbines: a review. *International Journal of Green Energy*, *15*(4), 232–253. https://doi.org/10.1080/15435075.2018.1431546

Sarjas, H., Goljandin, D., Kulu, P., Mikli, V., Surženkov, A., & Vuoristo, P. (2012). Wear resistant thermal sprayed composite coatings based on iron self-fluxing alloy and recycled cermet powders. *Medziagotyra*, *18*(1), 34–39. https://doi.org/10.5755/j01.ms.18.1.1338

Schmitt, J., Offermann, F., Söder, M., Frühauf, C., & Finger, R. (2022). Extreme weather events cause significant crop yield losses at the farm level in German agriculture. *Food Policy*, *112*(August). https://doi.org/10.1016/j.foodpol.2022.102359

Schrijvers, D., Hool, A., Blengini, G. A., Chen, W. Q., Dewulf, J., Eggert, R., van Ellen, L., Gauss, R., Goddin, J., Habib, K., Hagelüken, C., Hirohata, A., Hofmann-Amtenbrink, M., Kosmol, J., Le Gleuher, M., Grohol, M., Ku, A., Lee, M. H., Liu, G., … Wäger, P. A. (2020). A review of methods and data to determine raw material criticality. *Resources, Conservation and Recycling*, *155*(October 2019), 104617. https://doi.org/10.1016/j.resconrec.2019.104617

Selvakkumaran, S., & Limmeechokchai, B. (2013). Energy security and co-benefits of energy efficiency improvement in three Asian countries. *Renewable and Sustainable Energy Reviews*, *20*, 491–503. https://doi.org/10.1016/j.rser.2012.12.004

Serres, N., Hlawka, F., Costil, S., Langlade, C., & Machi, F. (2010). Microstructures and environmental assessment of metallic NiCrBSi coatings manufactured via hybrid plasma spray process. *Surface and Coatings Technology*, *205*(4), 1039–1046. https://doi.org/10.1016/j.surfcoat.2010.03.048

Serres, N., Hlawka, F., Costil, S., Langlade, C., & MacHi, F. (2011). Corrosion properties of in situ laser remelted NiCrBSi coatings comparison with hard chromium coatings. *Journal of*

Materials Processing Technology, *211*(1), 133–140. https://doi.org/10.1016/j.jmatprotec.2010.09.005

Serres, N., Hlawka, F., Costil, S., Langlade, C., Machi, F., & Cornet, A. (2009). Dry coatings and ecodesign part. 1 - Environmental performances and chemical properties. *Surface and Coatings Technology*, *204*(1–2), 187–196. https://doi.org/10.1016/j.surfcoat.2009.07.012

Shah, I. H., Hadjipantelis, N., Walter, L., Myers, R. J., & Gardner, L. (2023). Environmental life cycle assessment of wire arc additively manufactured steel structural components. *Journal of Cleaner Production*, *389*(October 2022), 136071. https://doi.org/10.1016/j.jclepro.2023.136071

Siligardi, C., Barbi, S., Casini, R., Tagliaferri, L., & Remigio, V. (2017). Recycling of yttria-stabilized zirconia waste powders in glazes suitable for ceramic tiles. *International Journal of Applied Ceramic Technology*, *14*(6), 1236–1247. https://doi.org/10.1111/ijac.12702

Sobol, I. M. (2001). Global sensitivity indices for nonlinear mathematical models and their Monte Carlo estimates. *Mathematics and Computers in Simulation*, *55*(1–3), 271–280. https://doi.org/10.1016/S0378-4754(00)00270-6

Sollars, R., & Beitelman, A. D. (2011). *Cavitation-Resistant Coatings for Hydropower Turbines Construction Engineering*. *June*.

Sonoya, K., & Kitiara, S. (1997). Life cycle assessment for spray coatings applied to the heating tubes of PFBC boiler. *Tetsu-to-Hagane*, *83*, 78–83.

Spreafico, C. (2024). Prospective life cycle assessment of titanium powder atomization. *Journal of Cleaner Production*, *468*(July), 143104. https://doi.org/10.1016/j.jclepro.2024.143104

Spreafico, C., Landi, D., & Russo, D. (2023). A new method of patent analysis to support prospective life cycle assessment of eco-design solutions. *Sustainable Production and Consumption*, *38*(March), 241–251. https://doi.org/10.1016/j.spc.2023.04.006

Stenberg, V., Rydén, M., & Lind, F. (2023). Evaluation of bed-to-tube heat transfer in a fluidized bed heat exchanger in a 75 MWth CFB boiler for municipal solid waste fuels. *Fuel*, *339*(October 2022), 1–9. https://doi.org/10.1016/j.fuel.2022.127375

Strafford, K. N., & Subramanian, C. (1995). Surface engineering: An enabling technology for manufacturing industry. *Journal of Materials Processing Technology*, *53*, 393–403. https://doi.org/10.1016/0924-0136(95)01996-R

Takuma, Y., Sugimori, H., Ando, E., Mizumoto, K., & Tahara, K. (2018). Comparison of the environmental impact of the conventional nickel electroplating and the new nickel electroplating. *International Journal of Life Cycle Assessment*, *23*(8), 1609–1623. https://doi.org/10.1007/s11367-017-1375-y

Tang, Z. (2022). *Personal communication with Zhaolin Tang of Mettech. Phone call, 20 December 2022*.

Tejero-Martin, D., Rezvani Rad, M., McDonald, A., & Hussain, T. (2019). Beyond Traditional Coatings: A Review on Thermal-Sprayed Functional and Smart Coatings. In *Journal of Thermal Spray Technology* (Vol. 28, Issue 4). Springer US. https://doi.org/10.1007/s11666-019-00857-1

Thévenot, A., Rivera, J. L., Wilfart, A., Maillard, F., Hassouna, M., Senga-Kiesse, T., Le Féon, S., & Aubin, J. (2018). Mealworm meal for animal feed: Environmental assessment and sensitivity analysis to guide future prospects. *Journal of Cleaner Production*, *170*, 1260–1267. https://doi.org/10.1016/j.jclepro.2017.09.054

Thomassen, G., Van Passel, S., & Dewulf, J. (2020). A review on learning effects in prospective technology assessment. *Renewable and Sustainable Energy Reviews*, *130*(June), 109937. https://doi.org/10.1016/j.rser.2020.109937

Tokimatsu, K., Wachtmeister, H., McLellan, B., Davidsson, S., Murakami, S., Höök, M., Yasuoka, R., & Nishio, M. (2017). Energy modeling approach to the global energy-mineral nexus: A first look at metal requirements and the 2 °C target. *Applied Energy*, *207*, 494–509. https://doi.org/10.1016/j.apenergy.2017.05.151

Tripathy, K. P., Mukherjee, S., Mishra, A. K., E., M. M., & Williams, A. P. (2023). Climate change will accelerate the high- end risk of compound drought and heatwave events. *Proceedings of the National Academy of Sciences*, *120*(28), e2219825120. https://doi.org/10.1073/pnas.2219825120

Tsoy, N., Prado, V., Wypkema, A., Quist, J., & Mourad, M. (2019). Anticipatory Life Cycle Assessment of sol-gel derived anti-reflective coating for greenhouse glass. *Journal of Cleaner Production*, *221*, 365–376. https://doi.org/10.1016/j.jclepro.2019.02.246

Tucker Jr., R. C. (2013). Introduction to Thermal Spray Technology. In Robert C Tucker Jr. (Ed.), *Thermal Spray Technology* (Vol. 5A, p. 0). ASM International. https://doi.org/10.31399/asm.hb.v05a.a0005706

Turconi, R., Boldrin, A., & Astrup, T. (2013). Life cycle assessment (LCA) of electricity generation technologies: Overview, comparability and limitations. *Renewable and Sustainable Energy Reviews*, *28*, 555–565. https://doi.org/10.1016/j.rser.2013.08.013

Ulion, N. E., Maloney, M. J., Trubelja, M. F., & Litton, D. A. (2005). *Thermal barrier coating having an interfacial layer for spallation life enhancement and low conductivity* (Patent No. EP1591550B1). European Patent Office.

US Department of Energy. (2020a). *Average Annual Vehicle Miles Traveled by Major Vehicle Category*. https://afdc.energy.gov/data/10309

US Department of Energy. (2020b). *What is generation capacity?* https://www.energy.gov/ne/articles/what-generation-capacity#:~:text=The Capacity Factor,power all of the time.

USA Today. (2012). *Ask the Captain: How far does a jet fly during its lifetime*. https://www.usatoday.com/story/travel/columnist/cox/2012/11/19/ask-the-captain-how-far-does-a-jet-fly-during-its-lifetime/1712269/

van der Giesen, C., Cucurachi, S., Guinée, J., Kramer, G. J., & Tukker, A. (2020). A critical view on the current application of LCA for new technologies and recommendations for improved practice. *Journal of Cleaner Production*, *259*. https://doi.org/10.1016/j.jclepro.2020.120904

van Nes, N., & Cramer, J. (2006). Product lifetime optimization: a challenging strategy towards more sustainable consumption patterns. *Journal of Cleaner Production*, *14*(15–16), 1307–1318. https://doi.org/10.1016/j.jclepro.2005.04.006

van Oers, L., Guinée, J. B., Heijungs, R., Schulze, R., Alvarenga, R. A. F., Dewulf, J., & Drielsma, J. (2024). Top-down characterization of resource use in LCA: from problem definition of

resource use to operational characterization factors for resource inaccessibility of elements in a short-term time perspective. *International Journal of Life Cycle Assessment*, *29*(7), 1315–1338. https://doi.org/10.1007/s11367-024-02297-8

Van Vuuren, D. P., Den Elzen, M. G. J., Lucas, P. L., Eickhout, B., Strengers, B. J., Van Ruijven, B., Wonink, S., & Van Houdt, R. (2007). Stabilizing greenhouse gas concentrations at low levels: An assessment of reduction strategies and costs. *Climatic Change*, *81*(2), 119–159. https://doi.org/10.1007/s10584-006-9172-9

Vandepaer, L., Panos, E., Bauer, C., & Amor, B. (2020). Energy System Pathways with Low Environmental Impacts and Limited Costs: Minimizing Climate Change Impacts Produces Environmental Cobenefits and Challenges in Toxicity and Metal Depletion Categories. *Environmental Science & Technology*, *54*(8), 5081–5092. https://doi.org/10.1021/acs.est.9b06484

Vardelle, A., Moreau, C., Akedo, J., Ashrafizadeh, H., Berndt, C. C., Berghaus, J. O., Boulos, M., Brogan, J., Bourtsalas, A. C., Dolatabadi, A., Dorfman, M., Eden, T. J., Fauchais, P., Fisher, G., Gaertner, F., Gindrat, M., Henne, R., Hyland, M., Irissou, E., … Vuoristo, P. (2016). The 2016 Thermal Spray Roadmap. *Journal of Thermal Spray Technology*, *25*(8), 1376–1440. https://doi.org/10.1007/s11666-016-0473-x

Vaßen, R., Jarligo, M. O., Steinke, T., Mack, D. E., & Stöver, D. (2010). Overview on advanced thermal barrier coatings. *Surface and Coatings Technology*, *205*(4), 938–942. https://doi.org/10.1016/j.surfcoat.2010.08.151

Vassen, R., & Mauer, G. (2013). Renewable Energy Applications. In *Thermal Spray Technology* (Vol. 5, Issue A, pp. 318–321). ASM International. https://doi.org/10.31399/asm.hb.v05a.a0005708

Viscusi, A., Perna, A. S., & Astarita, A. (2023). A Preliminary Study on the Sustainability of Metallization of Polymer Matrix Composites through Cold Spray. *Journal of Materials Engineering and Performance*, *32*(9), 3888–3895. https://doi.org/10.1007/s11665-023-07853-1

Viswanathan, R., Henry, J. F., Tanzosh, J., Stanko, G., Shingledecker, J., Vitalis, B., & Purgert, R.

(2005). U.S. Program on materials technology for ultra-supercritical coal power plants. *Journal of Materials Engineering and Performance*, *14*(3), 281–292. https://doi.org/10.1361/10599490524039

VOITH. (2021). *Francis turbines*.

Von Pfingsten, S., Broll, D. O., Von Der Assen, N., & Bardow, A. (2017). Second-Order Analytical Uncertainty Analysis in Life Cycle Assessment. *Environmental Science and Technology*, *51*(22), 13199–13204. https://doi.org/10.1021/acs.est.7b01406

Vuoristo, P. (2014). Thermal Spray Coating Processes. In *Comprehensive Materials Processing* (Vol. 4). Elsevier. https://doi.org/10.1016/B978-0-08-096532-1.00407-6

Waldbillig, D., & Kesler, O. (2011). Effect of suspension plasma spraying process parameters on YSZ coating microstructure and permeability. *Surface and Coatings Technology*, *205*(23–24), 5483–5492. https://doi.org/10.1016/j.surfcoat.2011.06.019

Wan, H., Xia, J., Zhang, L., She, D., Xiao, Y., & Zou, L. (2015). Sensitivity and interaction analysis based on Sobol' method and its application in a distributed flood forecasting model. *Water (Switzerland)*, *7*(6), 2924–2951. https://doi.org/10.3390/w7062924

Wang, P., Li, W., & Kara, S. (2018). Dynamic life cycle quantification of metallic elements and their circularity, efficiency, and leakages. *Journal of Cleaner Production*, *174*, 1492–1502. https://doi.org/10.1016/j.jclepro.2017.11.032

Wang, Qiang, Jiang, X. ting, Ge, S., & Jiang, R. (2019). Is economic growth compatible with a reduction in CO2 emissions? Empirical analysis of the United States. *Resources, Conservation and Recycling*, *151*(July), 104443. https://doi.org/10.1016/j.resconrec.2019.104443

Wang, Qinqiang, Jin, Z., Zhao, Y., Niu, L., & Guo, J. (2021). A comparative study on tool life and wear of uncoated and coated cutting tools in turning of tungsten heavy alloys. *Wear*, *482–483*(November 2020), 203929. https://doi.org/10.1016/j.wear.2021.203929

Wang, T. (2017). The gas and steam turbines and combined cycle in IGCC systems. In *Integrated Gasification Combined Cycle (IGCC) Technologies*. Elsevier Ltd. https://doi.org/10.1016/B978-0-08-100167-7.00028-7

Wang, X., Feng, F., Klecka, M. A., Mordasky, M. D., Garofano, J. K., El-Wardany, T., Nardi, A., & Champagne, V. K. (2015). Characterization and modeling of the bonding process in cold spray additive manufacturing. *Additive Manufacturing*, *8*, 149–162. https://doi.org/10.1016/j.addma.2015.03.006

Wei, W., Larrey-Lassalle, P., Faure, T., Dumoulin, N., Roux, P., & Mathias, J. D. (2015). How to conduct a proper sensitivity analysis in life cycle assessment: Taking into account correlations within LCI data and interactions within the LCA calculation model. *Environmental Science and Technology*, *49*(1), 377–385. https://doi.org/10.1021/es502128k

Wernet, G., Bauer, C., Steubing, B., Reinhard, J., Moreno-Ruiz, E., & Weidema, B. (2016). The ecoinvent database version 3 (part I): overview and methodology. *International Journal of Life Cycle Assessment*, *21*(9), 1218–1230. https://doi.org/10.1007/s11367-016-1087-8

Wigger, H., Steinfeldt, M., & Bianchin, A. (2017). Environmental benefits of coatings based on nano-tungsten-carbide cobalt ceramics. *Journal of Cleaner Production*, *148*, 212–222. https://doi.org/10.1016/j.jclepro.2017.01.179

Wolf, P., Groen, E. A., Berg, W., Prochnow, A., Bokkers, E. A. M., Heijungs, R., & de Boer, I. J. M. (2017). Assessing greenhouse gas emissions of milk production: which parameters are essential? *International Journal of Life Cycle Assessment*, *22*(3), 441–455. https://doi.org/10.1007/s11367-016-1165-y

Xiao, Y. Q., Yang, L., Zhou, Y. C., Wei, Y. G., & Wang, N. G. (2017). Dominant parameters affecting the reliability of TBCs on a gas turbine blade during erosion by a particle-laden hot gas stream. *Wear*, *390–391*(November 2016), 166–175. https://doi.org/10.1016/j.wear.2017.07.013

Yang, F., Cai, Z., Chen, Y., Dong, S., Deng, C., Niu, S., Zeng, W., & Wen, S. (2022). A Robotic Polishing Trajectory Planning Method Combining Reverse Engineering and Finite Element Mesh Technology for Aero-Engine Turbine Blade TBCs. *Journal of Thermal Spray Technology*, *31*(7), 2050–2067. https://doi.org/10.1007/s11666-022-01434-9

Yousefzadeh, Z. (2021). *Prospective Life Cycle Assessment in Surface engineering: Case Studies on a Novel Thermal Spray Coating System and a Novel Coating Removal Method* (Issue July).

Concordia University.

Yousefzadeh, Z., Rezvani Rad, M., McDonald, A., & Lloyd, S. M. (2022). Life Cycle Assessment of a Thermal Sprayed Al2O3-NiCr Resistive Heating Coating for Pipe Freeze Protection. *Journal of Thermal Spray Technology*, *31*(3), 378–395. https://doi.org/10.1007/s11666-021-01308-6

Zargar, S., Yao, Y., & Tu, Q. (2022). A review of inventory modeling methods for missing data in life cycle assessment. *Journal of Industrial Ecology*, *26*(5), 1676–1689. https://doi.org/10.1111/jiec.13305

Zhai, Q., Li, T., & Liu, Y. (2021). Life cycle assessment of a wave energy converter: Uncertainties and sensitivities. *Journal of Cleaner Production*, *298*, 126719. https://doi.org/10.1016/j.jclepro.2021.126719

Zhang, Y. (2019). *Effect of Slot Wall Jet on Combustion Process in a 660 MW Opposed Wall Fired Pulverized Coal Abstract :* 1–13. https://doi.org/10.1515/ijcre-2018-0110

Zhao, M., Dong, Y., & Guo, H. (2021). Comparative life cycle assessment of composite structures incorporating uncertainty and global sensitivity analysis. *Engineering Structures*, *242*(April), 112394. https://doi.org/10.1016/j.engstruct.2021.112394

Zheng, B., Zhang, Y. W., Geng, Y., Wei, W., Ge, Z., & Gao, Z. (2022). Investigating lanthanum flows and stocks in China: A dynamic material flow analysis. *Journal of Cleaner Production*, *368*(3), 133204. https://doi.org/10.1016/j.jclepro.2022.133204

Zhou, F., Guo, D., Zhang, X., Xu, B., Wang, Y., Liu, M., & Wang, Y. (2022). In-situ synthesized nanostructured t-ZrO2/La2(Zr0.75Ce0.25)2O7 composite thermal barrier coatings. *Ceramics International*, *48*(20), 31054–31059. https://doi.org/10.1016/j.ceramint.2022.06.246

Zimmermann, T. (2017). Uncovering the Fate of Critical Metals: Tracking Dissipative Losses along the Product Life Cycle. *Journal of Industrial Ecology*, *21*(5), 1198–1211. https://doi.org/10.1111/jiec.12492

Zimmermann, T., & Gößling-Reisemann, S. (2013). Critical materials and dissipative losses: A screening study. *Science of the Total Environment*, *461–462*, 774–780. https://doi.org/10.1016/j.scitotenv.2013.05.040

Zimmermann, T., & Gößling-Reisemann, S. (2014). Recycling potentials of critical metals-analyzing secondary flows from selected applications. *Resources*, *3*(1), 291–318. https://doi.org/10.3390/resources3010291

APPENDIX A SUPPLEMENTARY INFORMATION FOR ARTICLE 1

This chapter contains additional data for the article. The first section shows how the vintage tracking was performed in detail. The second section contains the LCA for the coating materials used in the energy sector and the ecoinvent flows used. The last part contains additional figures including the ecosystem quality and human health impacts and the sensitivity analysis on the efficiency improvements from coating.

Vintage Tracking

We used a stock-driven model to estimate the in-use stock (in our case energy supplied) as suggested by Pauliuk et al. (2012). This model could be characterized by equation (A.1):

$$\Delta S(t) = I(t) - O(t) \qquad (A.1)$$

Where: $\Delta S(t)$: Stock change; gap of energy supply between t and t-1 (in kWh)

$I(t)$: Inflow; energy supplied by new installed capacity at t (in kWh)

$O(t)$: Outflow; energy supplied by decommissioned capacity at t (in kWh)

Figure A.1 Shows how the vintage tracking was performed.

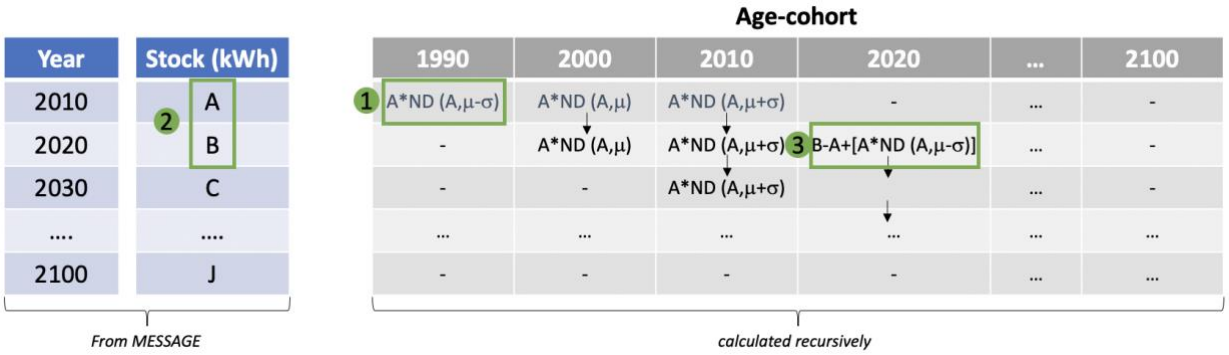

Figure A.1 Overview of the vintage tracking process. A-J refer to the energy supplied from the studied technology in a specific region ate a given year, retrieved from the output of the MESSAGE model, ND refers to normal distribution, μ refers to the mean of the normal distribution, σ refers to the standard deviation of the normal distribution.

Assuming that gas turbines, wind turbines and solar panels have a fixed lifetime of 30 years and coal power plants 40 years (E. G. Hertwich et al., 2015; Turconi et al., 2013), the entire age-cohort

would be decommissioned after 30 and 40 years, respectively. For the sake of illustration, the methodology explains the case of 30 years, which can be followed for the coal power plant. Because no data is provided about the age-cohort of the energy infrastructure at t_0-1 (the year 2010 in our case), a normal distribution with a mean μ = 20 years old, and a standard deviation σ = 10 years was taken to allocate the total energy demand into three age groups: 10, 20 and 30 years remaining. In the age-cohort table, this means that the capacity needed to supply the demand was installed in the years 1990, 2000, and 2010 respectively. For the coming years, a recursive procedure is repeated (Figure A.1 shows the steps as numbered below for year t=2020):

1 Calculate the outflow O(t), which is the energy supplied from the decommissioned capacity from the existing energy supply stock S(t). This includes the energy supplied from the capacity that served its 30 years lifetime. At t=2020, this is the energy supplied from the capacity that was installed in 1990.

2 Calculate the gap ΔS(t) between the stock scenario (energy supplied at year t) and the remaining stock (energy supplied at year t-1). At t=2020, ΔS(t) = B - A.

3 Set the inflow I(t), which is the energy supplied by the installed capacity at that year, to fill the calculated gap based on the energy supplied from the decommissioned capacity. I(t) = ΔS(t) + O(t). I(t) could be negative in some cases when ΔS(t) is negative. In this case, I(t) is set to 0 (i.e. no new capacity is added that year), and ΔS(t) is added to the age-cohort of the oldest technology, indicating early decommissioning of the capacity.

Repeat steps 1-3 for the remaining years.

LCA of coating energy systems

Goal and Scope

Goal:

The goal of the study is to identify the environmental impact of applying surface engineering to energy conversion technologies.

Functional unit:

1 kWh of electricity generated by a coated energy conversion technology.

System boundary:

In this study we are interested in the coating process of energy technologies. Accordingly, the substrate material (i.e., component to be coated) is outside the system boundaries (to avoid double counting when comparing it with the baseline system). Information about the post-treatment of the coated components is missing in the literature and assumed not to take place for the applications in our study. Finally, Building the power generation plants is excluded to avoid double counting when comparing with the baseline system. In the electricity generation phase, the benefits of coating are analyzed separately and included later in the integrated assessment model provided in the article. Figure A.2 shows the system boundaries.

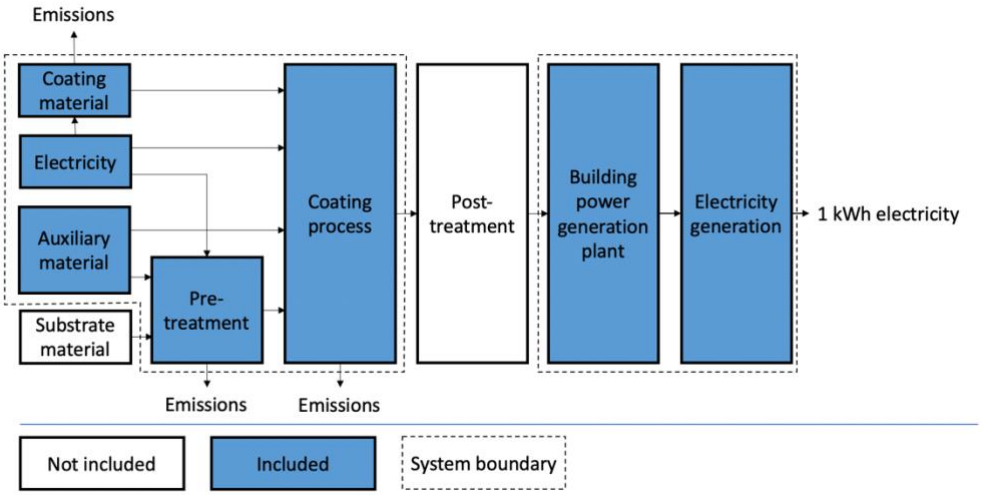

Figure A.2 System boundaries of the model. Dashed lines represent the system boundary.

LCI

Coating material per functional unit

The first step is to identify the needed amount of coating per functional unit to achieve the desired benefits, which is retrieved mainly from surface engineering literature.

In coal power plants, the density of the NiCrBSi is 8.2 g/cm^3 and the thickness needed for the anticorrosive coating is 520 μm (Hidalgo et al., 2001). The area to be coated is around 5300 m^2 for a 660 MW power plant. based on the dimensions provided by Zhang (2019). Based on this, the amount of NiCrBSi is 34240g/MW. In ecoinvent, a typical coal power plant with a capacity of 500MW has an operation time of 150000hrs (Wernet et al., 2016). Accordingly, the amount of NiCrBSi needed is **$2.3x10^{-4}$ g/kWh**.

In gas turbines, the density of GZ is 6.32 g/cm^3 and the thickness needed in the TBC is 100 μm (Mahade, Curry, et al., 2019). The area coated with TBC is an average of 0.29m^2/MW (Zimmermann & Gößling-Reisemann, 2014). Based on this, the amount of GZ is 183 g/MW. In ecoinvent, a typical combined cycle gas turbine with a capacity of 400MW has an operation time of 180000hrs (Wernet et al., 2016). Accordingly, the amount of GZ needed is **10^{-6} g/kWh**.

For solar panels, 7.5mL of nano SiO_2 solution (superhydrophobic coating) is needed per m^2 of a solar panel (Alamri et al., 2020). To make the SiO_2 solution, 0.02g/mL of SiO_2 is used (Manca et al., 2009). In ecoinvent, a typical solar farm with a capacity of 570KW_p with an area of 4273.5 m^2 generates 847.5 MWh of electricity annually for 30 years (Wernet et al., 2016). Accordingly, the amount of SiO_2 needed is **$2.5x10^{-5}$ g/kWh**.

In wind turbines, to achieve the anti-icing properties for the blade, we need to coat them with 10g of PVDF per blade with a dimension of 0.2m (C. Peng et al., 2012). In ecoinvent, a 2MW wind turbine operates for around 32000 hours during its lifetime, with a rotor diameter of 80m (so there are 3 blades of 40m each) (Wernet et al., 2016). Accordingly, the amount of PVDF needed is **$9x10^{-5}$ g/kWh**.

Coating process per functional unit

The second step is to scale the inventory of LCA studies of different coating technologies to match our functional unit by scaling down with respect to the amount of coating needed per kWh.

Coal and Gas:

Since both coal and gas require atmospheric plasma spray (APS), the inventory of the coating process is taken from the same LCA study, and the numbers are scaled to reflect the amount of coating material calculated in the previous section. The results are summarized in Table A.1.

Table A.1 System boundaries of the model. Dashed lines represent the system boundary.

Process	**APS Baseline study** (Serres et al., 2009)	**APS Coal**	**APS Gas**
Degreasing			
Acetone (kg)	7.86×10^{-5}	1.2×10^{-8}	5×10^{-11}
Grit blasting			
Al_2O_3 (kg)	50	7.3×10^{-3}	3.2×10^{-5}
Electricity (kWh)	3	4.4×10^{-4}	1.9×10^{-6}
Coating material			
NiCrBSi powder (kg)	**1.567×10^{-3}**	**2.3×10^{-7}**	**-**
GZ powder (kg)	**-**	**-**	**1×10^{-9}**
Coating process			
Ar (kg)	1.665×10^{-5}	2.4×10^{-9}	1×10^{-11}
H_2 (kg)	1.958×10^{-6}	2.9×10^{-10}	1.3×10^{-12}
Electricity	1.501×10^{-2}	2.2×10^{-6}	9.6×10^{-9}

For coal power plants, the composition of the NiCrBSi powder (Serres et al., 2011) is given in Table A.2.

Table A.2 Composition of the NiCrBSi powder

	Chemical composition (wt.%)						
Powder	C	Ni	Fe	Cr	Si	B	O
NiCrBSi	0.76	72.33	3.87	15.16	4.65	3.19	0.043

With a lack of data about the process to prepare GZ powder for the gas turbines, the process to prepare Zircon powder (Moign et al., 2010) was used as a proxy (Table A.3). Data from patents shows a Gd_2O_3 content of 59wt% and ZrO_2 content of 41wt% (Ridgeway, 2016; Ulion et al., 2005), so we divide the 1.611 kg of Zircon in the study between Gd (59%) Zircon (41%) for our study.

Table A.3 Inventory data for the process to prepare GZ powder

Input	
Ammonia, liquid (kg)	0.363
Hydrochloric acid (kg)	1.286
Gadolinium (kg)	0.950
Soda powder (kg)	1.411
Zircon (kg)	0.661
Electricity (kWh)	1.885
Output	
GZ powder (kg)	**1**

Solar:

Table A.4 summarizes the inventory for the sol-gel coating of the solar panels. Note that the amount of acetic acid and acetone in the referenced study was not realistic (263.33 kg/m^3 for acetone). Accordingly, we assumed they are actually in grams (we tried to contact the authors to confirm but got no answer).

Table A.4 Summary of the inventory data for the sol-gel coating of solar panels

Process	**Baseline study** (Pini et al., 2017)	**Sol-gel solar**
Cleaning		
Acetone (kg)	$2.6x10^{-1}$	$1x10^{-6}$
Acetic acid (kg)	$4.37x10^{-3}$	$1.9x10^{-8}$
Electricity (kWh)	244.4	$1x10^{-3}$
Coating material		
$NanoTiO_2$ (kg)	**$5.84x10^{-3}$**	**-**
$NanoSiO_2$ (kg)	**-**	**$2.5x10^{-8}$**

The process to make nanoSiO_2 sol (Roes et al., 2010) is given in Table A.5. The calorific value of natural gas for modelling later was taken as 44MJ/kg.

Table A.5 Inventory data for the process of making nanoSiO2 sol

Input	
Sodium silicate (kg)	3.9
Sulfuric acid (kg)	0.66
Natural gas (MJ)	20
Output	
NanoSiO_2 (kg)	**1**

Wind:

Table A.6 summarizes the inventory for the coating preparation of the wind turbines. The density of N,N-dimethylformamide is taken as 0.948 kg/L for modelling later.

Table A.6 Inventory data for coating preparation of the wind turbines

Process	**Baseline study** (C. Peng et al., 2012)	**Wind**
Coating material		
PVDF (kg)	**$1x10^{-2}$**	**$9x10^{-8}$**
N,N-dimethylformamide (mL)	$9.48x10^{-2}$	$8.5x10^{-7}$
Ammonium bicarbonate (kg)	$2x10^{-3}$	$1.8x10^{-8}$

Table A.7 includes the ecoinvent 3.5 (Wernet et al., 2016) flows used for modelling. The electricity flows are based on the output of our model linking MESSAGE scenarios with their impacts in ecoinvent 3.5, and their corresponding flows are provided in Table A.8. Since Carbon Capture and

Storage technologies are not available in ecoinvent 3.5, the impact of those flows were adjusted based on the results of Hertwich et al. (2015).

Table A.7 Mapping of the processes/materials used, and the corresponding flows used to model them in ecoinvent

Process/Material	**Ecoinvent flow**
Acetone	acetone production, liquid | acetone, liquid | Cutoff, U - RER
Acetic acid	acetic acid production, product in 98% solution state | acetic acid, without water, in 98% solution state | Cutoff, U - RER
Alumina	aluminium oxide production | aluminium oxide | Cutoff, U - IAI Area, EU27 & EFTA
Ammonia	ammonia production, steam reforming, liquid | ammonia, liquid | Cutoff, U - RER
Ammonium bicarbonate	ammonium bicarbonate production | ammonium bicarbonate | Cutoff, U - RER
Argon	argon production, liquid | argon, liquid | Cutoff, U - RER
Boron	boron carbide production | boron carbide | Cutoff, U - GLO
Chromium	chromium oxide production, flakes | chromium oxide, flakes | Cutoff, U - RER
Iron	iron sulfate production | iron sulfate | Cutoff, U - RER
Gadolinium	rare earth oxides production from bastnäsite concentrate | samarium europium gadolinium concentrate, 94% rare earth oxide | Cutoff, U - RoW

Table A.7 Mapping of the processes/materials used, and the corresponding flows used to model them in ecoinvent (cont'd and end)

Hydrochloric acid	hydrochloric acid production, from the reaction of hydrogen with chlorine | hydrochloric acid, without water, in 30% solution state | Cutoff, U - RER
Hydrogen	hydrogen cracking, APME | hydrogen, liquid | Cutoff, U - RER
Natural gas	natural gas liquids production | natural gas liquids | Cutoff, U - GLO
Nickel	nickel sulfate production | nickel sulfate | Cutoff, U - GLO
N,N-dimethylformamide	N,N-dimethylformamide production | N,N-dimethylformamide | Cutoff, U - RER
PVDF	polyvinylfluoride production | polyvinylfluoride | Cutoff, U - RoW
Silicon	silicon carbide production | silicon carbide | Cutoff, U - RER
Soda powder	soda production, solvay process | sodium bicarbonate | Cutoff, U - RER
Sodium silicate	sodium silicate production, furnace liquor, product in 37% solution state | sodium silicate, without water, in 37% solution state | Cutoff, U - RER
Sulfuric acid	sulfuric acid production | sulfuric acid | Cutoff, U - RER
Zircon	heavy mineral sand quarry operation | zircon, 50% zirconium | Cutoff, U - RoW

Table A.8 Mapping of the energy conversion technology flows in the MESSAGE model with the corresponding flows in ecoinvent 3.5 and Hertwich et al. (2015). CCS: Carbon capture and storage

Energy technology in MESSAGE	**Flow**	**Source**
Secondary Energy|Electricity|Biomass|w/ CCS		
R5.2ASIA	Biopower, with CCS, attributional, TAX30_betr_rf | Baseline | 2010 | Absolute - China	Hertwich
R5.2LAM	Biopower, with CCS, attributional, TAX30_betr_rf | Baseline | 2010 | Absolute - Latin America	Hertwich
R5.2MAF	Biopower, with CCS, attributional, TAX30_betr_rf | Baseline | 2010 | Absolute - Africa and Middle East	Hertwich
R5.2OECD	Biopower, with CCS, attributional, TAX30_betr_rf | Baseline | 2010 | Absolute - OECD Europe	Hertwich
R5.2 REF	Biopower, with CCS, attributional, TAX30_betr_rf | Baseline | 2010 | Absolute - Economies in transition	Hertwich
Secondary Energy|Electricity|Biomass|w/o CCS		
R5.2ASIA	electricity production, wood, future | electricity, high voltage | Cutoff, U – GLO	Ecoinvent
R5.2LAM	electricity production, wood, future | electricity, high voltage | Cutoff, U – GLO	Ecoinvent
R5.2MAF	electricity production, wood, future | electricity, high voltage | Cutoff, U – GLO	Ecoinvent

Table A.8 Mapping of the energy conversion technology flows in the MESSAGE model with the corresponding flows in ecoinvent 3.5 and Hertwich et al. (2015). CCS: Carbon capture and storage (cont'd)

R5.2OECD	electricity production, wood, future | electricity, high voltage | Cutoff, U – GLO	Ecoinvent
R5.2 REF	electricity production, wood, future | electricity, high voltage | Cutoff, U – GLO	Ecoinvent
Secondary Energy|Electricity|Coal|w/ CCS		
R5.2ASIA	Coal, SCPC w CCS | Baseline | 2010 | Absolute – China	Hertwich
R5.2LAM	Coal, SCPC w CCS | Baseline | 2010 | Absolute - Latin America	Hertwich
R5.2MAF	Coal, SCPC w CCS | Baseline | 2010 | Absolute - Africa and Middle East	Hertwich
R5.2OECD	Coal, SCPC w CCS | Baseline | 2010 | Absolute - OECD Europe	Hertwich
R5.2 REF	Coal, SCPC w CCS | 2010 | Absolute - Economies in transition	Hertwich
Secondary Energy|Electricity|Coal|w/o CCS		
R5.2ASIA	electricity production, hard coal | electricity, high voltage | Cutoff, U - CN-JS	Ecoinvent
R5.2LAM	electricity production, hard coal | electricity, high voltage | Cutoff, U – BR	Ecoinvent

Table A.8 Mapping of the energy conversion technology flows in the MESSAGE model with the corresponding flows in ecoinvent 3.5 and Hertwich et al. (2015). CCS: Carbon capture and storage (cont'd)

R5.2MAF	electricity production, hard coal | electricity, high voltage | Cutoff, U – RoW	Ecoinvent
R5.2OECD	Gas, NGCC w CCS | Baseline | 2010 | Absolute - OECD Europe	Hertwich
R5.2 REF	Gas, NGCC w CCS | Baseline | 2010 | Absolute - Economies in transition	Hertwich
Secondary Energy|Electricity|Gas|w/o CCS		
R5.2ASIA	electricity production, natural gas, combined cycle power plant | electricity, high voltage | Cutoff, U – TH	Ecoinvent
R5.2LAM	electricity production, natural gas, conventional power plant | electricity, high voltage | Cutoff, U – BR	Ecoinvent
R5.2MAF	electricity production, natural gas, conventional power plant | electricity, high voltage | Cutoff, U – SA	Ecoinvent
R5.2OECD	electricity production, natural gas, combined cycle power plant | electricity, high voltage | Cutoff, U – MX	Ecoinvent
R5.2 REF	electricity production, natural gas, conventional power plant | electricity, high voltage | Cutoff, U – RU	Ecoinvent
Secondary Energy|Electricity|Geothermal		
R5.2ASIA	electricity production, deep geothermal | electricity, high voltage | Cutoff, U – RoW	Ecoinvent

Table A.8 Mapping of the energy conversion technology flows in the MESSAGE model with the corresponding flows in ecoinvent 3.5 and Hertwich et al. (2015). CCS: Carbon capture and storage (cont'd)

R5.2LAM	electricity production, deep geothermal | electricity, high voltage | Cutoff, U – RoW	Ecoinvent
R5.2MAF	electricity production, deep geothermal | electricity, high voltage | Cutoff, U – RoW	Ecoinvent
R5.2OECD	electricity production, deep geothermal | electricity, high voltage | Cutoff, U – RoW	Ecoinvent
R5.2 REF	electricity production, deep geothermal | electricity, high voltage | Cutoff, U – RoW	Ecoinvent
Secondary Energy|Electricity|Hydro		
R5.2ASIA	electricity production, hydro, run-of-river | electricity, high voltage | Cutoff, U - CN-SC	Ecoinvent
R5.2LAM	electricity production, hydro, reservoir, tropical region | electricity, high voltage | Cutoff, U – BR	Ecoinvent
R5.2MAF	electricity production, hydro, run-of-river | electricity, high voltage | Cutoff, U – IR	Ecoinvent
R5.2OECD	electricity production, hydro, reservoir, alpine region | electricity, high voltage | Cutoff, U – NO	Ecoinvent
R5.2 REF	electricity production, hydro, run-of-river | electricity, high voltage | Cutoff, U – RU	Ecoinvent

Table A.8 Mapping of the energy conversion technology flows in the MESSAGE model with the corresponding flows in ecoinvent 3.5 and Hertwich et al. (2015). CCS: Carbon capture and storage (cont'd)

Secondary Energy|Electricity|Nuclear		
R5.2ASIA	electricity production, nuclear, pressure water reactor | electricity, high voltage | Cutoff, U - CN-GD	Ecoinvent
R5.2LAM	electricity production, nuclear, pressure water reactor | electricity, high voltage | Cutoff, U – BR	Ecoinvent
R5.2MAF	electricity production, nuclear, pressure water reactor | electricity, high voltage | Cutoff, U – ZA	Ecoinvent
R5.2OECD	electricity production, nuclear, pressure water reactor | electricity, high voltage | Cutoff, U – FR	Ecoinvent
R5.2 REF	electricity production, nuclear, pressure water reactor | electricity, high voltage | Cutoff, U – RU	Ecoinvent
Secondary Energy|Electricity|Solar		
R5.2ASIA	electricity production, photovoltaic, 570kWp open ground installation, multi-Si | electricity, low voltage | Cutoff, U - CN-QH	Ecoinvent
R5.2LAM	electricity production, photovoltaic, 3kWp slanted-roof installation, multi-Si, panel, mounted | electricity, low voltage | Cutoff, U – BR	Ecoinvent
R5.2MAF	electricity production, photovoltaic, 3kWp slanted-roof installation, multi-Si, panel, mounted | electricity, low voltage | Cutoff, U – ZA	Ecoinvent

Table A.8 Mapping of the energy conversion technology flows in the MESSAGE model with the corresponding flows in ecoinvent 3.5 and Hertwich et al. (2015). CCS: Carbon capture and storage (cont'd and end)

R5.2OECD	electricity production, photovoltaic, 570kWp open ground installation, multi-Si | electricity, low voltage | Cutoff, U – IT	Ecoinvent
R5.2 REF	electricity production, photovoltaic, 3kWp slanted-roof installation, multi-Si, panel, mounted | electricity, low voltage | Cutoff, U – UA	Ecoinvent
Secondary Energy|Electricity|Wind		
R5.2ASIA	electricity production, wind, 1-3MW turbine, onshore | electricity, high voltage | Cutoff, U - CN-NM	Ecoinvent
R5.2LAM	electricity production, wind, 1-3MW turbine, onshore | electricity, high voltage | Cutoff, U – BR	Ecoinvent
R5.2MAF	electricity production, wind, <1MW turbine, onshore | electricity, high voltage | Cutoff, U – IR	Ecoinvent
R5.2OECD	electricity production, wind, 1-3MW turbine, onshore | electricity, high voltage | Cutoff, U – DK	Ecoinvent
R5.2 REF	electricity production, wind, 1-3MW turbine, onshore | electricity, high voltage | Cutoff, U – UA	Ecoinvent

LCIA

Table A.9 shows the impacts of the SE coating process. The coating impact (without electricity flows) was calculated using OpenLCA software with the ecoinvent 3.5 database (Wernet et al., 2016) and the IMPACTWorld+ (Bulle et al., 2019) impact assessment method. Note that Ecosystem quality and human health indicators exclude the endpoint impact from climate change.

The impact of electricity flows in the coating process vary each year depending on the projections of the model, to account for the efficiency gains achieved from SE in the previous decade. Thus, their impacts were calculated directly in out model based on the results we got. In Table A.9, the results are shown only for the year 2030 in SSP2 baseline, but per kWh, it is almost the same for the upcoming years, because the impact of electricity in the coating process is negligible.

Table A.9 Life cycle impacts of coatings for different energy technologies and regions

Energy technology	**Climate Change [kgCO_2 eq/kWh]**	**Ecosystem quality [PDF.m^2.yr/kWh]**	**Human health [DALY/kWh]**
Coal	1.2E-4	4.84E-3	1.12E-9
Gas	5.95E-5	2.45E-3	5.64E-10
Solar	2.55E-6	3.42E-6	1.12E-11
Wind	3.69E-6	1.38E-5	1.71E-11

Additional Figures

Figure A.3 and A.4 show the impacts on ecosystem quality and human health, respectively, excluding the "climate change, long term" endpoint indicator. The impact factors for both areas of protection were taken from IMPACTWorld+ (Default Recommended Damage 1.47) (Bulle et al., 2019) with the ecoinvent 3.5 (Wernet et al., 2016) database. Both indicators show that adding SE to the energy conversion technologies would lead to a net environmental benefit (the dashed line representing technologies with SE is always lower than the solid line where SE is not applied). Impacts on human health follow the same trend as climate change that was discussed in the article. For ecosystem quality, the 1.5 D policy scenario of SSP1 has a higher impact than the baseline scenario. This could be attributed to the higher share of solar and biomass electricity, having a higher impact on land transformation. Nevertheless, this was not caused by the application of SE technologies.

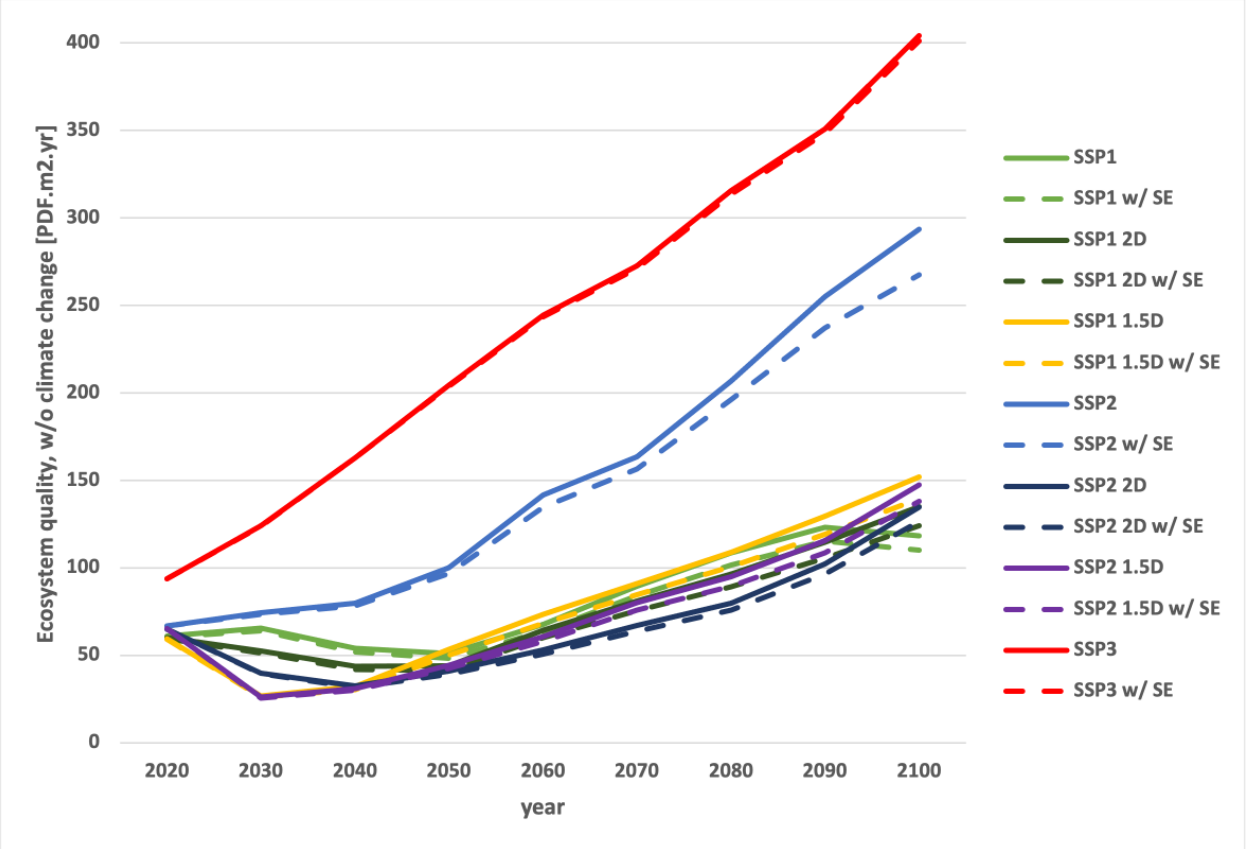

Figure A.3 Ecosystem quality indicator from global electricity production based on different shared socio-economic pathways (SSPs) with (dashed lines) and without (solid lines) novel surface engineering technologies. 1.5D and 2D are mitigation scenarios corresponding to the 1.5 degree and 2 degree rising temperature targets in the Paris Agreement, respectively.

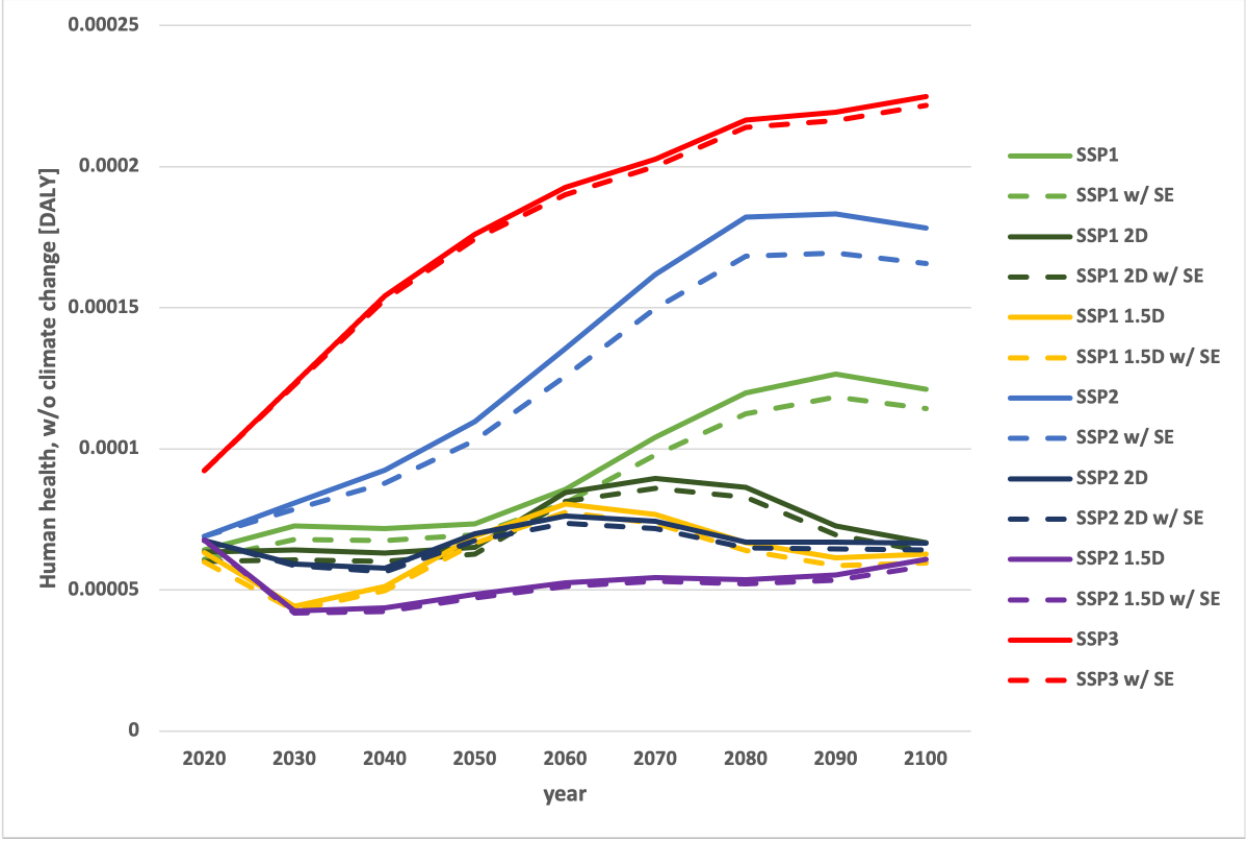

Figure A.4 Human health indicator from global electricity production based on different shared socio-economic pathways (SSPs) with (dashed lines) and without (solid lines) novel surface engineering technologies. 1.5D and 2D are mitigation scenarios corresponding to the 1.5 degree and 2 degree rising temperature targets in the Paris Agreement, respectively.

Figure A.5 shows the breakeven point of efficiency gains where the benefits in terms of efficiency gains overcome the impacts of the coating. In terms of GHG emissions, for all the energy conversion technologies and impact categories, the breakeven points occur at very low efficiency improvements. Accordingly, if SE leads to an improvement of at least 0.9%, the impacts from the SE coating process would be acceptable. This figure is higher for the ecosystem quality (17.4%), because the impact of producing the NiCrBSi powder for the coating is high.

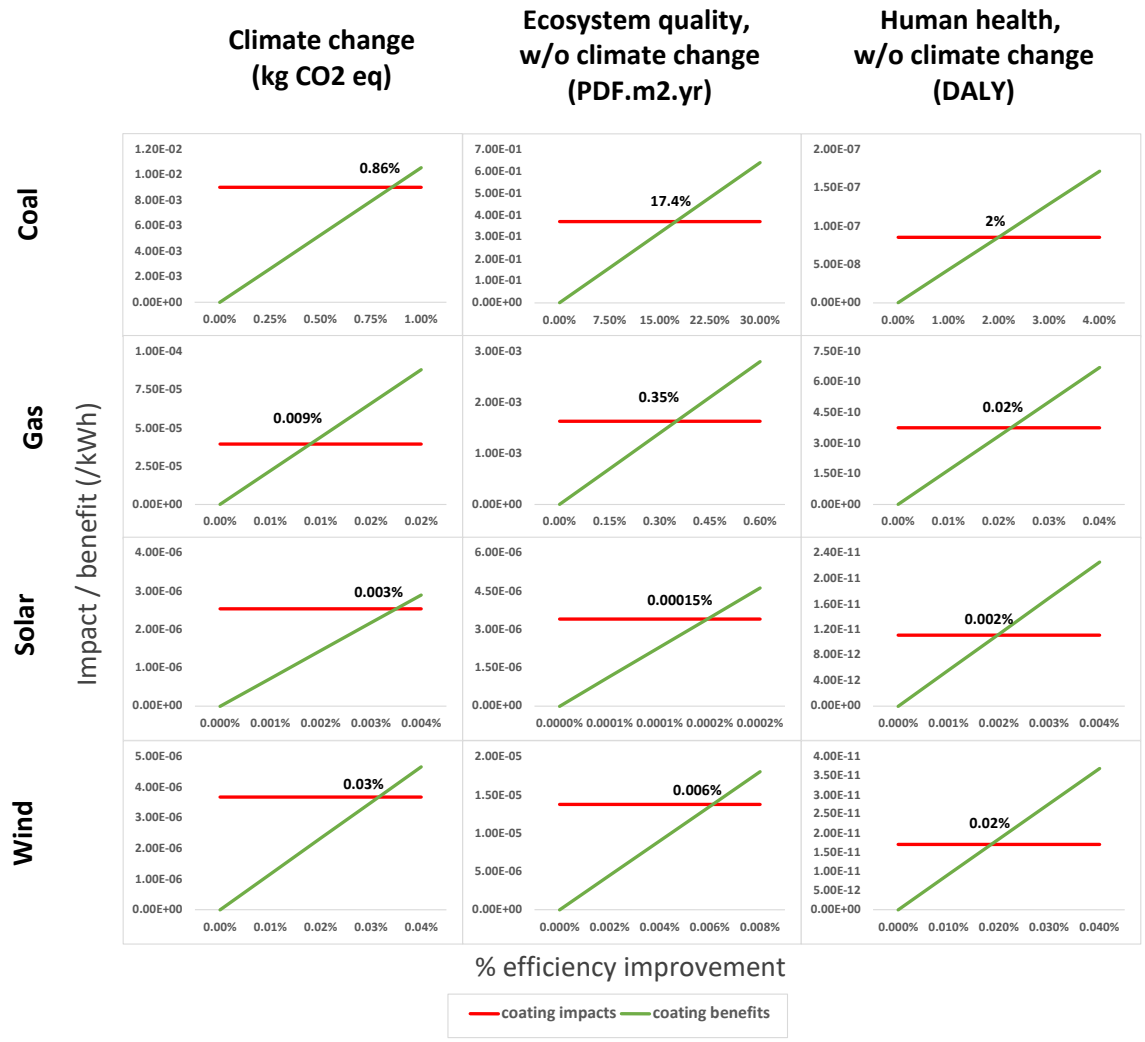

Figure A.5 The breakeven point at which the impact of the SE coating process equals the environmental benefits achieved from the coating for different energy conversion technologies and impact categories.

All studied energy conversion technologies (except for wind turbine) result in a net reduction in GHG emissions when applying the innovative SE technology for the range of possible efficiency improvement achieved (Figure A.6). In the case of wind turbines, the low efficiency improvement (0.005%) falls below the breakeven point, resulting in an increase of emissions. Besides, even in the high efficiency improvement case (50%), the achieved GHG reduction is 3 orders of magnitude lower than that achieved by coal power plants. This is due to the limited geographical areas where there are cold climates, and limited temporal range when it is cold.

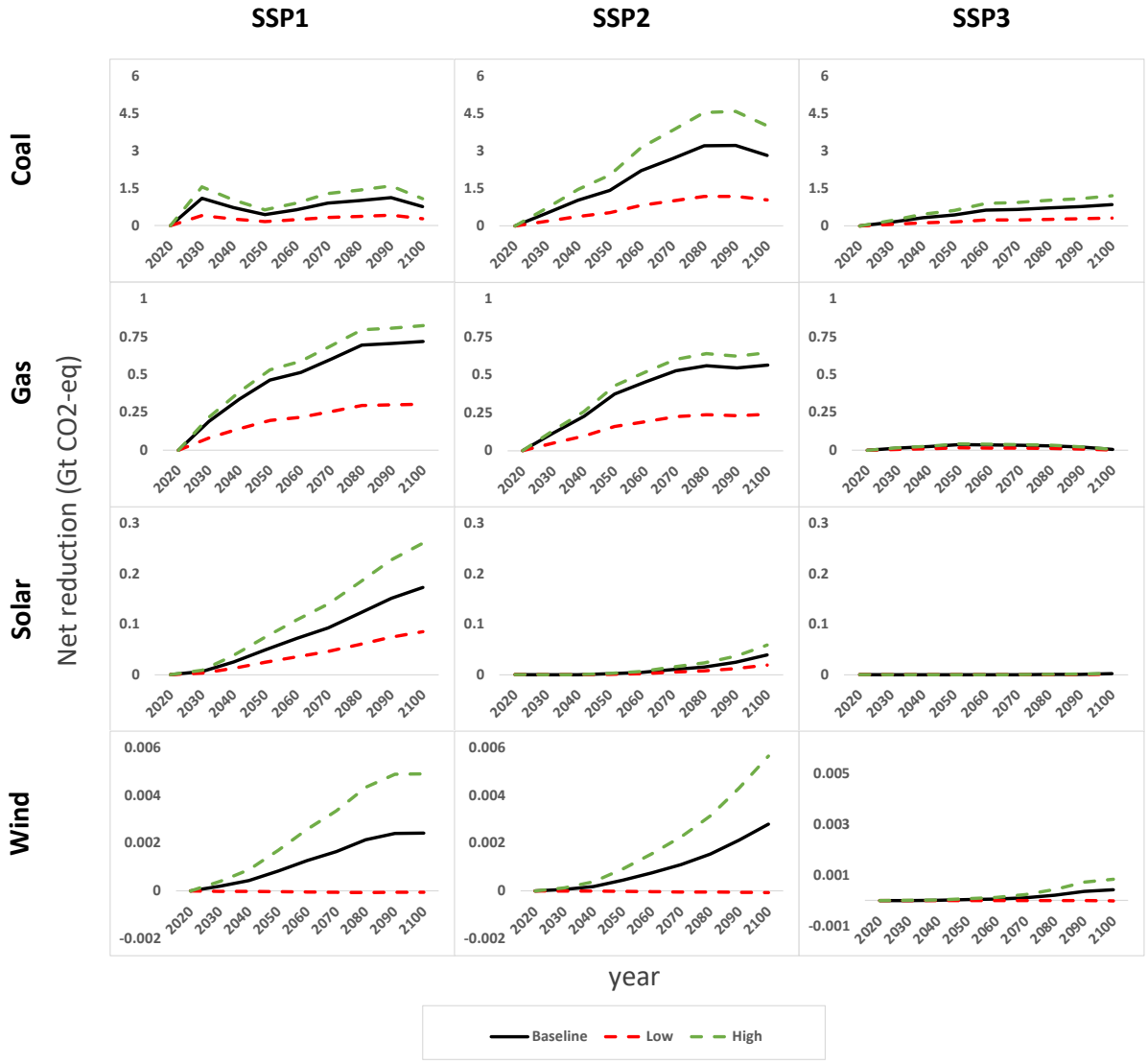

Figure A.6 Sensitivity analysis showing the net reduction of GHG emissions (in GTCO2-eq) achieved from applying SE to the four energy conversion technologies in different SSPs as a function of different improvement in energy conversion (baseline, low and high).

Another sensitive parameter is the adoption rate of the innovative SE technologies in the energy conversion technologies. SSP3 is the most sensitive to this parameter, with an additional 4.8 $GtCO_2$-eq reduction achieved between 2020 and 2100 with each one percentage point increase in the adoption rate (Table A.10). This is expected where the highest reduction comes from applying innovative SE technologies to coal power plants, and SSP3 has the highest capacity of them.

Table A.10 Sensitivity analysis showing the reduction in GHG emissions (GtCO2-eq) achieved with a 1%-point increase in the adoption rates between 2020 and 2100

SSP scenario	**Reduced emissions (GtCO2-eq)**
SSP1	1.2
SSP2	2.6
SSP3	4.8

APPENDIX B SUPPLEMENTARY INFORMATION FOR ARTICLE 2

This chapter contains additional data for the article. The first section contains the inventory with their sources and any additional calculation needed. The second section explains the parameters used in the model. The third section explains how the scale-up was done. The fourth section contains the ecoinvent processes used for modelling. This follows with information about the experts questioned in the study. The last section contains additional results including the Sankey diagrams per 1 kg of coated material, dynamic MFA showing when maintenance and EOL occurs, material dissipation per application, and material dissipation per material.

Inventory

Table B.1 summarises the different parameters needed to calculate the amount of coating needed for each application, together with the sources of the data. When further calculations were needed, the formulas are given below the table.

Table B.1 Parameters needed to calculate the inventory (coating amount per applications)

Parameter	**Value**	**Unit**	**Source**
Piston rings			
Coating material	Mo	-	(Miyamoto, 2013)
Coating density	10.22	g/cm^3	(MatWeb, 2023a)
Coating thickness	0.1	mm	(Miyamoto, 2013)
Piston diameter	62.4	mm	(Lakatos et al., 2011)
Piston width	3	mm	(Lakatos et al., 2011)
Coated area	187.2	mm^2	Calculated below
Rings	4	Items/vehicle	(Lakatos et al., 2011)
Coating amount	**2.4**	**g/vehicle**	Calculated below
Piston			
Coating material	NiCrSi	-	(Baba et al., 2014)
Coating density	8.53	g/cm^3	(MatWeb, 2023b)
Coating thickness	0.4	mm	(Baba et al., 2014)
Piston diameter	62.4	mm	(Lakatos et al., 2011)

Table B.1 Parameters needed to calculate the inventory (coating amount per applications) (cont'd)

Piston height	51	mm	(Lakatos et al., 2011)
Coated area	100	cm^2	Calculated below
Coating amount	**34**	**g/vehicle**	Calculated below
Gas turbine			
Coating material	YSZ	-	(Zimmermann, 2017)
Amount Y	118	g/MW	(Zimmermann, 2017)
Amount Y in YSZ	0.108	g/g	Stoichiometry
Coating amount	**1**	**kg/MW**	Calculated
Aircraft engine			
Coating material	YSZ	-	(Zimmermann, 2017)
Amount Y	685	g/engine	(Zimmermann, 2017)
Amount Y in YSZ	0.108	g/g	Stoichiometry
Engines	2	Items/aircraft	(Zimmermann, 2017)
Coating amount	**12.7**	**kg/aircraft**	Calculated
Landing gear			
Coating material	WCCoCr	-	(Eybel, 2023)
Coating density	15.7	g/cm^3	(MatWeb, 2023c)
Coating thickness	0.075	mm	(Eybel, 2023)

Table B.1 Parameters needed to calculate the inventory (coating amount per applications) (cont'd)

Cylinder diameter	5 (20)	cm	(Eybel, 2023)
Cylinder height	15 (152)	cm	(Eybel, 2023)
Coated area	243 (9,729)	cm^2	Calculated below
Cylinders	29 (1)	Items/landing gear	(Eybel, 2023)
Landing gears	3	Items/aircraft	(Eybel, 2023)
Coating amount	**2.5**	**kg/aircraft**	Calculated below
Biomass boiler			
Coating material	NiCrSi	-	(Vassen & Mauer, 2013)
Coating density	8.53	g/cm^3	(MatWeb, 2023b)
Coating thickness	0.65	mm	(Vassen & Mauer, 2013)
Powerplant capacity	75	MW	(Stenberg et al., 2023)
Heat transfer area	44	m2	(Stenberg et al., 2023)
Coating amount	**3.25**	**kg/MW**	Calculated
Hydropower blades			
Coating material	WCCoCr	-	(Badina, 2023; Vassen & Mauer, 2013)
Coating density	15.7	g/cm^3	(MatWeb, 2023c)

Table B.1 Parameters needed to calculate the inventory (coating amount per applications) (cont'd and end)

Coating thickness	0.3	mm	(Vassen & Mauer, 2013)
Average capacity	529	MW	(VOITH, 2021)
Average diameter	7.2	m	(VOITH, 2021)
Blades	13	Items/turbine	(VOITH, 2021)
Coated area	42	m^2	calculated below
Coating amount	**377**	**g/MW**	Calculated below

Piston rings

The piston rings were proxied as cylinders, and the lateral surface area was calculated as:

$$Coated\ area\ = 2 \times \pi \times radius \times width \qquad (B.1)$$

To calculate the coating amount, the volume is multiplied by the density as:

$$Coating\ amount\ =\ density \times volume = density\ \times\ area\ \times\ thickness \qquad (B.2)$$

Pistons

The piston was proxied as cylinders, and the surface area was calculated as:

$$Coated\ area\ = (2 \times \pi \times radius \times height) + (2 \times \pi\ \times\ radius^2) \qquad (B.3)$$

To calculate the coating amount, the volume is multiplied by the density as:

$$Coating\ amount\ =\ density \times volume = density\ \times\ area\ \times\ thickness \qquad (B.4)$$

Landing gears

In landing gears, we usually spray 125-150μm, then go to 75μm after processing (Eybel, 2023). Post processing is done because the surface is very rough and won't achieve the desired

functionality. The landing gear is composed of around 150 tubular components, 30 of which are thermally sprayed (Eybel, 2023). One of the cylinders is around 5 ft tall with 8 in diameter, and the rest are 6 in tall with 2 in diameter (Eybel, 2023). We assumed that we have 2 landing gears in a typical plane (can be more for larger planes). The area of each cylinder was calculated as:

$$Coated\ area\ = 2 \times \pi \times radius \times height \qquad (B.5)$$

To calculate the coating amount, the volume is multiplied by the density as:

$$Coating\ amount\ =\ density \times volume = density\ \times\ area\ \times\ thickness \qquad (B.6)$$

Hydropower

For hydropower plants, Pelton turbines are mainly coated because they are more subject to abrasion, but Francis turbine started being coated recently where water has high sediments (Badina, 2023). For Francis turbines, only the entrance of the blade and the pressure side are coated (Badina, 2023), so we assumed 1/2 of the area is coated to be conservative. To get the coated area per MW of hydropower plants, data for Francis turbines with a capacity greater than 200 MW was used (VOITH, 2021). In total, 20 hydropower plants met the criteria, and the average capacity and diameter of the blades was documented. The blades were proxied as rectangles, and the surface area was calculated as:

$$Coated\ area\ = \frac{1}{2} \times length \times width \qquad (B.7)$$

Where the 1/2 represents that half of the blades are coated, length is the radius, and the width was assumed to be 1/2 of the length, so the coated area would be:

$$Coated\ area\ = \frac{1}{2} \times \frac{diameter}{2} \times \frac{diameter}{4} = \frac{diameter^2}{16} \qquad (B.8)$$

To calculate the coating amount, the volume is multiplied by the density as:

$$Coating\ amount\ =\ density \times volume = density\ \times\ area\ \times\ thickness \qquad (B.9)$$

Dissipative losses parameters

Table B.2 lists the used parameters with the description and source of each. The values of different parameters for different applications are in the supplementary excel file.

Table B.2 Description of parameters

Parameter	**Description**	**Source**
E_m	*Mining efficiency:* ratio of material extracted to the ore mined. This includes the concentrator recovery rate and the smelter/refinery recovery rate (%)	(Nassar et al., 2021)
E_p	*Powder production efficiency:* ratio of powder produced to material sieved (%)	(Azevedo et al., 2018)
$E_{d,th}$	*Theoretical deposition efficiency:* ratio of powder adhered on the substrate from the total powder deposited (based on deposition parameters and technology used) (%)	(Nagy, 2023; Poirier, 2022)
$E_{d,ta}$	*Target deposition efficiency:* ratio of powder adhered on the substrate from the total powder deposited (based on the time the robot is positioned away from the target while changing the path) (%)	(Eybel, 2023; Nagy, 2023; Poirier, 2022)
$E_{d,pp}$	*Post-processing efficiency:* ratio of powder adhered on the substrate from the total powder deposited (based on the amount removed in post processing) (%)	(Eybel, 2023; Poirier, 2022)

Table B.2 Description of parameters (cont'd)

R_c	*Corrosion ratio:* ratio of coating lost due to corrosion during one maintenance interval to the coating deposited (kg_{lost} / $kg_{deposited}$)	(Momber & Marquardt, 2018)
R_f	*Friction loss ratio:* ratio of coating lost due to friction during one maintenance interval to the coating deposited (kg_{lost} / $kg_{deposited}$)	n.a.
R_{tf}	*Thermal fatigue loss ratio:* ratio of coating lost due to thermal fatigue during one maintenance interval to the coating deposited (kg_{lost} / $kg_{deposited}$)	n.a.
R_w	*Wear ratio:* ratio of coating lost due to wear during one maintenance interval to the coating deposited (kg_{lost} / $kg_{deposited}$)	n.a.
LT_c	*Component lifetime* (*years*)	n.a.
LT_p	*Product lifetime* (*years*)	(Eybel, 2023; Turconi et al., 2013)
I_m	*Maintenance interval* (*years*)	n.a.
RR_c	*Coating recycling rate:* ratio of the powder collected during coating that is sent to recycling to the total powder (%)	n.a.
RR_m	*Maintenance recycling rate:* ratio of stripped material sent to recycling to the total material stripped (%)	n.a.
RR_{eol}	*EOL recycling rate:* ratio of the coating material at the EOL that is sent to recycling to the total coating material at the EOL (%)	n.a.

Table B.2 Description of parameters (cont'd and end)

S_p	*Product scaling factor:* Amount of coating material needed per product (*kg/product*)	(see section: Inventory)
S_e	*Economy scaling factor:* Amount of products in a sector (*product/sector* or *TW/sector*)	(IEA, 2017)

Large scale

Tables B.3, B.4, and B.5 contain the energy generation and transportation demand from IEA ETP (IEA, 2017) needed to scale-up the use to the 2014 scale. Only 2014 was used for the study, others could be used in future prospective studies.

Table B.3 Gross electricity generation (TWh)

	2014	**2025**	**2030**	**2035**	**2040**	**2045**	**2050**	**2055**	**2060**
Natural gas	5155	6583	7764	8695	9395	10058	10586	10981	11702
Biomass and waste	496	1032	1267	1463	1693	1894	2198	2522	2731
Hydro (excl. pumped storage	3895	4939	5422	5867	6261	6649	7037	7430	7836

Table B.4 Passenger kilometers (billion)

	2014	**2025**	**2030**	**2035**	**2040**	**2045**	**2050**	**2055**	**2060**
Air	6323	9365	11416	13721	16192	18776	21377	23963	26530
Road	40303	51356	56761	61443	65488	69482	72589	75001	76062

Table B.5 Freight tonne kilometers (billion)

	2014	**2025**	**2030**	**2035**	**2040**	**2045**	**2050**	**2055**	**2060**
Road	27789	41662	50445	59270	67869	76259	84753	93506	102382

Electricity generation (TWh to TW)

To get the capacity, we multiply the capacity factor by the hours per year (8760 hours) to get the hours of operation per year (Table B.6). Then we divide the energy generated (in TWh) by the number of hours of operations to get the capacity (in TW).

Table B.6 Capacity factors for energy technologies

Technology	**Capacity factor**	**Capacity, 2014 (TW)**	**Source**
Natural gas	0.544	1.08	(US Department of Energy, 2020b)
Biomass and waste	0.635	0.09	(US Department of Energy, 2020b)
Hydro	0.371	1.2	(US Department of Energy, 2020b)

Vehicles (passenger km and tonne km to vehicles)

To get the number of passenger vehicles, we need to know the number of passengers per vehicle and the annual distance of the vehicle (Table B.7). For freight vehicles, we need the load factor, the load capacity, and the annual distance.

Table B.7 Parameters to calculate the amount of vehicles entering the fleet in 2014

Parameter	**Value**	**Unit**	**Source**
Passenger vehicles			
Occupancy rate	1.7	passenger/vehicle	(NTM, 2023b)
Annual distance	18,450	km	(US Department of Energy, 2020a)
Freight vehicles			
Load factor	0.4	-	(NTM, 2023c)
Load capacity	14	tonnes	(NTM, 2023c)
Annual distance	101,000	km	(US Department of Energy, 2020a)
Total vehicles, 2014	**1,334**	**Million vehicles**	calculated

Aircrafts (passenger km to aircrafts)

To get the number of aircrafts, we need to know the load factor of the aircraft, the nominal passenger capacity, and the annual distance covered by the aircraft (Table B.8).

Table B.8 Parameters to calculate the amount of aircrafts entering the fleet in 2014

Parameter	**Value**	**Unit**	**Source**
Load factor	0.65	-	(NTM, 2023a)
Passenger capacity	200	passenger/aircraft	assumed
Annual flight time	3,500	hours/year	(USA Today, 2012)
Load capacity	500	miles/hr	(USA Today, 2012)
Annual distance	101,000	km	calculated
Total aircrafts, 2014	**17.3**	**Thousand aircrafts**	calculated

Since all the data was calculated for all the stocks in the year 2014, it is important to know the lifetimes of products and components (Tables B.9 and B.10, respectively) to estimate how much of this stock was introduced that year. This is done using the survival function.

Table B.9 Lifetime of products

Product	**Lifetime (years)**	**source**
Aircraft	30	(USA Today, 2012)
Gas turbine	20	(Turconi et al., 2013)
Biomass plant	15	(Turconi et al., 2013)
Hydropower plant	50	(Turconi et al., 2013)
Vehicle	15	150,000 km (Hawkins et al., 2013) at 10,000 km/year

Table B.10 Lifetime of components

Component	**Lifetime (years)**	**source**
Aircraft engine	6	(Nagy, 2023)
Gas turbine blades	4	(Nagy, 2023)
Landing gear	20	(Eybel, 2023)
Biomass boiler	15	same as product
Hydropower blades	20	Assumed every 2 maintenance cycles
Piston rings	15	same as product
Pistons	15	same as product

To account for the losses happening during the maintenance, Table B.11 includes the maintenance intervals of the components.

Table B.11 Maintenance interval for the components

Component	**Maintenance interval (years)**	**source**
Aircraft engine	3	(Nagy, 2023)
Gas turbine blades	1	(Nagy, 2023)
Landing gear	10	(Eybel, 2023)
Biomass boiler	3	(Castolin Eutectic, 2015)
Hydropower blades	10	(Sollars & Beitelman, 2011)
Piston rings	n.a.	n.a.
Pistons	n.a.	n.a.

Ecoinvent processes

Table B.12 shows the ecoinvent 3.8 – cutoff processes used to get the emissions factors of the materials. The processes where adjusted by removing transportation flows to account only for the material extraction.

Table B.12 ecoinvent processes used to get the emission factors of the materials

Metal	**ecoinvent process**
Chromium	market for chromium oxide, flakes | chromium oxide, flakes | Cutoff, U
Cobalt	market for cobalt sulfate | cobalt sulfate | Cutoff, U
Molybdenum	molybdenum trioxide | molybdenum trioxide production | Cutoff, U
Nickel	market for nickel sulfate | nickel sulfate | Cutoff, U
Silicon	market for silicon carbide | silicon carbide | Cutoff, U
Tungsten	market for tungsten concentrate | tungsten concentrate | Cutoff, U
Yttrium	market for yttrium oxide | yttrium oxide | Cutoff, U
Zirconium	market for zirconium oxide | zirconium oxide | Cutoff, U

Experts' judgement

A phone and email communication with surface engineering experts was needed for some assumptions in the study. Most of the experts are part of the GreenSEAM network, where surface engineering researchers and industries work on the next generation surface engineering, with the focus on the green thinking. Table B.13 explains the relevance of each expert for the study. Please not the information provided is based on the expertise of the experts in their field, and not necessarily reflecting the data or views of their respective company.

Table B.13 Information about the experts questioned in the study

Expert	**Relevance to the study**
(Badina, 2023)	Performance and safety hydraulic expert, experience with hydropower plants
(Eybel, 2023)	Material expert, part of GreenSEAM, experience with landing gears
(Nagy, 2023)	Industrial Gas Turbine components repair manager, part of GreenSEAM, experience with both aerospace and power generation gas turbines
(Poirier, 2022)	Research officer, part of GreenSEAM, experience with thermal spray
(Tang, 2022)	VP R&D for a thermal spray technology company, part of GreenSEAM, experience in atmospheric plasma spray

Additional results

Figure B.1 shows the Sankey diagram for coating 1 kg on a component over the lifecycle of the product. The recoating of the gas turbine engine is responsible of most of the losses due to the low maintenance interval. This result could be helpful if better inventory results for the coating on components becomes available, and the large scales results would be more robust.

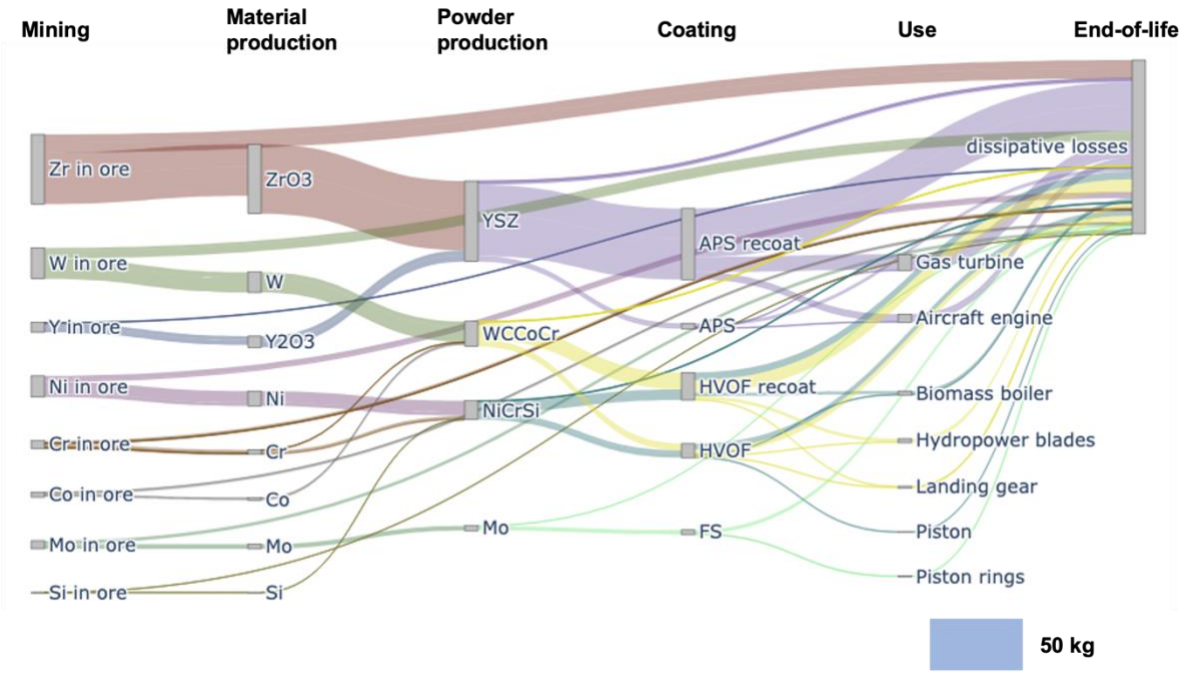

Figure B.1 Sankey diagram of coating 1 kg on a component over the product lifetime

Figure B.2 shows the dynamic MFA for the 2014 cohort. In this figure, we differentiate between the dissipative losses at the maintenance and EOL stage. This is helpful in the scenario setting, where during maintenance the coating is stripped before a new coating is added. At the EOL of the component, the whole component is replaced, and it might be harder to strip and collect the coating and would probably be recycled with the substrate material.

Figure B.2 Dynamic MFA for the 2014 cohort of different applications

Figure B.3 shows the contribution of the materials lost for each application. This clearly shows that Pistons are responsible for most of the losses, where NiCrSi is used.

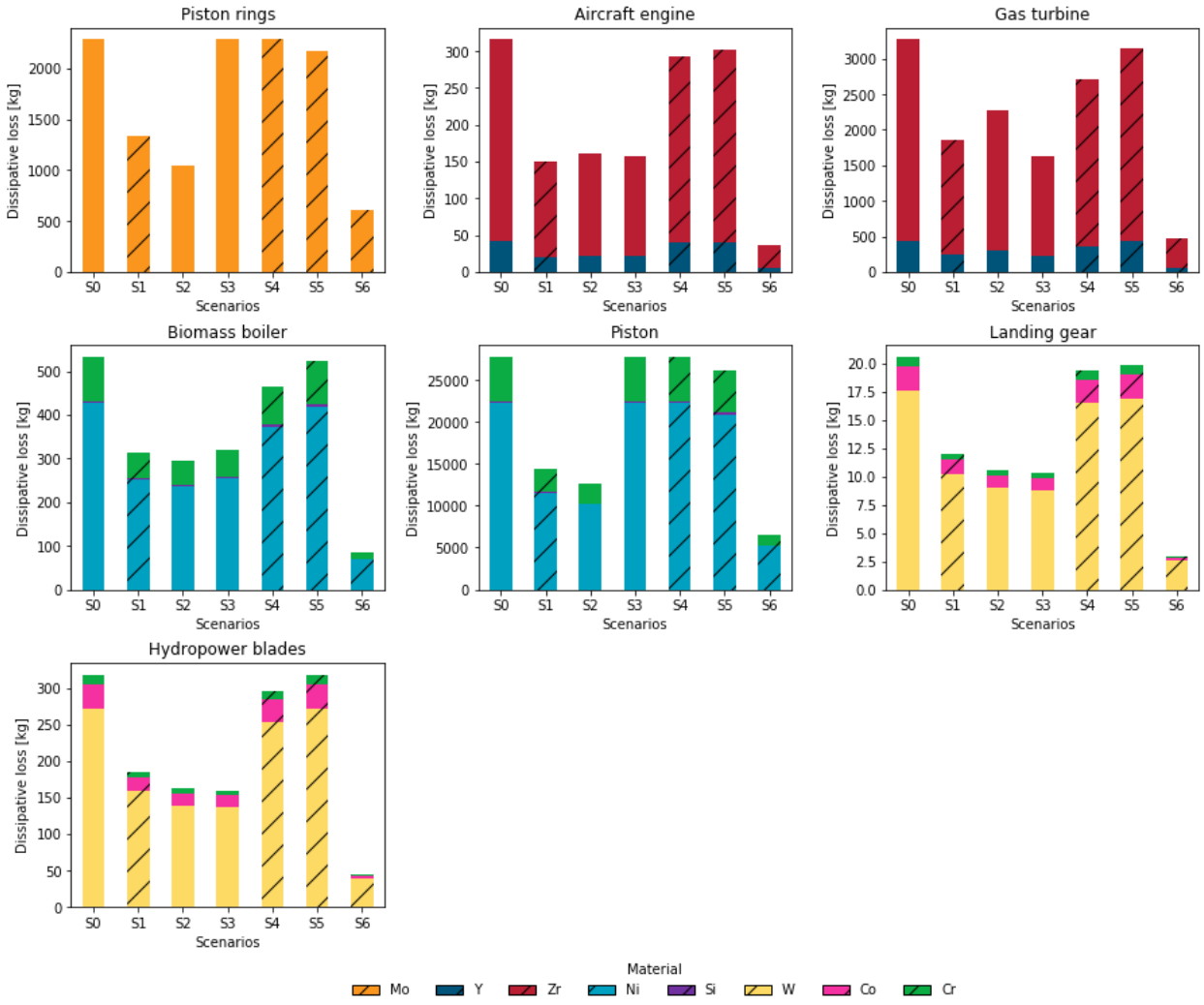

Figure B.3 Contribution of material losses to each application for each scenario

Figure B.4 shows the contribution of the application for each material lost. It is another way to represent Figure B.3.

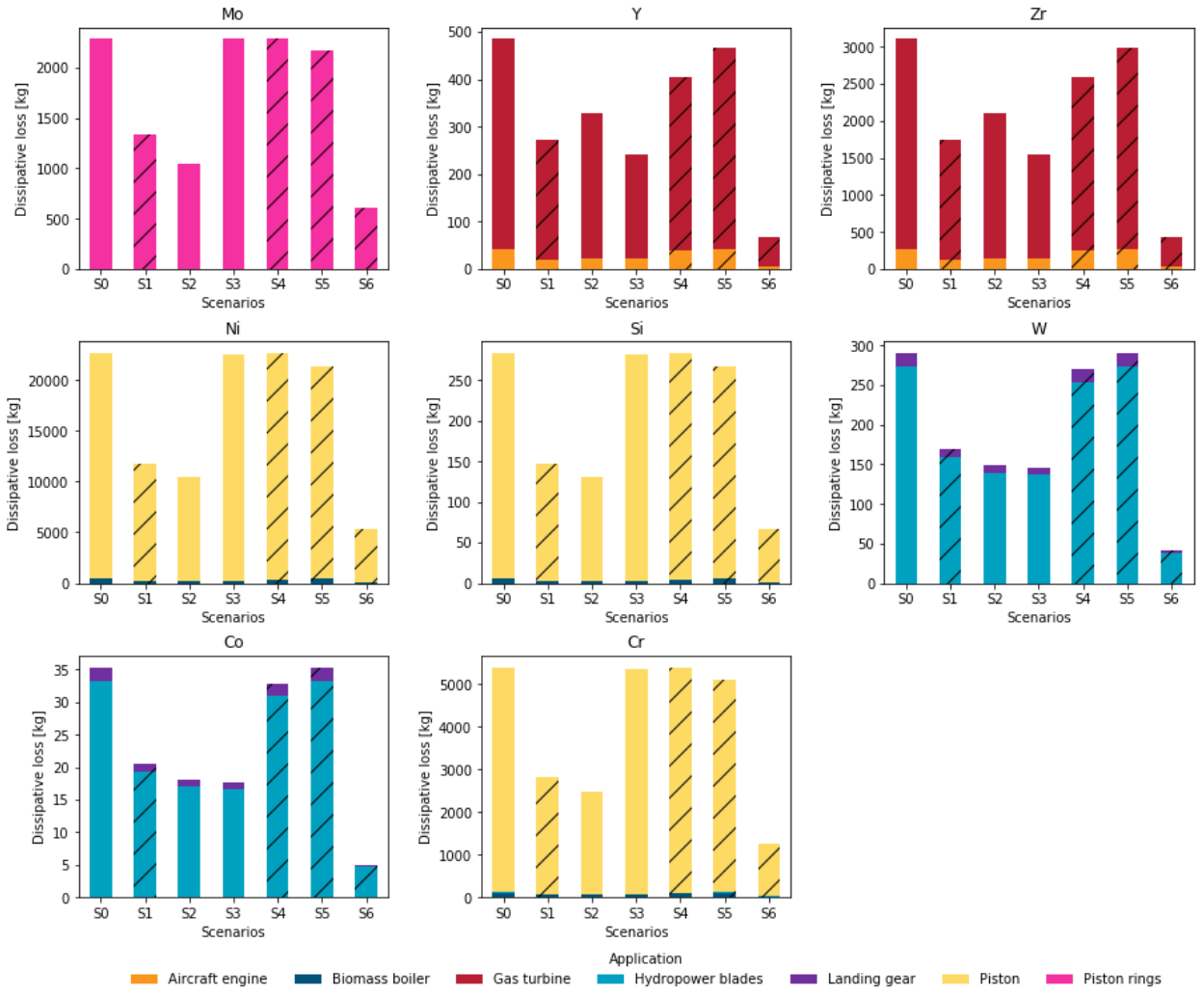

Figure B.4 Contribution of applications to each material lost for each scenario

APPENDIX C SUPPLEMENTARY INFORMATION FOR ARTICLE 3

This chapter contains additional data for the article. The first section contains extended methodology sections, particularly the flow diagram of the wire arc additive manufacturing (WAAM) and the pedigree matrix for the applicability uncertainty. The second section contains additional results including the probability distribution functions of the parameters, the impacts of the background processes, and the applicability of the background process. I also include the global sensitivity analysis of the background processes and the deterministic results.

Additional methodology and data

Calculating the first order Sobol' index

The are steps taken to sample and calculate the first order Sobol' indices for different parameters:

1) Parameters definition:

p: Set of sampled values for a single input parameter using the numpy uniform random function in python.

GWP: The corresponding output values (GWP) from a formula as a function of the inputs parameters **p**.

# of iterations: The total number of samples / iterations used in the sampling of parameters and the Monte Carlo simulation. This is 1,000 in our case.

# of bins: The number of bins into which the samples are divided for calculating bin-wise means and variances. This is 20 in our case.

2) Bin size calculation:

The bin size is defined as:

$$Bin\ size\ = \frac{\#\ \text{of iterations}}{\#\ \text{of bins}} \qquad (C.1)$$

3) Monte Carlo simulation:

Run the Monte Carlo simulation, and for each iteration calculate the the output (the difference in GWP between A and B) based on a defined formula as a function of the sampled parameters and store the results in a list **GWP**.

4) Pairing input and output:

The input-output pairs (parameter **p** and corresponding output **GWP** are combined into a two-column array called **pairs**. Each row represents a single iteration, where the first column contains the values of **GWP** and the second column contains corresponding values of **p**.

5) Sorting by input

The rows of the **pairs** array are sorted based on the values of **p** (second column). This sorting step groups the output values **GWP** according to the increasing values of the parameter **p**, which allows for analyzing the effect of different ranges of **p** on the output **GWP**.

6) Extracting sorted outputs (GSA):

The first column (sorted outputs **GWP**) is extracted into an array called **GSA**. This will be used to calculate the variance contributions.

7) Reshaping output into bins:

The sorted output **GSA** (in practice, this is still **GWP** but sorted) is reshaped into a 2D array with dimensions (*# of bins*, *bin size*). Each group corresponds to a different range of input values **p**.

8) Calculating the mean of each bin:

The mean of the output **GSA** (in practice, this is still **GWP** but sorted) is calculated for each bin and stored as *bin means*. This gives an array of means, where each mean corresponds to the average **GWP** for a specific range of the input **p**.

9) First-order Sobol' Index calculation:

The first-order Sobol' index (SI) is calculated as:

$$\text{SI} = \frac{Var\ (bin\ means)}{Var\ (GWP)} \qquad (C.2)$$

The variance of the bin means captures the variance of the model output (**GWP**) due to the variation in the input parameter (**p**). This is divided by the total variance of the output (**GWP**), which is how the first-order Sobol' index is defined.

More information on how the GSA calculation is conducted is available in the GSAPDaC jupyter notebook.

System boundaries

Figure C.1 shows the flow chart for the wire arc additive manufacturing (WAAM) and illustrates how different uncertainty distributions are applied across the different life cycle stages. The orange boxes are the uncertainties based on the background data (pedigree matrix in ecoinvet) and shown in Figure C.3. The green boxes represent the applicability uncertainty (Figure C.3), which act as a scaling factor, and its distribution is based on our defined pedigree scores (Table C.1). For example, aluminum casting (adjusted to exclude the aluminum input) is used as a proxy for the steel casting process, and we account for that by having a wider uncertainty distribution. Blue boxes are the foreground data, where the parameters affecting the input are shown, and are modeled using a uniform distribution (Figure C.2).

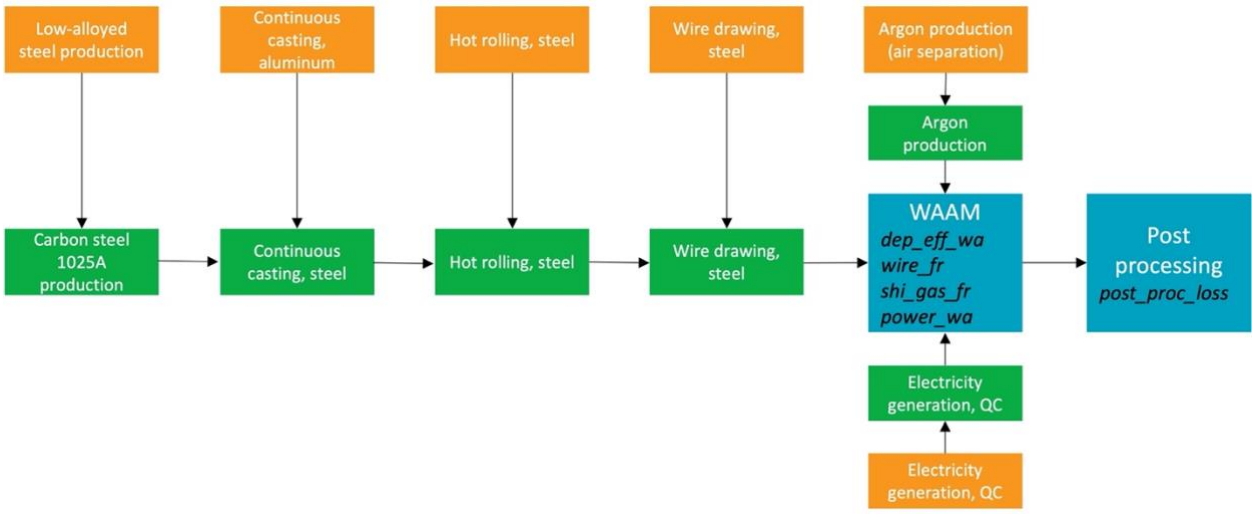

Figure C.1 Flow chart of WAAM

Table C.1 shows our scoring for the pedigree matrix for the applicability uncertainty (which is based on the ecoinvent pedigree matrix). The lower the score, the more applicable it is for our specific study.

Table C.1 The pedigree scores used to generate the uncertianty associated with the applicability of the background dataset

	Reliability	**Completeness**	**Temporal correlation**	**Geographical correlation**	**Technological correlation**
Electricity	1 Verified data based on statistics	1 Representative relevant data from all energy sources	2 Data is less than 6 years old	1 Data from QC-CA	2 Data from processes under study, different enterprise
Argon	2 Verified data based on literature and estimations	2 Representative relevant data for most cryogenic technologies	5 Data is more than 15 years old	1 Data from QC-CA	2 Data from material under study, different enterprise
Wire drawing	3 Non-verified data	2 Representative relevant data for most steel processes	5 Data is more than 15 years old	5 Data from RoW (but contains EU data)	2 Data from material under study, different enterprise
Wire rolling	3 Non-verified data	2 Representative relevant data for average techniques	5 Data is more than 15 years old	5 Data from RoW (but contains EU data)	2 Data from material under study, different enterprise

Table C.1 The pedigree scores used to generate the uncertianty associated with the applicability of the background dataset (cont'd and end)

Continuous casting	3 Non-verified data	2 Representative relevant data for average techniques	4 Data is less than 15 years old	1 Data from QC-CA	4 Data on related material (aluminum)
Steel	2 Verified data based on literature	2 Representative relevant data for most steel alloys	4 Data is less than 15 years old	1 Data from QC-CA	3 Data from material under study, different alloy
Nitrogen	2 Verified data based on literature and estimations	2 Representative relevant data for most cryogenic technologies	5 Data is more than 15 years old	1 Data from QC-CA	2 Data from material under study, different enterprise
Heat	1 Verified data based on measurements	3 Representative relevant data for EU technologies	5 Data is more than 15 years old	5 Data from QC-CA (but based on EU data)	2 Data from material under study, different enterprise

Additional results

Figure C.2 shows the probability distribution functions of the input parameters modelled with a uniform distribution. The dashed lines are the deterministic values.

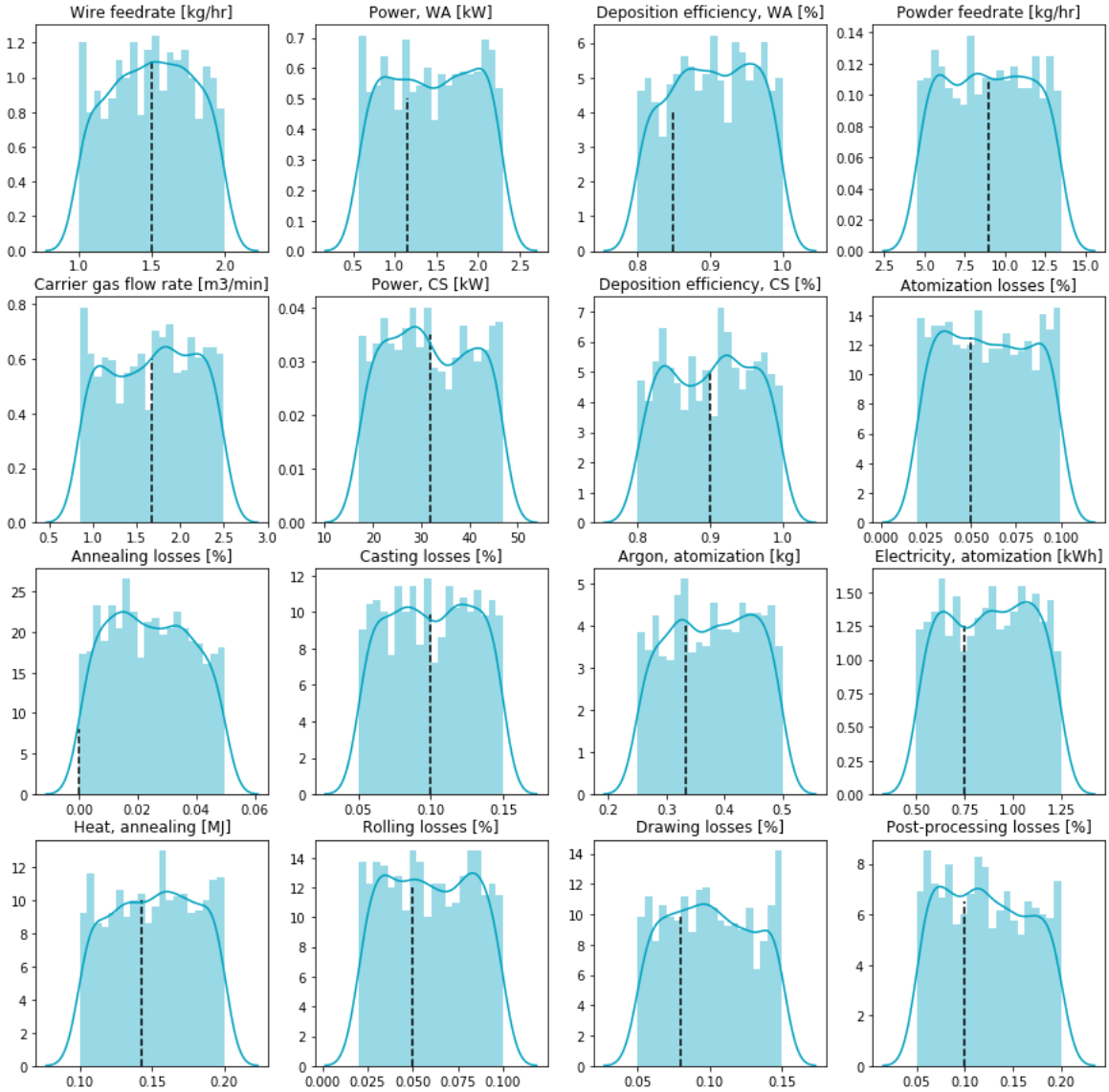

Figure C.2 Probability distribution functions of the input parameters

Figure C.3 shows the probability distribution functions of the uncertainty of the impacts of the background data (green) and the applicability uncertainty (orange). The uncertainty on the background impacts are based on a 1000 Monte Carlo analysis done with Activity Browser. The reason behind using the impact directly is the way our model is defined in python, which allows us to have a parametrized model. The dashed lines are the deterministic values.

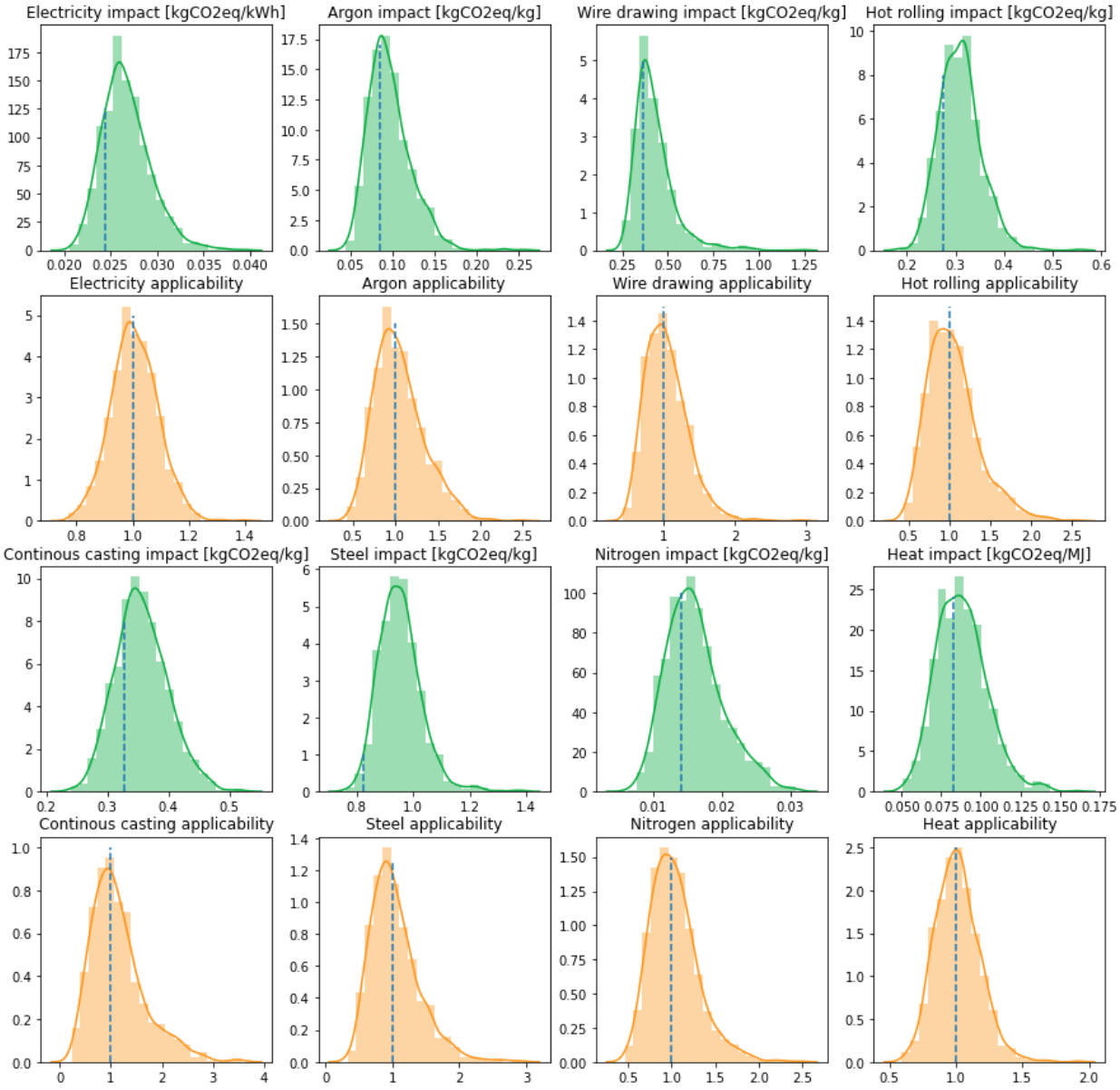

Figure C.3 Probability distribution functions of the impact of the background data and the applicability uncertainty

Figure C.4 shows the results of the GSA of the ecoinvent background processes. Those results were calculated manually using the Activity Browser, where the three highest contributors to the uncertainty (based on the Sobol' Index) are presented. The black bar present elementary flows and the gray bars economic flows. This is useful if our results show that the uncertainty comes from the background data, where its processes are not included in our GSA.

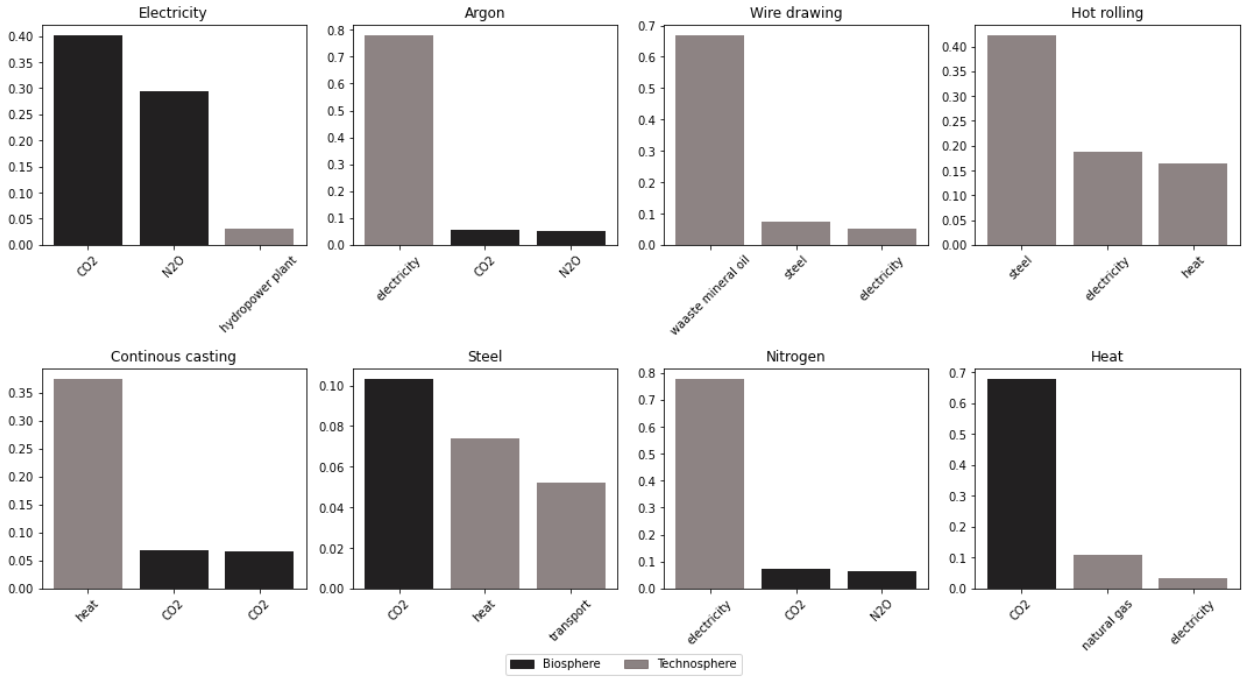

Figure C.4 GSA of the background processes

Figure C.5 shows the deterministic results for the initial iteration, where WAAM has a higher GWP than CSAM (2.36 and 1.77 kg CO_2-eq/f.u., respectively). The impact of WAAM is dominated by the steel wire production phase (99%), while for CSAM, 67% of the impact is from the steel powder production and 28% is from the nitrogen carrier gas.

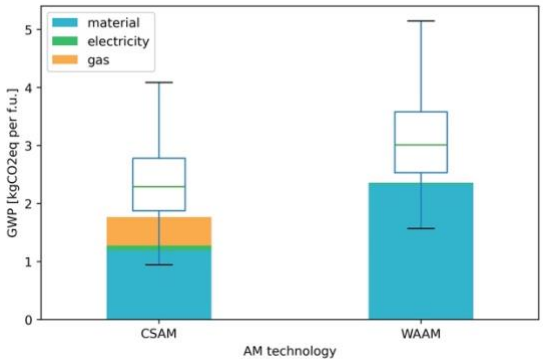

Figure C.5 Deterministic results of the initial iteration

Figure C.6 show the contribution analysis after the final iteration. Compared to the initial, we see that the electricity is higher (mainly due improving the data of the powder feed rate affecting the duration in the second iteration, and the power in the final iteration), while the gas is lower (due to lower gas flow rate in the third iteration).

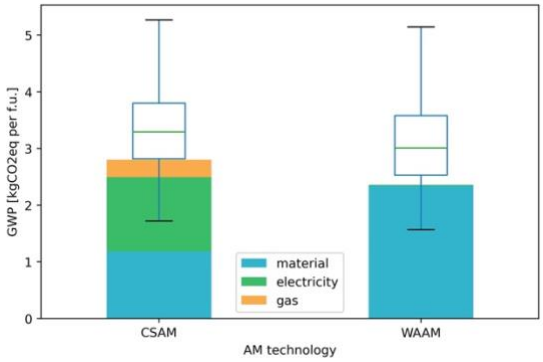

Figure C.6 Deterministic results after the last iteration

APPENDIX D SURFACE ENGINEERING GLOSSARY

Appendix D includes a short glossary of the main surface engineering technologies mentioned in the thesis, and a description of how each technology works.

Atmospheric plasma spray (APS)

Plasma Spray Coating is a thermal spray technology that utilizes a plasma gun that melts coating powder particles and sprays them on the substrate (Fotovvati et al., 2019).

Cold spray (CS)

Cold Spray coating, while labeled a thermal spray technology, does not rely on a heat source, where powder materials are fed to a stream of high-velocity inert gases that spray the coating material with high-velocity to achieve a critical kinetic energy required for the deformation of coating particles inside the substrate (Fotovvati et al., 2019).

Chemical vapor deposition (CVD)

Chemical vapor deposition processes involve the injection of volatile coating material in high vacuum, which in turn deposits on the surface of the substrate, also known as the wafer, as a result of a respective chemical reaction. CVD coating is largely used in the semiconductors industry for a resulting solid, high quality, and high resistance coating that provides protection against corrosion and wear. The process starts by vacuum pumping the coating material through an injector and then a vaporizer, that in turn shoots the coating material onto the wafer that would be ideally placed in a heated reactor that facilitates the chemical reaction between the wafer and the volatile material (Fotovvati et al., 2019).

Electrodeposition

Electrodeposition is a coating process that utilizes an electrochemical cell consisting of two electrodes: the substrate (cathode) and the coating material (anode). The two electrodes are submerged in an electrolyte solution that facilitates the transfer of metallic ions from the negatively charged anode to the positively charged cathode. Thus, a coating layer is formed on the substrate under the effect of electron transfer due to potential difference. It is suggested by extensive research that the coating layer highly enhances the corrosion properties of the substrate, in addition to high

prospects for producing superhydrophobic polymeric coatings as polythiophene (Fotovvati et al., 2019).

High-Velocity Oxy-Fuel (HVOF)

High-Velocity Oxy-Fuel is a category of thermal spray coating where a mix of fuel and oxygen combust and melt down the coating material, then the products are shot through a high-speed jet over the substrate, thus providing corrosion and wear-resistant layers (Fotovvati et al., 2019).

Physical vapor deposition (PVD)

Physical vapor deposition is a family of thin films that is mainly used for corrosion and wear resistance. The process is initiated by transforming the base material for coating into the vapor phase by means of thermal energy. The vaporized base material then travels in vacuum and condensates on the subtract. An important advantage of this method is the adjustability of the corrosion, mechanical, and aesthetic properties of coating layers (Fotovvati et al., 2019).

Surface engineering (SE)

Surface engineering is "a specialized activity that is applied at or very near the final stage of material manufacture" (Dearnley, 2017). SE is mainly used to allow for the adjustment of four surface properties: mechanical (wear and friction), chemical (corrosion, permeation, temperature insulation, bio-compatibility, wettability), electrical (conductivity) and optical (transmission, reflection, absorption and color) (Bewilogua et al., 2009).

Thermal Spray Coating (TSC)

Thermal Spray Coating is a group of coating techniques that rely on melting down the coating base material by means of plasma, electric, or chemical combustion then spraying the molten material on the designated substrate, that may be of non-conductive material, through a high- speed jet. This technique allows for using coating feedstock material that include refractory metals, metallic alloys, ceramics, plastics, and composites. It also permits achieving a variable thickness of coating from 20 micrometers up to a few millimeters, which is much higher than that achieved via electroplating, CVD, or PVD (Fotovvati et al., 2019).

APPENDIX E LITERATURE REVIEW OF LCA OF SURFACE ENGINEERING TECHNOLOGIES

A literature review covered publications in peer-reviewed journals and conference proceedings using the Web of Science Core Collection database. Two keyword categories were combined in the search, and the search fields included the topic. One category was related to life cycle assessment ("LCA" OR "Life Cycle Assessment" OR "Life Cycle Analysis") and the other referring to the surface engineering technology name or acronym presented in Figure 2.1 ("Surface Engineering Technology" OR "SET"). The Surface Engineering Technologies included were Physical Vapor Deposition (PVD), Chemical Vapor Deposition (CVD), Sol gel, electroplating, electrodeposition, plasma spray, high velocity oxygen fuel (HVOF) and cold spray. An initial screening allowed the exclusion of irrelevant articles, mainly because no LCA was done, or the acronyms referred to something else (LCA and CVD were not referring to life cycle assessment and chemical vapor deposition, respectively). Besides, other articles were excluded because they use SE technologies to synthesize materials and not to deposit coating layers. The overview of the identified articles is presented in Table E.1.

Table E.1 Literature review of LCA studies on surface engineering technologies with the scope of each.

Reference	**SE technology**	**Coating material**	**Functional unit**	**System boundaries**	**SE characteristics**
(E. Rúa Ramirez et al., 2024)	APS HVOF CS	WCCo	1 m2 of WC-Co coating applied on a C-steel substrate using the optimized process parameters for each deposition technique available	Use and EOL phases excluded	X

Table E.1 Literature review of LCA studies on surface engineering technologies with the scope of each. (cont'd)

(Baiocco et al., 2024)	EP	GNP	coating 5 μm thick on steel samples of size 2×4 cm^2	Use and EOL phases excluded	Improvement in tribological properties and coefficient of friction less than 0.2.
(Baranda et al., 2024)	HVOF	Ni50Cr	1 kg of of the material	Use phase excluded	X
(Q. Li et al., 2024)	CVD	Cu	1 m^2 of the graphene transparent electrode production	Use and EOL phases excluded, impact of industrial material recycling included.	X
(Edwin Rúa Ramirez et al., 2024)	APS HVOF CS	WC-12Co	coating applied on a low carbon steel plate with dimensions 50 × 20 × 5 mm^3	Use and EOL phases excluded	X
(Furberg & Arvidsson, 2024)	CVD	ND	1 cm^2 diamond film with a 10 μm thickness, corresponding to 3.2 mg diamond film with a density of about 3200 kg/m^3	Use and EOL phases excluded	X

Table E.1 Literature review of LCA studies on surface engineering technologies with the scope of each. (cont'd)

(Merlo et al., 2023)	HVOF EP	WCCo Cr	a coating of 1 m^2 on a cylinder whose thickness will be 150 μm	Use and EOL phases excluded	X
(D. Kumar et al., 2023)	CS	Al	An aluminum alloy flange	Use and EOL phases excluded	X
(Viscusi et al., 2023)	CS	Al	80 x 80 mm panel	Use and EOL phases excluded	X
(Yousefzadeh et al., 2022)	FS CS	Al_2O_3 Ni-50Cr	protection of a 5-meter aboveground carbon steel water pipe (2-inch diameter) from freezing during frost days in Alberta for 10 years.	EOL excluded	The thickness of the coating reflects its electrical insulation and heat-conducting properties
(Fiameni et al., 2021)	PVD	AlTiN	50 coated samples, each one with an area of 25 cm^2 and an AlTiN film thickness of 3 μm	Use and EOL phases excluded	X

Table E.1 Literature review of LCA studies on surface engineering technologies with the scope of each. (cont'd)

(J. Liu et al., 2021)	APS	FeNiCrBSi	1 m^2 Fe-based coating by plasma spraying	Use and EOL phases excluded	microhardness and porosity were evaluated with the LCA to assess the "greenness"
(Merlo & Léonard, 2021)	PVD EP	Cr	coating of 20 µm thick chromium film on 1m^2 area	Use and EOL phases excluded	The thickness in the functional unit reflects the improvement in tribological properties
(Bianco et al., 2020)	EP	X	one painted car	Use and EOL phases excluded	X
(Igartua et al., 2020)	PVD HVOF EP	CrN CrN Cr (VI)	1 m^2 coated surface area of component	EOL excluded	An evaluation of the durability through a tribology test was included
(S. Peng et al., 2019)	EP APS	$NiSO_4$	a restoring process with certain deposition layer (720 mm^3)	Use and EOL phases excluded	Bonding strength, substrate deformation, hardness and porosity were included

Table E.1 Literature review of LCA studies on surface engineering technologies with the scope of each. (cont'd)

(Tsoy et al., 2019)	Sol gel - dip coating	SiO_2	the production of 1692.30 kg of tomatoes in greenhouses for 30 years (under 1m^2 coated glass)	EOL phase excluded	Antireflective coating increases light transmittance, which increases crops yield
(Encinas-Sánchez et al., 2018)	Sol gel - dip coating	YSZ	1 cm^2 in accordance with the gravimetric analysis performed in the corrosion study	Use and EOL phases excluded	Coating resists corrosion, which increases lifetime
(Takuma et al., 2018)	EP	Ni	plating 1 kg part	Use phase excluded	X
(Guarino et al., 2017)	EP	Ag GNP + Cu	Coating an 8 cm electrical conductor	Use phase excluded	Graphene coating increases the thermal properties of the metallic circuit breaker
(Wigger et al., 2017)	EP HVOF	Cr (VI) WC-Co	300 μm thickness coating over an area of 1 m^2	Cradle-to-grave	X

Table E.1 Literature review of LCA studies on surface engineering technologies with the scope of each. (cont'd)

(Arvidsson et al., 2016)	CVD	graphene	A layer with a surface area of 1 cm^2	Use and EOL phases excluded	transparence measured in optical transmission and electrical conductivity measured in sheet resistance
(Louwen et al., 2015)	PVD PECVD EP	ITO Si Cu	one kilowatt-hour of alternating current electricity delivered by a PV system	EOL phase excluded	Module efficiency included
(Sánchez-Cruces et al., 2014)	EP Sol gel - dip coating	Co	1 m^2 of coating	Use and EOL phases excluded	optical properties studied
(García et al., 2013)	EP	Cr (III)	square meter of passivated product	Use phase excluded	X
(Espinosa et al., 2012)	Roll-to-roll	Al/Cr	1 m^2 of processed area (290 mm width)	EOL phase excluded	Active area coverage and module efficiency assessed

Table E.1 Literature review of LCA studies on surface engineering technologies with the scope of each. (cont'd)

(Posset et al., 2012)	EP PVD	WO_3 IrO_x Ni Ti Ta_2O_5 In_2O_3Sn	one unit of an electrochromic/tropic shading device, i.e., one piece of product, 20 cm x 30 cm in size	Cradle-to-grave	X
(Espinosa et al., 2011)	Roll-to-roll	Co_3O_4	1 m^2 of coating	Use and EOL phases excluded	Active area coverage and module efficiency assessed
(Serres et al., 2011)	APS EP	NiCrBSi	the elaboration with a specific technology of a coating which is remelted (or not) after deposition	Cradle-to-grave	In situ laser remelting improves corrosion resistance
(Moign et al., 2010)	SPPS SPS APS	YSZ	1 μm thick layer of YSZ on 1 m^2 surface	Use and EOL phases excluded	X

Table E.1 Literature review of LCA studies on surface engineering technologies with the scope of each. (cont'd)

(Serres et al., 2010)	APS FS	NiCrBSi	realization with a specific technology of a coating which is remelted (or not) after deposition	Cradle-to-grave	The microstructure of the coating was assessed
(Haapala et al., 2009)	EP	NiP NiNP	50mm x 50mm device, with a length of about 10mm	Use and EOL phases excluded	X
(Serres et al., 2009)	APS HVOF EP	NiP AISI316L Cr	the surface of a Ø = 25 mm, S = 491 mm^2 cylindrical C38 steel sample covered with a thick coating (380 μm for APS and HVOF coatings, 250 μm for EP)	Cradle-to-grave	FU thickness based on corrosion resistance
(Bauer et al., 2008)	PVD	TiN TiAlN	The coating of 100,000 drills, diameter of 6 mm	EOL phase excluded	improved material properties like friction, abrasion resistance, tribological oxidation and surface fatigue --> longer lifespan of tools and a higher resistance of components to deformity

Table E.1 Literature review of LCA studies on surface engineering technologies with the scope of each. (cont'd and end)

(Andrae et al., 2004)	PVD	Cu Ni60Cr40	one gallium arsenide (GaAs) Mon lithic Microwave Integrated Circuit (MMIC)	Use and EOL phases excluded	X
(Meijer et al., 2003)	CVD	InGaP	PV module with a capacity of 1 kW under Dutch meteorological conditions	Use and EOL phases excluded	The new coating improves the solar cell conversion efficiency
(Hart et al., 2000)	CVD PVD	YSZ	2 million 10 cm x 10 cm x 50 um thick YSZ electrolyte thick film per year	Use and EOL phases excluded	X
(Sonoya & Kitiara, 1997)	FS HVOF APS	MSFNi-4 Cr_3C_2 + NiCr Al_2O_3	1 mm of coated surface	Cradle-to-grave	Wear resistance was also assessed

APS: Atmospheric plasma spray; EP: Electroplating; EOL: End of life; FS: Flame spray; HVOF: High velocity oxy-fuel; ND: Nano diamond; PVD: Physical vapor deposition; SPPS: Solution precursor plasma spray; SPS: Suspension plasma spray; YSZ: Yttrium stabilized zirconium; X: not clear